8-2024

Effects of the Sea Level Rise and Hurricanes in the Coastal Forest of South Carolina

Siddhartha Regmi
sregmi@clemson.edu

EFFECTS OF THE SEA LEVEL RISE AND HURRICANES IN THE COASTAL FOREST OF SOUTH CAROLINA

A Thesis
Presented to the Graduate
School of Clemson
University

In Partial Fulfillment of the
Requirements for the Degree
Master of Science
Forest Resources

---

by
Siddhartha Regmi
August 2024

Accepted by:
Dr. Bo Song, Committee Chair
Dr. Thomas M. Williams
Dr. Thomas L. O'Halloran
Dr. Nilesh Timilsina

ABSTRACT

Accessing the mortality of the trees following any disturbances is of great interest to researchers in forestry science. This thesis project assessed topographic factors to explain the patterns of tree mortality after Hurricane Hugo in 1989 and investigated continuous tree mortality in relationship to important covariates using long-term data. Aerial photographs were taken one year after Hurricane Hugo, and long-term monitoring plots were set up five years after the hurricane to collect multi-year data. Analysis and visualization showed higher mortality in concave areas near the marsh at approximately 1-2m elevation and 120-180m far from streams after Hurricane Hugo. A model was derived using the logistic regression analysis, and tree mortality after Hurricane Ian 2023 was predicted based on the model. The actual tree mortality map was generated using the Leaf Area Index change. Two maps were compared visually, and the model underestimated the mortality. Using the data from the long-term monitoring plots, we performed a nonparametric Kaplan-Meier method to describe the effects of covariates (biotic, climatic and hydrologic) on the survival probability of trees. The Kaplan-Meier Curve indicated that any tree has a survival probability of around 20% after 29 years or upon reaching a diameter at breast height (DBH) of 10 cm. Understanding how various factors interact and contribute to tree mortality will enhance our capacity to evaluate the susceptibility of coastal forests to mortality due to periodic hurricane events and how they shape the growth and resilience of coastal forests.

ACKNOWLEDGEMENTS

I am deeply grateful to several individuals and organizations whose support and guidance have been instrumental in completing this thesis. First and foremost, I would like to sincerely thank the College of Agriculture, Forestry, and Life Sciences for providing me with a graduate fellowship to pursue my degree, the Belle W. Baruch Foundation and the United States Forest Service for their invaluable logistical and financial support.

I am particularly grateful to the Baruch Institute of Coastal Ecology and Forest Science for their collaboration and assistance in my research on forest disturbances. I would also like to thank the Society of American Foresters for Kurt Gottschalk Science Fund grant support for accommodation and fuel during field visits in the summer of 2023. A special thank you to the Department of Forestry and Environmental Conservation at Clemson University for providing an excellent academic environment and the resources needed for my research. The faculty and staff have been incredibly supportive and encouraging.

I would also like to express my deepest appreciation to my committee members Dr. Bo Song, Dr. Thomas M. Williams, Dr. Thomas L. O'Halloran and Dr. Nilesh Timilsina. Their insights, feedback, and constant motivation have been crucial in completing this thesis. I want to express my heartfelt thanks to Ms. Suraksha Adhikari and Mr. Brian Williams for their unwavering support and encouragement. Lastly, I am deeply indebted to my family for their unconditional love and support. Their belief in me and their encouragement has been the foundation upon which I have built my academic career.

TABLE OF CONTENTS

EFFECTS OF THE SEA LEVEL RISE AND HURRICANES IN THE COASTAL FOREST OF SOUTH CAROLINA i

ABSTRACT ii

ACKNOWLEDGEMENTS iii

TABLE OF CONTENTS iv

LIST OF FIGURES vii

LIST OF TABLES x

LIST OF APPENDICES x

CHAPTER 1 1

INTRODUCTION 1

REFERENCES 4

CHAPTER 2 8

LITERATURE REVIEW 8

Historical Overview of Sea Level Rise and Hurricanes in South Carolina 8

Hurricane Impacts in Coastal Forests 10

Tree Mortality and Biotic factors 13

Tree Mortality and Climatic Factors 15

Tree Mortality and Hydrologic Factors 16

Tree Mortality and Topographic Factors 17

Remote Sensing and Quantify Hurricane Damage 19

Survival Analysis. 21

REFERENCES 24

CHAPTER 3 47

SPATIAL PATTERNS OF TREE MORTALITY IN A COASTAL FOREST OF HOBCAW BARONY AFTER HURRICANE HUGO. 47

Abstract 47

Introduction 48

Methodology 51

Results 61

Discussion 74

Limitations of the study 77

Conclusion 77

REFERENCES 79

CHAPTER 4 84

TREE MORTALITY DUE TO HURRICANES AND ASSOCIATED VARIABLES IN THE COASTAL FOREST IN SOUTH CAROLINA. 84

Abstract 84

Introduction 85

Methodology 89

Results 95

Discussion 109

Limitations of the study 113

Conclusion 113

REFERENCES 115

APPENDICES 124

LIST OF FIGURES

Figure 2.1: Hurricanes near Georgetown, South Carolina, Since 1989. 10

Figure 2.2: Tree mortality patch in between the forest *(Credit: Dr. Thomas Williams*)..... 13

Figure 2.3: Sea water clogged in concave areas after the storm surge. (*Pic credit: Dr. Thomas Williams*) 19

Figure 3.1: Study area map showing part of Hobcaw Barony Forest, South Carolina. 53

Figure 3.2: Methodology layout showing the steps from acquiring images for analysis to comparing the mortality maps…….. 60

Figure 3.3: Tree Mortality Areas after Hurricane Hugo in 1989 in the Hobcaw Barony Forest, South Carolina. 61

Figure 3.4:Tree mortality by curvature classes after Hurricane Hugo (1989) in Hobcaw Barony, South Carolina, USA…….63

Figure 3.5: Tree mortality by distance from stream networks after Hurricane Hugo (1989) in Hobcaw Barony, South Carolina, USA..... 64

Figure 3.6: Tree mortality with distance from marsh after Hurricane Hugo (1989) in Hobcaw Barony, South Carolina, USA. 65

Figure 3.7: Tree mortality by elevation classes after Hurricane Hugo (1989) in Hobcaw Barony, South Carolina, USA. 66

Figure 3.8: Density plots of pixel distribution of independent variables for healthy areas after Hurricane Hugo and tree mortality areas in Hurricane Hugo and Ian. 67

Figure 3.9: Differences in the distribution of the pixels of independent variables for tree mortality and healthy areas after Hurricane Hugo in 1989 in the Hobcaw Barony forest, South Carolina, USA..... 68

Figure 3.10: Pearson correlation matrix plots among the variables used in the analysis. 69

Figure 3.11: ROC Curve for the accuracy estimation..... 71

Figure 3.12: Tree mortality areas were predicted after Hurricane Ian based on the logistic regression model prediction..... 72

Figure 3.13: Actual tree mortality areas after Hurricane Ian based on the LAI change. Blue shades depict tree mortality areas after Hurricane Ian, which also fall inside the areas of tree mortality after Hurricane Hugo..... 74

Figure 4.1: Annual tree mortality for a whole tree data set collected from 1994 to 2023 in the sample plots in Hobcaw Barony. Mean dashed line shows the mean annual mortality rate over the period of 29 years..... 95

Figure 4.2: Annual mortality rates in the four sample plots in the Hobcaw Barony. Mean dashed line in each plot shows the mean annual mortality over the period of 29 years. 96

Figure 4.3: Major species counts observed in the sample plots from 1994 to 2023. 97

Figure 4.4: The mortality rate of major species over 29 years in a coastal forest in Hobcaw Barony, South Carolina, USA..... 98

Figure 4.5: Evergreen and Deciduous Species..... 99

Figure 4.6: Mortality rate by year for Evergreen and Deciduous Species. 100

Figure 4.7: Violin plot for DBH distribution for all trees in the dataset and for trees of major species that have died..... 100

Figure 4.8: Patterns of mean annual temperature and precipitation from 1994 to 2023 in the Hobcaw Barony Forest, South Carolina, USA. 101

Figure 4.9: Mortality rate by year for temperature and precipitation variables. 101

Figure 4.10: Highest tides since 1994 and increasing trend of the tide heights. 102

Figure 4.11: Annual mortality rate and the highest tide in the past three years for the period of 29 years from 1994-2003. 103

Figure 4.12: Kaplan Meier curve for the tree mortality with DBH and period of observation in years (Time) as a time variable. 104

Figure 4.13: Kaplan Meier Survival Analysis for major species over the period of 29 years from 1994 to 2023. 105

Figure 4.14: Kaplan-Meier Survival Analysis curve for the biotic variables for the period of 29 years. Biotic variables included the DBH, leaf habit and total basal area in a plot. DBH is further categorized as small, medium and large. 106

Figure 4.15: Kaplan-Meier Survival Analysis curve for the climatic variables for the period of 29 years. Climatic variables included temperature and precipitation data for the past three years, as well as for a lagged period corresponding to the observation duration during the survival of each tree. 107

Figure 4.16: Kaplan-Meier Survival Analysis curve for the hydrologic variables for the period of 29 years. Hydrologic variables included the tide frequency and the highest tide in the past three years in each tree. 108

LIST OF TABLES

Table 3.1: Summary of the logistic regression analysis final model..... 69

Table 4.1: Variable selection for the model and analysis 92

LIST OF APPENDICES

Table A - 1: Correlation among the variables..... 124

Table A - 2: Annual mortality rate over the years for the period of 29 years (1994-2023)..... 124

Table A - 3: Plotwise annual mortality rate 125

Table A - 4: Species-wise annual mortality rate (%) for major species 128

Table A - 5: Species code, common name, scientific name, counts and leaf habits. 129

Table A - 6: Temperature, Precipitation and Highest tide Variables from 1994 to 2023..... 130

CHAPTER 1

INTRODUCTION

Coastal forests are more vulnerable due to global warming and rising sea levels. Although coastal plant death has various causes, the impacts of climate change and sea-level rise are becoming more apparent (Sippo et al., 2018). While there is a lack of extensive long-term data, available site-specific records over significant durations indicate an increase in mortality rates over time (Lewis et al., 2016; Kirwan et al., 2016; Demopoulos et al., 2018; Noe et al., 2018; Schieder & Kirwan, 2019). Certain hotspots, like the eastern coast of North America, have emerged where rising sea levels, land subsidence, a weakening Gulf Stream, and flat topography have caused extensive plant death (Kirwan & Gedan, 2019; Sallenger et al., 2012; Schieder et al., 2018; Smith, 2013; Smith et al., 2017, 2021; Smith & Kirwan, 2021; Ury et al., 2021). Extensive evidence from regional and global studies indicates that coastal plant death rates are rising.

Moreover, variations in mortality rates among different species are significant factors of ecological succession (Kobe et al., 1995; Purves et al., 2008), species' geographical ranges (Loehle et al., 1998; Purves et al., 2009), stand structure (such as stem size distributions: (Muller-Landau et al., 2006; Coomes et al., 2003) and how forests respond to climate change (van Mantgem et al., 2007). Understanding the factors and mechanisms driving coastal woody plant mortality in a changing climate is essential for predicting forest mortality (Kirwan & Gedan, 2019). Advanced measurements are needed to develop and evaluate models using these measurements (Collier et al., 2018; Dietze et al., 2018; Medlyn et al., 2015).

Obtaining precise information on the nature, magnitude, and causes of tree mortality in coastal forests is challenging. To better understand how woodland environments might respond to projected climate changes and rising sea levels, it is crucial to use all available information and analytical tools, including remote sensing (Allen et al., 2015). Remote sensing's unique ability to provide spatially explicit maps of tree mortality offers an invaluable foundation for studying potential mortality drivers (Anderegg et al., 2016).

Since 1996, the southeastern United States has experienced a rise in the frequency of hurricane landfalls, a trend expected to persist in the coming years (Goldenberg et al., 2001; Emanuel, 2005; Webster et al., 2005). This heightened hurricane activity presents a valuable opportunity to systematically study how a series of hurricanes may create cumulative and potentially irreversible impacts on coastal ecosystems. This thesis investigates the effects of these extreme events on the Hobcaw Barony Forest, focusing on tree mortality patterns and the factors influencing survival. By leveraging long-term monitoring data and advanced spatial analysis techniques, this research aims to enhance our understanding of how hurricanes and sea level rise shape coastal forest dynamics and inform future management frameworks.

The first chapter of the thesis is “Spatial Patterns of Tree Mortality in a Coastal Forest of Hobcaw Barony After Hurricane Hugo.” It uses remote sensing, such as satellite imagery and aerial photographs, to analyze the spatial patterns of tree mortality following Hurricane Hugo. This chapter assesses topographic factors, including elevation, proximity to marshes, drainage capacity, and land curvature, to explain tree mortality patterns. A logistic regression model incorporating these variables was developed and used to predict tree mortality following Hurricane Ian.

The second chapter of the thesis is "Tree Mortality Due to Hurricanes and Associated Variables in the Coastal Forests of South Carolina." It focuses on long-term tree mortality trends and the relationship between tree survival and biotic, climatic, and hydrologic variables. Data were collected from monitoring plots established in 1994 in the pine-dominated Hobcaw Barony Forest. This chapter employs simple graphical illustrations, a nonparametric survival analysis technique, and a Kaplan-Meier Estimator to assess the effects of covariates on survival probability.

In conclusion, this thesis provides valuable insights into the complex interactions between hurricanes, sea level rise, and tree mortality in coastal forests. This could be helpful in developing effective management strategies for the sustainability of coastal forests in the face of ongoing sea level rise.

REFERENCES

1. Allen, C. D., Breshears, D. D., & McDowell, N. G. (2015). On underestimation of global vulnerability to tree mortality and forest die-off from hotter drought in the Anthropocene. *Ecosphere*, *6*(8), 1-55.
2. Anderegg, W. R., Klein, T., Bartlett, M., Sack, L., Pellegrini, A. F., Choat, B., & Jansen, S. (2016). Meta-analysis reveals that hydraulic traits explain cross-species patterns of drought-induced tree mortality across the globe. *Proceedings of the National Academy of Sciences*, *113*(18), 5024-5029.
3. Collier, N., Hoffman, F. M., Lawrence, D. M., Keppel-Aleks, G., Koven, C. D., Riley, W. J., ... & Randerson, J. T. (2018). The International Land Model Benchmarking (ILAMB) system: design, theory, and implementation. *Journal of Advances in Modeling Earth Systems*, *10*(11), 2731-2754.
4. Coomes, D. A., Duncan, R. P., Allen, R. B., & Truscott, J. (2003). Disturbances prevent stem size-density distributions in natural forests from following scaling relationships. *Ecology letters*, *6*(11), 980-989.
5. Demopoulos, A. W., Bourque, J. R., Durkin, A., & Cordes, E. E. (2018). The influence of seep habitats on sediment macrofaunal biodiversity and functional traits. *Deep Sea Research Part I: Oceanographic Research Papers*, *142*, 77-93.
6. Dietze, M. C., Fox, A., Beck-Johnson, L. M., Betancourt, J. L., Hooten, M. B., Jarnevich, C. S., ... & White, E. P. (2018). Iterative near-term ecological forecasting: Needs, opportunities, and challenges. *Proceedings of the National Academy of Sciences*, *115*(7), 1424-1432.

7. Emanuel, K. (2005). Increasing destructiveness of tropical cyclones over the past 30 years. *Nature*, *436*(7051), 686-688.
8. Goldenberg, S. B., Landsea, C. W., Mestas-Nuñez, A. M., & Gray, W. M. (2001). The recent increase in Atlantic hurricane activity: Causes and implications. *Science*, *293*(5529), 474-479.
9. Kirwan, M. L., & Gedan, K. B. (2019). Sea-level driven land conversion and the formation of ghost forests. Nature Climate Change, 9, 450–457.
10. Kirwan, M. L., Temmerman, S., Skeehan, E. E., Guntenspergen, G. R., & Fagherazzi, S. (2016). Overestimation of marsh vulnerability to sea level rise. *Nature Climate Change*, *6*(3), 253-260.
11. Kobe, R. K., Pacala, S. W., Silander Jr, J. A., & Canham, C. D. (1995). Juvenile tree survivorship as a component of shade tolerance. *Ecological applications*, *5*(2), 517-532.
12. Krauss, K. W., Noe, G. B., Duberstein, J. A., Conner, W. H., Stagg, C. L., Cormier, N., Jones, M. C., Bernhardt, C. E., Lockaby, B. G., From, A. S., Doyle, T. W., Day, R. H., Ensign, S. H., Pierfelice, K. N., Hupp, C. R., Chow, A. T., & Whitbeck, J. L. (2018). The role of the upper tidal estuary in wetland blue carbon storage and flux. Global Biogeochemical Cycles, 32(5), 817–839.
13. Lewis, R. R., Milbrandt, E. C., Brown, B., Krauss, K. W., Rovai, A. S., Beever, J. W., III, & Flynn, L. L. (2016). Stress in mangrove forests: Early detection and preemptive rehabilitation are essential for future successful worldwide mangrove forest management. Marine Pollution Bulletin, 109(2), 764–771.
14. Loehle, C. (1998). Height growth rate tradeoffs determine northern and southern range limits for trees. *Journal of biogeography*, *25*(4), 735-742.

15. Medlyn, B. E., Zaehle, S., De Kauwe, M. G., Walker, A. P., Dietze, M. C., Hanson, P. J., ... & Norby, R. J. (2015). Using ecosystem experiments to improve vegetation models. *Nature Climate Change*, *5*(6), 528-534.
16. Muller-Landau, H. C., Condit, R. S., Harms, K. E., Marks, C. O., Thomas, S. C., Bunyavejchewin, S., ... & Ashton, P. (2006). Comparing tropical forest tree size distributions with the predictions of metabolic ecology and equilibrium models. *Ecology letters*, *9*(5), 589-602.
17. Purves, D. W. (2009). The demography of range boundaries versus range cores in eastern US tree species. *Proceedings of the Royal Society B: Biological Sciences*, *276*(1661), 1477-1484.
18. Purves, D. W., Lichstein, J. W., Strigul, N., & Pacala, S. W. (2008). Predicting and understanding forest dynamics using a simple tractable model. *Proceedings of the National Academy of Sciences*, *105*(44), 17018-17022.
19. Sallenger, A., Doran, K., & Howd, P. (2012). Hotspot of accelerated sealevel rise on the Atlantic coast of North America. Nature Climate Change, 2, 884–888.
20. Schieder, N. W., & Kirwan, M. L. (2019). Sea-level driven acceleration in coastal forest retreat. Geology, 47, 1151–1155.
21. Schieder, N. W., Walters, D. C., & Kirwan, M. L. (2018). Massive upland to wetland conversion compensated for historical marsh loss in Chesapeake Bay, USA. Estuaries and Coasts, 41(4), 940–951.
22. Sippo, J., Lovelock, C. E., Santos, I. R., Sanders, C. J., & Maher, D. T. (2018). Mangrove mortality in a changing climate: An overview. Estuarine, Coastal and Shelf Science, 215, 241–249.

23. Smith, A. J., & Kirwan, M. L. (2021). Sea level-driven marsh migration results in rapid net loss of carbon. Geophysical Research Letters, 48(13), e2021GL092420.

24. Smith, J. A. M. (2013). The role of Phragmites australis in mediating inland salt marsh migration in a mid-Atlantic estuary. PLoS One, 8(5), e65091.

25. Smith, J. A. M., Hafner, S. F., & Niles, L. J. (2017). The impact of past management practices on tidal marsh resilience to sea level rise in the Delaware Estuary. Ocean and Coastal Management, 149, 33–41.

26. Ury, E. A., Yang, X., Wright, J. P., & Bernhardt, E. S. (2021). Rapid deforestation of a coastal landscape driven by sea-level rise and extreme events. Ecological Applications, 31(5), e02339.

27. Van Mantgem, P. J., & Stephenson, N. L. (2007). Apparent climatically induced increase of tree mortality rates in a temperate forest. *Ecology letters*, *10*(10), 909-916.

28. Webster, P. J., Holland, G. J., Curry, J. A., & Chang, H. R. (2005). Changes in tropical cyclone number, duration, and intensity in a warming environment. *Science*, *309*(5742), 1844-1846.

CHAPTER 2

LITERATURE REVIEW

Historical Overview of Sea Level Rise and Hurricanes in South Carolina

Severe hurricanes are projected to increase due to human-induced climate change. (Knutson et al., 2010; Intergovernmental Panel on Climate Change [IPCC], 2012). Numerous studies also conclude that the increasing wind hazards from hurricanes along the eastern U.S. coastline and notable variations in hurricane frequencies, both annually and seasonally, may be attributed to climate change. (Lin et al., 2012; Mudd et al.,2014). Hurricanes, characterized by wind speeds exceeding 33 m s−1, impact 1.2 million hectares of U.S. land each year, leading to substantial ecological and economic damage to forests (Dale et al., 2001). Many hurricanes, such as Hugo, Irene, Floyd, Matthew, Irma, Florence, Dorian, and Ian, occurred in the recent few decades in South Carolina. (Figure 2.1)

In addition to sea-level rise, hurricane-induced storm surges exacerbate coastal flooding. Hurricane Hugo landed just north of Charleston, SC, at Sullivan's Island around midnight on September 22, 1989, as a Category 4 storm. The hurricane caused massive wind and storm surge damage along the coast and significant wind damage far inland; Hugo then generated the highest storm tide heights recorded on the U.S. East Coast. In South Carolina, around 1.8 million hectares of forest land were damaged by wind and water (National Weather Service, n.d.-a). Hurricane Irene formed from a low-pressure area in the western Caribbean Sea, becoming a tropical storm on October 13 and a hurricane on October 15, 1999, in the Straits of Florida. It caused agricultural losses and long-term ecological impacts expected in the Everglades and

estuaries. (National Weather Service, n.d.-b). Hurricane Floyd landed on September 16, 1999, at Cape Fear, North Carolina, as a Category 2 storm on the Saffir-Simpson Hurricane Scale. The primary impact of Floyd was extensive flooding, with Southport receiving the highest rainfall total of 24.06 inches. (National Weather Service, n.d.-c). Hurricane Gaston led to a tropical storm warning and a hurricane watch from Little River Inlet, South Carolina (SC) on August 29, 2004, causing heavy rains and strong winds and damaging many trees. (National Weather Service, n.d.-d)

Hurricane Charley landed on Florida's southwest coast near Cayo Costa, just west of Ft. Myers, at approximately 3:45 p.m. EDT on August 13, 2004. The hurricane caused an estimated $14 billion in economic losses. On October 8, 2016, Hurricane Matthew made landfall, producing the third-highest tide levels ever recorded at Charleston Harbor since Hugo and surpassing the early October 2015 flood event by over a foot. The hurricane affected Florida, Georgia, North Carolina, and South Carolina. Hurricane Florence, initially a category four storm, was downgraded to a category 1 when it landed on September 17, 2018. Surge levels reached 3.75 feet in Beaufort, South Carolina, where local inundation typically occurs. (Runkle et al., 2018). Hurricane Dorian came across northeastern South Carolina and eastern North Carolina on Wednesday, September 5, 2019. Luckily, it kept its center offshore as it neared Cape Fear that evening. (National Weather Service. n.d.-e)

Hurricane Isaias landed near Ocean Isle Beach, North Carolina, on August 3, 2020. The initial storm surge forecast predicted 2 to 4 feet of inundation from Edisto Beach, South

Carolina, to Cape Fear, North Carolina. Coastal South Carolina received 5-7 inches of rain. (National Hurricane Center, 2021). More recently, Hurricane Ian struck near Georgetown, SC, on September 30, 2022, as a Category 1 hurricane had high winds reaching 37 m s−1 near the area (Armstrong, 2022). The verified height of the tide was up to 2.35 m above mean sea level in the Springmaid Pier, Myrtle Beach (NOAA, 2024). It was the third most costly in U.S. history, following Hurricane Katrina in 2005 and Hurricane Sandy in 2012 (Bucci et al., 2023). In 2023, post-Hurricane Ian, mortality rates rose sharply in the mangrove. (Conservancy of Southwest Florida, 2024).

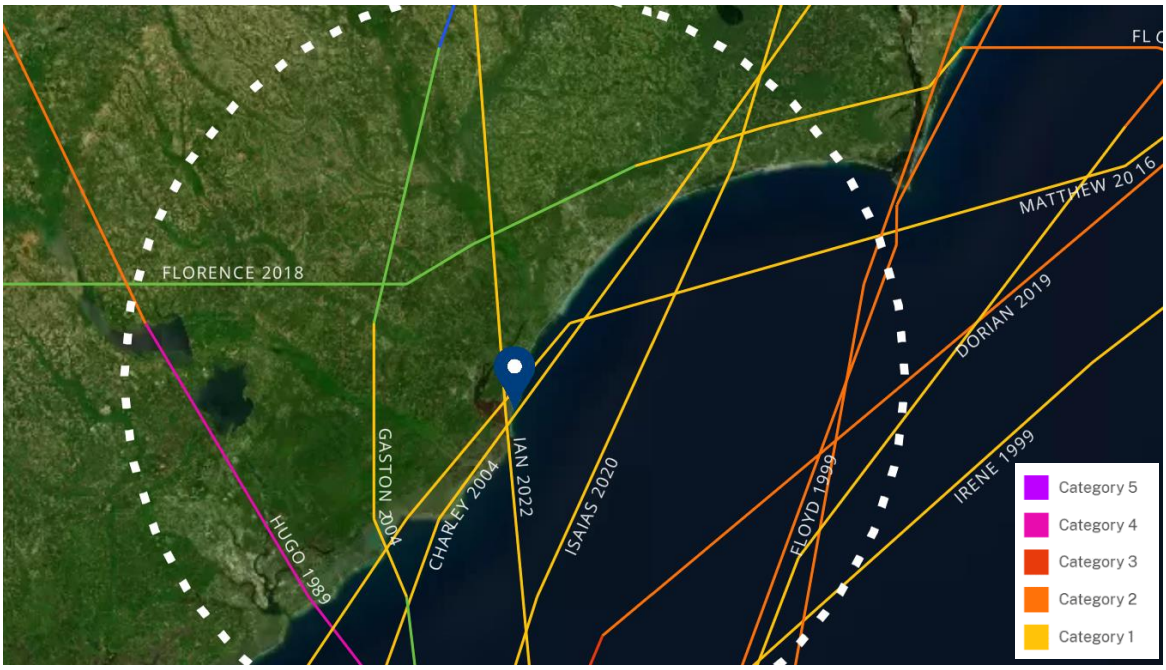

Figure 2.1: Hurricanes near Georgetown, South Carolina, Since 1989.

Hurricane Impacts in Coastal Forests

The impact of hurricane disturbances on tropical forests received significant interest from different researchers following Hurricane Hugo in 1989 (e.g., Walker, 1991a; Brokaw & Grear, 1991). Coastal and estuarine landscapes encompass a few of the world's most valuable and fragile ecosystems (Lotze et al., 2006; Barbier et al., 2011; Parker & Crichton, 2011). A rise in hurricane frequency and intensity likely exceeds the historical norms of southern forest ecosystems (Elsner et al., 2008; Pachauri et al., 2014; Kossin et al., 2020), raising concerns about the sustainability and future of coastal forests. In the southeastern United States, hurricanes are a significant natural disturbance affecting forest ecosystems. A powerful hurricane can dramatically alter these forests' composition, structure, and succession. (Foster, 1988; Boutet & Weishampel, 2003)

Storm surges and high winds from these storms can drastically affect the structure, growth, species makeup, and diversity of forests (Lugo, 2008). Rising sea levels lead to the gradual inward shift of shorelines and the forest-marsh boundary (Robichaud & Bégin, 1997; Kirwan et al., 2016). These stressors have resulted in decreased forest growth, regeneration failures, and dieback events (Mickler et al., 2012; Kirwan et al., 2016). For instance, the coastal forests in South Carolina saw increased mortality due to saltwater intrusion and severe wind damage from Hurricane Hugo in 1989 (Hook et al., 1991). Moreover, coastal forests on Florida's west coast have experienced regeneration failures due to rising sea levels (Williams et al., 1999).

Hurricanes impact forest ecosystems in various ways, resulting in patches of tree mortality within the forest (Figure 2.2). Hurricane Ivan in 2004 severely affected around 1

million hectares of land in Alabama alone (Springer et al., 2004). More recently, Hurricanes Irma in 2017 and Michael in 2018 caused significant wind disturbance to forests in Florida and Georgia. Hurricanes also cause saltwater intrusion and storm surge flooding in coastal ecosystems (Bianchette et al., 2009). Saltwater intrusion can kill trees, alter forest composition, and expand marshes into forested coastal areas (Bianchette et al., 2009; Doyle, 2007; Kearney et al., 2019).

Coastal ecosystems dominated by woody plants are undergoing significant mortality (Sippo et al., 2018). The emergence of 'ghost forests' due to inundation is becoming increasingly common globally for both halophytic and glycophytic woody plants (Kirwan & Gedan, 2019; Lovelock et al., 2017; Penfound & Hathaway, 1938; Shreve et al., 1910; Sippo et al., 2018; Wang et al., 2019). The rapid rise in relative sea levels and the growing frequency and intensity of storm surges are expected to continue (Vermeer & Rahmstorf, 2009; Jevrejeva et al., 2016). These changes are leading to increased coastal forest mortality (Schieder & Kirwan, 2019).

Hurricanes can damage or remove fruits, flowers, and leaves for varying periods. Additionally, these disturbances may prevent mature forests from transitioning to late-successional stages and can sometimes enhance ecosystem productivity and structural diversity (Conner et al., 1989). Forests disturbed by hurricanes can aid the growth of invasive species (Bhattarai et al., 2014; Besser et al., 2019). Consequently, hurricanes cause shifts in forest structure and composition. Understanding these structural and compositional changes over time is crucial for comprehending the complex ecological effects of hurricanes on forests (Shiels et al., 2014), which can inform forest management strategies to enhance forest resistance and

resilience. Several factors affect forest vulnerability and response to hurricane damage, with wind speed and forest structure particularly being crucial (Mitchell et al., 2013; Taylor et al., 2019). In coastal regions, saltwater intrusion and storm surge flooding from hurricanes significantly impact forest stands (Bianchette et al., 2009). Numerous studies have examined forest damage and responses following major storm events in the southern United States (e.g., Gresham et al., 1991; Xi et al., 2008; Song et al., 2012; Williams et al., 2013; Zampieri et al., 2020). Further research in this area is necessary to understand the risks of damage to coastal forests from severe hurricanes.

Figure 2.2: Tree mortality patch in between the forest *(Credit: Dr. Thomas Williams*)

Tree Mortality and Biotic factors

Tree mortality is also influenced by the size and age of the tree (van Mantgem et al., 2009; Peng et al., 2011). Mortality rates often exhibit a U-shaped, bimodal pattern relative to age, with high mortality among young trees due to competition and resource limitations and among old trees due to decreased physiological efficiency and higher susceptibility to damage

(Monserud & Sterba, 1999; Thurnher et al., 2016). Characteristics of individual trees, such as size, are expected to affect the likelihood of mortality and help infer the cause of death. Analyzing vegetation dynamics through comprehensive assessments of mortality, regeneration, and growth can enhance our understanding of the ecological mechanisms regulating plant communities (Phillips et al., 2011). Differences in the resilience of various plant species to inundation and saltwater exposure can lead to significant changes in vegetation structure and composition (Williams et al., 1999; Osland, 2016), which may become apparent long before a forest transition to a marsh (Field et al., 2016). Post-hurricane studies have revealed variations in tree resistance to damage and mortality rates (Walker, 1991b; Zimmerman et al., 1994). However, predicting such damage and mortality remains challenging due to the numerous factors influencing tree responses to hurricane winds, which operate at various spatial and temporal scales. The extent of damage to a tree may be related to its size (Lugo et al., 1983; Walker, 1991b; Herbert et al., 1999) or biogeographical origin (MacDonald et al., 1991).

Different tree species vary in sensitivity to hurricane events (Zimmerman et al., 1994; Canham et al., 2010) and their recovery pathways after the disturbances (e.g., Walker, 1991b; Canham et al., 2010). Resistance and responsiveness to hurricane disturbance differ among tree species (e.g., Gresham et al., 1991; Merrens & Peart, 1992; Zimmerman et al., 1994; Everham & Brokaw, 1996). Diameter at breast height (DBH) is an important variable in estimating tree growth and health. Larson et al. (2015) studied the spatial aspects of tree mortality in young and old-growth forests. They noted significant differences in mortality among the two forest types with different DBH classes. In young forests with smaller diameter trees, noncompetitive

mortality caused by insects, disease, or wind occurred in spatially aggregated patterns, increasing spatial heterogeneity. However, the relationship between sea level rise and DBH in coastal forests has received limited attention in the literature.

The type of leaf habit, whether deciduous or evergreen, greatly affects trees' ecological and physiological characteristics, as well as their allocation of metabolic resources, which in turn influences their growth rate and ability to cope with stress (Singh & Kushwaha, 2016). Deciduous forests tend to be less vulnerable to hurricane damage than evergreen forests (Yu & Gao, 2020). Evergreen forests had a higher tendency to die during disturbances in the Amazon forest (Aleixo et al., 2019).

Tree Mortality and Climatic Factors

Instead of attributing tree deaths solely to hurricane-induced saltwater intrusion, incorporating local climatic variables into models enhances their ability to illustrate how multiple factors collectively affect tree survival. Tree survival is expected to change with ongoing climate change due to shifts in average climatic conditions and the frequency and intensity of extreme weather events (van Mantgem et al., 2009; Allen et al., 2010), as well as changes in disturbance patterns (Seidl et al., 2014; Seidl et al., 2017). Climate-related abiotic and biotic disturbances will increase in magnitude and intensity under future climate scenarios, leading to heightened tree mortality (Seidl et al., 2017). Annual temperature was a significant factor in models for six out of eight hardwood species in the United States, with higher temperatures correlating significantly with increased mortality risk (Yaussy et al., 2013).

Elevated temperatures lead to higher respiration costs, heat stress, and increased risk of cavitation, all contributing to elevated tree mortality rates (McDowell et al., 2008; Allen et al., 2010). Mortality rates in trees have been associated with climate variations such as higher warm-season temperatures (Park Williams et al., 2013), longer and more intense dry seasons (Adams et al., 2017), wetter rainy seasons (Mori & Becker, 1991), and storms (Nelson et al., 2010).

Periods of extreme heat have been linked to mortality events, suggesting that rising temperatures exacerbate the effects of hypoxia and increased salinity (Allen et al., 2021; Lovelock et al., 2017). This trend aligns with observations and predictions for upland forests, indicating that higher temperatures contribute to increased tree mortality (Williams et al., 2013). Tree mortality may increase when high temperatures coincide with reduced summer precipitation (Bigler et al., 2006). However, in the western USA, precipitation-related variables did not predict tree mortality from any cause (McNellis et al., 2021).

Tree Mortality and Hydrologic Factors

Cyclones, tsunamis, high tides, and hurricanes frequently cause damage and mortality in coastal ecosystems (Lugo, 2008; Zeng et al., 2009). While flooding and saltwater intrusion often coincide during storms, they can also vary independently across space and time (Mulholland et al., 1997; Stanturf et al., 2007; Herbert et al., 2015). The frequency of tidal cycles and storm surges determines the overall impact of salinity on coastal lands. The direction and accumulation of water flow at lower elevations affect local moisture availability. Typically, saltwater accumulates in low-lying areas during and after hurricanes, increasing soil salinity and leading to

tree mortality. The inland reach of flooding and saltwater intrusion has expanded, affecting a larger area due to hurricanes and storm surges (Poulter & Halpin, 2008; Nicholls & Cazenave, 2010; Church et al., 2013).

Tree Mortality and Topographic Factors

The topographic position, particularly the elevation relative to sea or freshwater levels, is significant as it determines the potential frequency and duration of inundation. (Fagherazzi et al., 2019; Schieder & Kirwan, 2019; Smith et al., 2021; Smith & Kirwan, 2021; Taillie et al., 2019). Topographic variability impacts tree mortality rates as the sample plots are dispersed across varied topographic factors. Sea water clogged in concave areas after the storm surge, creating pools of standing water that can lead to increased salinity in the soil and hinder vegetation growth (Figure 2.3). Several research studies have examined how sea-level rise has influenced the distribution of upland forests along coastlines in the recent past (Clark, 1986; Ross et al., 1994) and have delved into how the decline of forest stands is related to changes in elevation. While high-elevation vegetation faced more significant damage during hurricanes in the mangroves (Yu & Gao, 2020), this pattern might vary in other coastal forests.

The curvature of the land, whether it is concave or convex, plays a role in directing the flow and collection of water (Ali & Roy, 2010; Gessler et al., 2000) and is assumed to contribute to the death of trees because it can lead to the accumulation of saltwater in the forest's path. Baguskas et al. (2014) included land curvature as one of the factors in their analysis of how drought-induced tree mortality is spatially distributed across the forest, noting that negative curvature values for most trees indicate they also grow in areas with convergent flow lines;

however, detailed research on tree mortality due to the curvature of the land is yet to be done in coastal forests.

Given the strong connection between the structure of forests and their hydrology, which is particularly pronounced in the gently sloping southeastern coastal plains, it is crucial to understand how flow accumulation and runoff are generated. This understanding is important because disruptions to forest structure can occur suddenly, such as during hurricanes, or gradually over longer periods, as with climate change (Dai et al., 2011, 2013). Following the storm, collections of surge water remained in swales with inadequate drainage for several weeks after the Hurricane Hugo in 1989. (Gardner et al., 1991). Moreover, Yu & Gao (2020) emphasized the significance of drainage capacity for the recovery of coastal mangroves, suggesting that better drainage capacity reduces the likelihood and duration of inundation, causing less soil salinity and thus lowering tree mortality. Comprehensive investigations regarding tree mortality's relationship to drainage capacity in the coastal forest are very limited.

Trees near the marsh area might face higher vulnerability to various stressors, potentially resulting in increased mortality rates (Kearney et al., 2019; Osland et al., 2013; Langston et al., 2017). Soon after the storm during Hurricane Hugo, the impact was severe, with trees and shrubs near the marsh's edge experiencing extensive leaf and needle damage due to salt and wind stress, while further inland, the spatial pattern of salt stress varied, vegetation showed less signs of stress (Garnder et al., 1991). Generally, salt levels decreased further inland from the forest marsh boundary over time, and trees along this boundary and in swales between remaining beach ridges have experienced needle or leaf loss or browning (Garnder et al., 1991). However, Field et al. (2016) mentioned that there is not sufficient evidence to strongly support a

significant recent rise in mortality rates near the marsh edge when considering the distance from the marsh in New England. These contrasting results brought more attention to our understanding of tree mortality and marsh transgression in the Hobcaw Barony of South Carolina.

Figure 2.3: Seawater clogged in concave areas after the storm surge. (*Pic credit: Dr. Thomas Williams*)

Remote Sensing and Quantify Hurricane Damage

To understand how forests will react to climate change, it is important to use all available data and tools, like remote sensing technology (Allen et al., 2015). Satellite remote sensing methods have been used to detect and measure the effects of forest disturbances across local to global scales and at various time intervals (Chambers et al., 2007; Frolking et al., 2009; Mildrexler et al., 2009; Zhu et al., 2012; Baumann et al., 2014; Negrón-Juárez et al., 2014).

Remote sensing provides a unique capability to create detailed maps of tree mortality, essential for investigating potential drivers of mortality (Anderegg et al., 2016). There are two primary approaches for using remote sensing to quantify tree mortality: (1) individual tree-based mortality mapping, which requires high spatial resolution data (Clark et al., 2004; Garrity et al., 2013; Guo et al., 2007; Waser et al., 2014); and (2) stand-level mortality mapping, which utilizes moderate spatial resolution data (Bullock et al., 2020; Coops et al., 2009; Fortin et al., 2020; Fraser & Latifovic, 2005; Macomber & Woodcock, 1994; Meigs et al., 2011; Van Gunst et al., 2016). This technology enables the identification of patterns that may be challenging to detect through ground-based studies (Chambers et al., 2007) and has been used to assess hurricane damage in coastal ecosystems (Cablk et al., 1994; Ramsey et al., 1997, 1998, 2001; Boutet & Weishampel, 2003; Wang, 2004; Ayala-Silva & Twumasi, 2004; Kiage et al., 2005; Gillespie et al., 2006; Chambers et al., 2007).

In satellite remote sensing, the Leaf Area Index (LAI) is typically derived from a spectral vegetation index (SVI), which combines multiple spectral bands into a single value (Franklin et al., 1997). Forest canopy characteristics are crucial when calculating LAI, as they directly influence physiological processes and contribute to vegetation dynamics models (Fang et al., 2019). The European Space Agency (ESA) operates Sentinel-2, consisting of two satellites, Sentinel-2A and Sentinel-2B. The LAI of loblolly pine was determined using Landsat 8 satellites via the simple ratio (SR) index (Blinn et al., 2019). Compared to Landsat 8, Sentinel-2 offers an advantage in forest management due to its four 10-meter spatial resolution bands sensitive to near-infrared (NIR), red, green, and blue electromagnetic radiation (Drusch et al., 2012). LAI is critical for monitoring forest cover and is recognized as a key variable in climate

change studies (GCOS, 2021). This study analyzes changes in LAI pre- and post-Hurricane Ian to assess tree mortality in Hobcaw Barony.

Survival Analysis.

Survival analysis, originally developed for analysis in medical sciences, has been adapted as a new technique in forest mortality analysis (Harcombe, 1987; Zens & Peart, 2003). Survival analysis encompasses a variety of statistical methods used to study the timing and occurrence of events, particularly death (Berkson & Gage, 1950; Cox & Oakes, 1984; Allison, 2010). The concept of applying survival analysis to forest mortality was initially proposed by Waters (1969), but its application has mainly focused on forest inventories in even-aged plantations (Morse & Kulman, 1984; Amateis et al., 1997; Volney, 1998; Wyckoff & Clark, 2000), research plots (Reams et al., 1988; Burgman et al., 1994; Preisler & Slaughter, 1997), and stand table projections (Rose, 2004). Researchers have dedicated significant efforts to developing estimation techniques for survival and hazard functions in forest research plots (Preisler & Slaughter, 1997; Volney, 1998). Survival analysis methods are adept at incorporating time-dependent variables and handling non-normal distributions (Collett, 1994; Allison, 1995), as well as handling censored data where the exact time of an event is unknown (Collett, 1994). Types of censoring include left censoring (the event occurred before a certain time), right censoring (follow-up ended before the event occurred), and interval censoring (the event happened within a known time interval). In forestry, right and interval censoring are common due to periodic inventories. Survival in this context is described by the survival function (S(t)), the hazard function, and the cumulative hazard function. The survival function, S(t), represents the probability that a tree survives past time t and is a decreasing function between 0 and 1.

Preisler and Slaughter (1997) used the lognormal distribution to explore how tree characteristics and locations affect the survival of individual trees in stands impacted by annosum root disease. Survival analysis methods were employed to create a model for individual tree mortality to detect, monitor, and address widespread forest health concerns (Woodall et al., 2005b). This model used DBH increment as the driving variable instead of the traditional time variable. More recently, Maringer et al. (2021) used almost 100 years of data to model tree mortality using the climate data using the Kaplan Meier estimator and AFT model.

Fan et al. (2006) investigated tree survival in oak forests by combining classification and regression tree analysis with survival analysis, employing the nonparametric Kaplan-Meier estimator. Burgman et al. (1994) applied a Cox model to create background mortality models for mountain ash (*Eucalyptus regnans)* and alpine ash *(Eucalyptus delegatensis*) in Australia, with the time scale defined as the difference between the age at study entry and the age at death or current age. Survival analysis has been successfully applied in forest research (e.g., Nothdurft, 2013; Neuner et al., 2015; Neumann et al., 2017). Rose et al. (2006) also utilized survival analysis to derive the model and predict individual tree survival probability in loblolly pine plantations using data from permanent plots measured annually, with the stand's age as the driving variable. This model also considered the effects of silvicultural treatments and various tree and stand characteristics on survival. In these models, most fundamental covariates are time-dependent, such as DBH, height, basal area plotwise, relative density, etc. However, conventional logistic regression cannot incorporate time-dependent covariates;

instead, it uses the covariate values at the beginning of the interval and assumes they remain constant throughout the period.

In contrast, survival analysis techniques can manage time-dependent and interval-censored data, allowing for testing the assumption of a constant hazard function and modeling dynamic hazard functions (Collett, 2003). Survival analysis techniques are advantageous for studying key variables that change over time, such as the effects of periodic hurricanes, droughts, winds, thinning, extreme temperature periods, etc. Therefore, the likely benefits of using survival analysis techniques for modeling individual tree mortality appear substantial, and this research uses the nonparametric Kaplan-Meier estimator (Kaplan & Meier, 1958).

REFERENCES

1. Adams, H. D., Zeppel, M. J., Anderegg, W. R., Hartmann, H., Landhäusser, S. M., Tissue, D. T., ... & McDowell, N. G. (2017). A multi-species synthesis of physiological mechanisms in drought-induced tree mortality. *Nature ecology & evolution*, *1*(9), 1285-1291.
2. Aleixo, I., Norris, D., Hemerik, L., Barbosa, A., Prata, E., Costa, F., & Poorter, L. (2019). Amazonian rainforest tree mortality driven by climate and functional traits. *Nature Climate Change*, *9*(5), 384-388. https://doi.org/10.1038/s41558-019-0458-0
3. Ali, G. A., & Roy, A. G. (2010). Shopping for hydrologically representative connectivity metrics in a humid temperate forested catchment. Water Resources Research, 46(12).
4. Allen, C. D., Breshears, D. D., & McDowell, N. G. (2015). On underestimation of global vulnerability to tree mortality and forest die-off from hotter drought in the Anthropocene. *Ecosphere*, *6*(8), 1-55.
5. Allen, C. D., Macalady, A. K., Chenchouni, H., Bachelet, D., McDowell, N., Vennetier, M., ... & Cobb, N. (2010). A global overview of drought and heat-induced tree mortality reveals emerging climate change risks for forests. *Forest ecology and management*, *259*(4), 660-684.
6. Allen, K. J., Verdon-Kidd, D. C., Sippo, J. Z., & Baker, P. J. (2021). Compound climate extremes driving recent sub-continental tree mortality in northern Australia have no precedent in recent centuries. *Scientific reports*, *11*(1), 18337.
7. Allison, P. D. (2010). *Survival analysis using SAS: a practical guide*. Sas Institute.

8. Amateis, R. L., Burkhart, H. E., & Liu, J. (1997). Modeling survival in juvenile and mature loblolly pine plantations. *Forest ecology and management*, *90*(1), 51-58.
9. Anderegg, W. R., Hicke, J. A., Fisher, R. A., Allen, C. D., Aukema, J., Bentz, B., ... & Zeppel, M. (2016). Tree mortality from drought, insects, and their interactions in a changing climate. *New Phytologist*, *208*(3), 674-683.
10. Armstrong, 2022 T. Armstrong Hurricane Ian: September 230, 2022.
11. Ayala-Silva, T. and Twumasi, Y.A., 2004. Hurricane Georges and vegetation change in Puerto Rico using AVHRR satellite data. International Journal of Remote Sensing, 25, 1629-1640.
12. Baguskas, S. A., Peterson, S. H., Bookhagen, B., & Still, C. J. (2014). Evaluating spatial patterns of drought-induced tree mortality in a coastal California pine forest. *Forest Ecology and Management*, *315*, 43-53.
13. Barbier, E. B., Hacker, S. D., Kennedy, C., Koch, E. W., Stier, A. C., & Silliman, B. R. (2011). The value of estuarine and coastal ecosystem services. *Ecological monographs*, *81*(2), 169-193.
14. Baumann, M., Ozdogan, M., Wolter, P. T., Krylov, A., Vladimirova, N., & Radeloff, V. C. (2014). Landsat remote sensing of forest windfall disturbance. *Remote sensing of environment*, *143*, 171-179.
15. Berkson, J., & RP, G. (1950, May). Calculation of survival rates for cancer. In *Proceedings of the staff meetings. Mayo Clinic* (Vol. 25, No. 11, pp. 270-286).

16. Besser, J., & Stuckey, J. (2019). The Long-Term Effects of Hurricane Hugo on the Growth and Recovery of South Carolina's Coastal Temperate Forests.
17. Bhattarai, G. P., & Cronin, J. T. (2014). Hurricane activity and the large-scale pattern of spread of an invasive plant species. *PLoS One*, *9*(5), e98478.
18. Bianchette, T. A., Liu, K. B., Lam, N. N., & Kiage, L. M. (2009). Ecological impacts of Hurricane Ivan on the Gulf Coast of Alabama: A remote sensing study. *Journal of Coastal Research*, 1622-1626.
19. Bigler, C., Bräker, O. U., Bugmann, H., Dobbertin, M., & Rigling, A. (2006). Drought as an inciting mortality factor in Scots pine stands of the Valais, Switzerland. *Ecosystems*, *9*, 330-343. Stanturf, J. A., Goodrick, S. L., & Outcalt, K. W. (2007). Disturbance and coastal forests: a strategic approach to forest management in hurricane impact zones. *Forest Ecology and Management*, *250*(1-2), 119-135. doi: 10.1016/j.foreco.2007.03.015
20. Blinn, C. E., House, M. N., Wynne, R. H., Thomas, V. A., Fox, T. R., & Sumnall, M. (2019). Landsat 8 based leaf area index estimation in loblolly pine plantations. Forests, 10(3), 222.
21. Boutet, J. C., & Weishampel, J. F. (2003). Spatial pattern analysis of pre-and post-hurricane forest canopy structure in North Carolina, USA. Landscape Ecology, 18, 553-559.
22. Brokaw, N. V., & Grear, J. S. (1991). Forest structure before and after Hurricane Hugo at three elevations in the Luquillo Mountains, Puerto Rico. *Biotropica*, 386-392.

23. Bucci, L., Alaka, L., Hagen, A., Delgado, S., & Beven, J. (2023). National Hurricane Center Tropical Cyclone Report. *Hurricane Ian (AL092022)*, 1-72.

24. Bullock, E. L., Woodcock, C. E., & Olofsson, P. (2020). Monitoring tropical forest degradation using spectral unmixing and Landsat time series analysis. *Remote sensing of Environment*, *238*, 110968. https://doi.org/10.1016/j.rse.2018.11.011

25. Burgman, M. A., Incoll, W., Ades, P. K., Ferguson, I., Fletcher, T. D., & Wohlers, A. (1994). Mortality models for mountain and alpine ash. Forest Ecology and Management, 67(1-3), 319-327.

26. Cablk, M.E.; Kjerfve, B.; Michener, W.K., and Jensen, J.R., 1994. Impacts of Hurricane Hugo on a coastal forest: assessment using Landsat TM data. Geocarto International, 9, 15-24.

27. Canham, C. D., Thompson, J., Zimmerman, J. K., & Uriarte, M. (2010). Variation in susceptibility to hurricane damage as a function of storm intensity in Puerto Rican tree species. *Biotropica*, *42*(1), 87-94.

28. Chambers, J. Q., Fisher, J. I., Zeng, H., Chapman, E. L., Baker, D. B., & Hurtt, G. C. (2007). Hurricane Katrina's carbon footprint on US Gulf Coast forests. *Science*, *318*(5853), 1107-1107. https://doi.org/10.1126/science.1148913

29. Church, J. A., Clark, P. U., Cazenave, A., Gregory, J. M., Jevrejeva, S., Levermann, A., ... & Unnikrishnan, A. S. (2013). *Sea level change*. PM Cambridge University Press.

30. Clark, D. B., Castro, C. S., Alvarado, L. D. A., & Read, J. M. (2004). Quantifying mortality of tropical rain forest trees using high-spatial-resolution satellite data. *Ecology Letters*, *7*(1), 52-59. https://doi.org/10.1046/j.1461-0248.2003.00547.x
31. Clark, J. S. (1986). Coastal forest tree populations in a changing environment, southeastern Long Island, New York. *Ecological Monographs*, *56*(3), 259-277.
32. Collett, D. (1994). Modelling Survival Data in Medical Research, Chapman & Hall/CRC, Boca Raton.
33. Collett, D. (2003). Modelling survival data in medical research. Chapman and Hall/CRC Press.
34. Collett, D. (2023). *Modelling survival data in medical research*. Chapman and Hall/CRC.
35. Conner, W. H., Day, J. W., Baumann, R. H., & Randall, J. M. (1989). Influence of hurricanes on coastal ecosystems along the northern Gulf of Mexico. *Wetlands ecology and Management*, *1*, 45-56.
36. Conservancy of Southwest Florida. (2024). *Clam Bay Report: 1999-2023*. Retrieved from https://conservancy.org/wp-content/uploads/2024/04/clam-bay-report-1999-2023-compressed.pdfhttps://conservancy.org/wp-content/uploads/2024/04/clam-bay-report-1999-2023-compressed.pdf
37. Coops, N. C., Waring, R. H., Wulder, M. A., & White, J. C. (2009). Prediction and assessment of bark beetle-induced mortality of lodgepole pine using estimates of stand vigor derived from remotely sensed data. *Remote Sensing of Environment*, *113*(5), 1058-1066. https://doi.org/10.1016/j.rse.2009.01.013

38. Cox, D. R., and Oakes, D. (1984). Analysis of Survival Data, London: Chapman and Hall.

39. Dai, Z., Amatya, D. M., Sun, G., Trettin, C. C., Li, C., & Li, H. (2011). Climate variability and its impact on forest hydrology on South Carolina coastal plain, USA. *Atmosphere*, *2*(3), 330-357.

40. Dai, Z., Trettin, C. C., & Amatya, D. (2013). *Effects of climate variability on forest hydrology and carbon sequestration on the Santee Experimental Forest in coastal South Carolina*. Asheville, NC, USA: United States Department of Agriculture, Forest Service, Southern Research Station.

41. Dale, V. H., Joyce, L. A., McNulty, S., Neilson, R. P., Ayres, M. P., Flannigan, M. D., ... & Wotton, B. M. (2001). Climate change and forest disturbances: climate change can affect forests by altering the frequency, intensity, duration, and timing of fire, drought, introduced species, insect and pathogen outbreaks, hurricanes, windstorms, ice storms, or landslides. BioScience, 51(9), 723-734.

42. Doyle, T. W., Conner, W. H., Day, R. H., Krauss, K. W., & Swarzenski, C. M. (2007). Wind damage and salinity effects of Hurricanes Katrina and Rita on coastal baldcypress forests of Louisiana. Farris, GS, 163-8.

43. Drusch, M., Del Bello, U., Carlier, S., Colin, O., Fernandez, V., Gascon, F., ... & Bargellini, P. (2012). Sentinel-2: ESA's optical high-resolution mission for GMES operational services. Remote sensing of Environment, 120, 25-36.

44. Elsner, J. B., Kossin, J. P., & Jagger, T. H. (2008). The increasing intensity of the strongest tropical cyclones. *Nature*, *455*(7209), 92-95.

45. Emanuel, K., Ravela, S., Vivant, E., & Risi, C. (2006). A statistical deterministic approach to hurricane risk assessment. Bulletin of the American Meteorological Society, 87(3), 299-314.

46. Everham, E. M., & Brokaw, N. V. (1996). Forest damage and recovery from catastrophic wind. *The botanical review*, *62*, 113-185.

47. Fagherazzi, S., Anisfeld, S. C., Blum, L. K., Long, E. V., Feagin, R. A., Fernandes, A., ... & Williams, K. (2019). Sea level rise and the dynamics of the marsh-upland boundary. Frontiers in environmental science, 7, 25.

48. Fan, Z., Kabrick, J. M., & Shifley, S. R. (2006). Classification and regression tree based survival analysis in oak-dominated forests of Missouri's Ozark highlands. Canadian Journal of Forest Research, 36(7), 1740-1748.

49. Fang, H., Baret, F., Plummer, S., & Schaepman-Strub, G. (2019). An overview of global leaf area index (LAI): Methods, products, validation, and applications. *Reviews of Geophysics*, *57*(3), 739-799. https://doi.org/10.1029/2018RG000608

50. Field, C. R., Gjerdrum, C., & Elphick, C. S. (2016). Forest resistance to sea-level rise prevents landward migration of tidal marsh. *Biological Conservation*, *201*, 363-369.

51. Fortin, J. A., Cardille, J. A., & Perez, E. (2020). Multi-sensor detection of forest-cover change across 45 years in Mato Grosso, Brazil. *Remote Sensing of Environment*, *238*, 111266. https://doi.org/10.1016/j.rse.2019.111266

52. Foster, D. R. (1988). Species and stand response to catastrophic wind in central New England, USA. *The Journal of Ecology*, pp. 135-151.

53. Franklin, S. E., Lavigne, M. B., Deuling, M. J., Wulder, M. A., & Hunt Jr, E. R. (1997). Estimation of forest leaf area index using remote sensing and GIS data for modelling net primary production. International Journal of Remote Sensing, 18(16), 3459-3471.

54. Fraser, R. H., & Latifovic, R. (2005). Mapping insect-induced tree defoliation and mortality using coarse spatial resolution satellite imagery. *International Journal of Remote Sensing*, *26*(1), 193-200. https://doi.org/10.1080/01431160410001716923

55. Frolking, S., Palace, M. W., Clark, D. B., Chambers, J. Q., Shugart, H. H., & Hurtt, G. C. (2009). Forest disturbance and recovery: A general review in the context of spaceborne remote sensing of impacts on aboveground biomass and canopy structure. *Journal of Geophysical Research: Biogeosciences*, *114*(G2). https://doi.org/10.1029/2008jg000911

56. Gardner, L. R., Michener, W. K., Blood, E. R., Williams, T. M., Lipscomb, D. J., & Jefferson, W. H. (1991). Ecological impact of Hurricane Hugo—salinization of a coastal forest. *Journal of Coastal Research*, 301-317.

57. Garrity, S. R., Allen, C. D., Brumby, S. P., Gangodagamage, C., McDowell, N. G., & Cai, D. M. (2013). Quantifying tree mortality in a mixed species woodland using multitemporal high spatial resolution satellite imagery. *Remote Sensing of Environment*, *129*, 54-65. https://doi.org/10.1016/j.rse.2012.10.029

58. GCOS. (2021). The Status of the Global Climate Observing System 2021: The GCOS Status Report (GCOS-240), pub WMO, Geneva.

59. Gessler, P. E., Chadwick, O. A., Chamran, F., Althouse, L., & Holmes, K. (2000). Modeling soil–landscape and ecosystem properties using terrain attributes. Soil Science Society of America Journal, 64(6), 2046-2056.

60. Gillespie, T. W., Zutta, B. R., Early, M. K., & Saatchi, S. (2006). Predicting and quantifying the structure of tropical dry forests in South Florida and the Neotropics using spaceborne imagery. Global Ecology and Biogeography, 15(3), 225-236.

61. Gresham, C. A., Williams, T. M., & Lipscomb, D. J. (1991). Hurricane Hugo wind damage to southeastern US coastal forest tree species. *Biotropica*, 420-426.

62. Guo, Q., Kelly, M., Gong, P., & Liu, D. (2007). An object-based classification approach in mapping tree mortality using high spatial resolution imagery. *GIScience & Remote Sensing*, *44*(1), 24-47. https://doi.org/10.2747/1548-1603.44.1.24

63. Harcombe, P. A. (1987). Tree life tables. *Bioscience*, *37*(8), 557-568.

64. Herbert, E. R., Boon, P., Burgin, A. J., Neubauer, S. C., Franklin, R. B., Ardón, M., ... & Gell, P. (2015). A global perspective on wetland salinization: ecological consequences of a growing threat to freshwater wetlands. Ecosphere, 6(10), 1-43.

65. Herbert, R. A. (1999). Nitrogen cycling in coastal marine ecosystems. *FEMS microbiology reviews*, *23*(5), 563-590.

66. Hook, D. D., Buford, M. A., & Williams, T. M. (1991). Impact of Hurricane Hugo on the South Carolina coastal plain forest. *Journal of Coastal Research*, 291-300.

67. Intergovernmental Panel on Climate Change (IPCC). (2012). *Managing the risks of extreme events and disasters to advance climate change adaptation* (p. 582). Geneva,

Switzerland: IPCC. Retrieved from http://ipcc-wg2.gov/SREX/ (accessed on January 15, 2022).

68. Jevrejeva, S., Jackson, L. P., Riva, R. E., Grinsted, A., & Moore, J. C. (2016). Coastal sea level rise with warming above 2 C. *Proceedings of the National Academy of Sciences*, *113*(47), 13342-13347.
69. Kaplan, E. L., & Meier, P. (1958). Nonparametric estimation from incomplete observations. *Journal of the American statistical association*, *53*(282), 457-481
70. Kearney, W. S., Fernandes, A., & Fagherazzi, S. (2019). Sea-level rise and storm surges structure coastal forests into persistence and regeneration niches. *PloS one*, *14*(5), e0215977.
71. Kiage, L.M.; Walker, N.D.; Balasubramanian, S.; Babin, A., and Barras, J., 2005. Applications of Radarsat-1 synthetic aperture radar imagery to assess hurricane-related flooding of coastal Louisiana. International Journal of Remote Sensing, 26, 5359-5380.
72. Kirwan, M. L., & Gedan, K. B. (2019). Sea-level driven land conversion and the formation of ghost forests. *Nature Climate Change*, *9*(6), 450-457.
73. Kirwan, M. L., Temmerman, S., Skeehan, E. E., Guntenspergen, G. R., & Fagherazzi, S. (2016). Overestimation of marsh vulnerability to sea level rise. *Nature Climate Change*, *6*(3), 253-260.
74. Knutson, T. R., McBride, J. L., Chan, J., Emanuel, K., Holland, G., Landsea, C., ... & Sugi, M. (2010). Tropical cyclones and climate change. *Nature geoscience*, *3*(3), 157-163.

75. Kossin, J. P., Knapp, K. R., Olander, T. L., & Velden, C. S. (2020). Global increase in major tropical cyclone exceedance probability over the past four decades. *Proceedings of the National Academy of Sciences*, *117*(22), 11975-11980.

76. Langston, A. K., Kaplan, D. A., & Putz, F. E. (2017). A casualty of climate change? Loss of freshwater forest islands on Florida's Gulf Coast. *Global Change Biology*, *23*(12), 5383-5397. https://doi.org/10.1111/gcb.13805

77. Larson, A. J., Lutz, J. A., Donato, D. C., Freund, J. A., Swanson, M. E., HilleRisLambers, J., ... & Franklin, J. F. (2015). Spatial aspects of tree mortality strongly differ between young and old-growth forests. https://doi.org/10.1890/15-0628.1

78. Lin, N., Emanuel, K., Oppenheimer, M., & Vanmarcke, E. (2012). Physically based assessment of hurricane surge threat under climate change. *Nature Climate Change*, *2*(6), 462-467.

79. Lotze, H. K., Lenihan, H. S., Bourque, B. J., Bradbury, R. H., Cooke, R. G., Kay, M. C., ... & Jackson, J. B. (2006). Depletion, degradation, and recovery potential of estuaries and coastal seas. *Science*, *312*(5781), 1806-1809.

80. Lovelock, C. E., Feller, I. C., Reef, R., Hickey, S., & Ball, M. C. (2017). Mangrove dieback during fluctuating sea levels. Sci. Rep. 7, 1680.

81. Lugo, A. E. (2008). Visible and invisible effects of hurricanes on forest ecosystems: an international review. *Austral Ecology*, *33*(4), 368-398.

82. Macomber, S. A., & Woodcock, C. E. (1994). Mapping and monitoring conifer mortality using remote sensing in the Lake Tahoe Basin. *Remote sensing of environment*, *50*(3), 255-266. https://doi.org/10.1016/0034-4257(94)90075-2

83. McDowell, N., Pockman, W. T., Allen, C. D., Breshears, D. D., Cobb, N., Kolb, T., ... & Yepez, E. A. (2008). Mechanisms of plant survival and mortality during drought: why do some plants survive while others succumb to drought?. *New phytologist*, *178*(4), 719-739.

84. McNellis, B. E., Smith, A. M., Hudak, A. T., & Strand, E. K. (2021). Tree mortality in western US forests forecasted using forest inventory and Random Forest classification. *Ecosphere*, *12*(3), e03419.

85. Meigs, G. W., Kennedy, R. E., & Cohen, W. B. (2011). A Landsat time series approach to characterize bark beetle and defoliator impacts on tree mortality and surface fuels in conifer forests. *Remote Sensing of Environment*, *115*(12), 3707-3718. https://doi.org/10.1016/j.rse.2011.09.009

86. Merrens, E. J., & Peart, D. R. (1992). Effects of hurricane damage on individual growth and stand structure in a hardwood forest in New Hampshire, USA. *Journal of Ecology*, 787-795.

87. Mickler, R. A., Birdsey, R. A., & Hom, J. (Eds.). (2012). *Responses of northern US forests to environmental change* (Vol. 139). Springer Science & Business Media.

88. Mildrexler, D. J., Zhao, M., & Running, S. W. (2009). Testing a MODIS global disturbance index across North America. *Remote Sensing of Environment*, *113*(10), 2103-2117.

89. Mitchell, S. J. (2013). Wind as a natural disturbance agent in forests: a synthesis. *Forestry*, *86*(2), 147-157.

90. Mori, S. A., & Becker, P. (1991). Flooding affects survival of Lecythidaceae in terra firme forest near Manaus, Brazil. *Biotropica*, *23*(1), 87-90.

91. Morse, B. W., & Kulman, H. M. (1984). Plantation white spruce mortality: estimates based on aerial photography and analysis using a life-table format. *Canadian Journal of Forest Research*, *14*(2), 195-200.

92. Mudd, L., Wang, Y., Letchford, C., & Rosowsky, D. (2014). Assessing climate change impact on the US East Coast hurricane hazard: temperature, frequency, and track. *Natural Hazards Review*, *15*(3), 04014001.

93. Mulholland, P. J., Best, G. R., Coutant, C. C., Hornberger, G. M., Meyer, J. L., Robinson, P. J., ... & Wetzel, R. G. (1997). Effects of climate change on freshwater ecosystems of the south-eastern United States and the Gulf Coast of Mexico. Hydrological Processes, 11(8), 949-970.

94. National Hurricane Center. (2021). *Tropical Cyclone Report: Hurricane Isaias (AL092020), 28 July – 4 August 2020*. National Oceanic and Atmospheric Administration. Retrieved from https://www.nhc.noaa.gov/data/tcr/AL092020_Isaias.pdf

95. National Oceanic and Atmospheric Administration. (2006). *Service assessment: Hurricane Charley, August 9-15, 2004*. National Weather Service. Retrieved from https://www.weather.gov/media/publications/assessments/Charley06.pdf

96. National Oceanic and Atmospheric Administration. (2019). *Atlantic high-activity eras: What does it mean for hurricane season?*

97. National Weather Service (n.d.-a). *Hurricane Hugo - September 21-22, 1989*. NOAA. Retrieved July 1, 2024, from https://www.weather.gov/chs/HurricaneHugo-Sep1989

98. National Weather Service. (n.d.-b). *1999 Irene*. NOAA. Retrieved July 1, 2024, from https://www.weather.gov/mfl/1999_irene

99. National Weather Service. (n.d.-c). Hurricane Floyd review: September 16, 1999. NOAA's National Weather Service Weather Forecast Office, Newport/Morehead City, NC. Retrieved July 1, 2024, from https://www.weather.gov/mhx/Sep161999EventReview

100. National Weather Service. (n.d.-d). *Hurricane Gaston - August 29, 2004*. National Oceanic and Atmospheric Administration. Retrieved July 1, 2024, from https://www.weather.gov/chs/HurricaneGaston-Aug2004

101. National Weather Service. (n.d.-e). *Hurricane Dorian: September 5-6, 2019*. National Oceanic and Atmospheric Administration. Retrieved July 1, 2024, from https://www.weather.gov/ilm/Dorian#:~:text=Hurricane%20Dorian%20was%20the%20strongest,surge%20greater%20than%2018%20feet

102. Negrón-Juárez, R., Baker, D. B., Chambers, J. Q., Hurtt, G. C., & Goosem, S. (2014). Multi-scale sensitivity of Landsat and MODIS to forest disturbance associated with tropical cyclones. *Remote Sensing of Environment*, *140*, 679-689. https://doi.org/10.1016/j.rse.2013.09.028

103. Nelson, R., Kokic, P., Crimp, S., Martin, P., Meinke, H., Howden, S. M., ... & Nidumolu, U. (2010). The vulnerability of Australian rural communities to climate variability and change: Part II—Integrating impacts with adaptive capacity. *Environmental Science & Policy*, *13*(1), 18-27.

104. Neumann, M., Mues, V., Moreno, A., Hasenauer, H., & Seidl, R. (2017). Climate variability drives recent tree mortality in Europe. Global change biology, 23(11), 4788-4797.

105. Neuner, S., Albrecht, A., Cullmann, D., Engels, F., Griess, V. C., Hahn, W. A., ... & Knoke, T. (2015). Survival of Norway spruce remains higher in mixed stands under a dryer and warmer climate. Global change biology, 21(2), 935-946.

106. Nicholls, R. J., & Cazenave, A. (2010). Sea-level rise and its impact on coastal zones. *science*, *328*(5985), 1517-1520.

107. NOAA (National Centers for Environmental Information), 2022. Monthly national climate report for 2022. https://www.ncei.noaa.gov/access/monitoring/monthlyreport/national/202209/supplemental/page-5 (accessed 29 March 2023).

108. NOAA [National Oceanic and Atmospheric Administration]. 2020 Atlantic Hurricane Season takes infamous top spot for busiest on record 2020 [cited 2020 November 11]. Available from: https://www.noaa.gov/news/2020-atlantic-hurricane-season-takes-infamous-top-spot-for-busiest-on-record.

109. Nothdurft, A. (2013). Spatio-temporal prediction of tree mortality based on long-term sample plots, climate change scenarios and parametric frailty modeling. Forest ecology and management, 291, 43-54.

110. Osland, M. J., Enwright, N. M., Day, R. H., Gabler, C. A., Stagg, C. L., & Grace, J. B. (2016). Beyond just sea-level rise: Considering macroclimatic drivers within coastal wetland vulnerability assessments to climate change. *Global Change Biology*, *22*(1), 1-11.

111. Osland, M. J., Enwright, N., Day, R. H., & Doyle, T. W. (2013). Winter climate change and coastal wetland foundation species: salt marshes vs. mangrove forests in the southeastern United States. *Global change biology*, *19*(5), 1482-1494. https://doi.org/10.1111/gcb.12126

112. Pachauri, R. K., Allen, M. R., Barros, V. R., Broome, J., Cramer, W., Christ, R., ... & van Ypserle, J. P. (2014). Climate change 2014: synthesis report. Contribution of Working Groups I, II and III to the fifth assessment report of the Intergovernmental Panel on Climate Change (p. 151). Ipcc.

113. Park Williams, A., Allen, C. D., Macalady, A. K., Griffin, D., Woodhouse, C. A., Meko, D. M., ... & McDowell, N. G. (2013). Temperature as a potent driver of regional forest drought stress and tree mortality. *Nature climate change*, *3*(3), 292-297.

114. Parker, S., & Crichton, G. (2011). *Effects of global climate change at the Virginia Coast Reserve*. The Nature Conservancy in Virginia: Report from the Virginia Coast Reserve climate change threats workshop.

115. Penfound, W. T., & Hathaway, E. S. (1938). Plant communities in the marshlands of southeastern Louisiana. *Ecological Monographs*, 4-56.

116. Peng, C., Ma, Z., Lei, X., Zhu, Q., Chen, H., Wang, W., ... & Zhou, X. (2011). A drought-induced pervasive increase in tree mortality across Canada's boreal forests. *Nature climate change*, *1*(9), 467-471.

117. Phillips, O. L., Lewis, S. L., Baker, T. R., & Malhi, Y. (2011). The response of South American tropical forests to recent atmospheric changes. *Tropical Rainforest Responses to Climatic Change*, 343-358.

118. Poulter, B., & Halpin, P. N. (2008). Raster modelling of coastal flooding from sea-level rise. *International Journal of Geographical Information Science*, *22*(2), 167-182.

119. Preisler, H. K., & Slaughter, G. W. (1997). A stochastic model for tree survival in stands affected by annosum root disease. Forest science, 43(1), 78-86.

120. Ramsey, E.W.; Chappell, D.K., and Baldwin, D., 1997. AVHRR imagery used to identify Hurricane Andrew damage in a forested wetland in Louisiana. Photogrammetric Engineering and Remote Sensing, 63, 293-297.

121. Ramsey, E.W.; Chappell, D.K.; Jacobs, D.M.; Sapkota, S.K., and Nelson, G.A., 1998. Resource management of forested wetlands: hurricane impact and recovery mapped by combining Landsat TM and NOAA AVHRR data. Photogrammetric Engineering and Remote Sensing, 64, 733- 738.

122. Ramsey, E.W.; Hodgson, M.E.; Sapkota, S.K., and Nelson, G.A., 2001. Forest impact estimated with NOAA AVHRR and Landsat TM data related to an empirical hurricane wind- field distribution. *Remote Sensing of Environment*, 11, 279- 292.

123. Reams, G. A., Brann, T. B., & Halteman, W. A. (1988). A nonparametric survival model for balsam fir during a spruce budworm outbreak. Canadian Journal of Forest Research, 18(6), 789-795.

124. Robichaud, A., & Begin, Y. (1997). The effects of storms and sea-level rise on a coastal forest margin in New Brunswick, eastern Canada. *Journal of Coastal Research*, 429-439.

125. Rose Jr, C. E., Clutter, M. L., Shiver, B. D., Hall, D. B., & Borders, B. (2004). A generalized methodology for developing whole-stand survival models. Forest Science, 50(5), 686-695.

126. Rose Jr, C. E., Hall, D. B., Shiver, B. D., Clutter, M. L., & Borders, B. (2006). A multilevel approach to individual tree survival prediction. *Forest Science*, 52(1), 31-43.

127. Ross, M. S., O'Brien, J. J., & da Silveira Lobo Sternberg, L. (1994). Sea-level rise and the reduction in pine forests in the Florida Keys. *Ecological Applications*, *4*(1), 144-156.

128. Runkle, J., Svendsen, E. R., Hamann, M., Kwok, R. K., & Pearce, J. (2018). Population health adaptation approaches to the increasing severity and frequency of weather-related disasters resulting from our changing climate: a literature review and

application to Charleston, South Carolina. Current environmental health reports, 5, 439-452.

129. Schieder, N. W., & Kirwan, M. L. (2019). Sea-level driven acceleration in coastal forest retreat. *Geology*, *47*(12), 1151-1155.

130. Seidl, R., Schelhaas, M. J., Rammer, W., & Verkerk, P. J. (2014). Increasing forest disturbances in Europe and their impact on carbon storage. Nature climate change, 4(9), 806-810.

131. Seidl, R., Thom, D., Kautz, M., Martin-Benito, D., Peltoniemi, M., Vacchiano, G., ... & Reyer, C. P. (2017). Forest disturbances under climate change. Nature climate change, 7(6), 395-402.

132. Shiels, A. B., González, G., & Willig, M. R. (2014). Responses to canopy loss and debris deposition in a tropical forest ecosystem: Synthesis from an experimental manipulation simulating effects of hurricane disturbance. *Forest Ecology and Management*, *332*, 124-133.

133. Shreve, F., Chrysler, M. A., Blodgett, F. H., & Besley, F. W. (1910). *The plant life of Maryland* (Vol. 3). Johns Hopkins Press.

134. Singh, K. P., & Kushwaha, C. P. (2016). Deciduousness in tropical trees and its potential as indicator of climate change: A review. *Ecological indicators*, *69*, 699-706.

135. Sippo, J. Z., Lovelock, C. E., Santos, I. R., Sanders, C. J., & Maher, D. T. (2018). Mangrove mortality in a changing climate: An overview. *Estuarine, Coastal and Shelf Science*, *215*, 241-249. https://doi.org/10.1016/j.ecss.2018.10.011

136. Smith, A. J., & Kirwan, M. L. (2021). Sea level-driven marsh migration results in rapid net loss of carbon. Geophysical Research Letters, 48(13), e2021GL092420.

137. Smith, D. M., Eade, R., Dunstone, N. J., Fereday, D., Murphy, J. M., Pohlmann, H., & Scaife, A. A. (2010). Skilful multi-year predictions of Atlantic hurricane frequency. *Nature geoscience*, *3*(12), 846-849.

138. Smith, I. M., Fiorino, G. E., Grabas, G. P., & Wilcox, D. A. (2021). Wetland vegetation response to record-high Lake Ontario water levels. Journal of Great Lakes Research, 47(1), 160-167.

139. Song, B., Gresham, C. A., Trettin, C. C., & Williams, T. M. (2012). Recovery of coastal plain forests from Hurricane Hugo in South Carolina, USA, fourteen years after the storm. *Tree For Sci Biotechnol*, *6*(Special Issue 1), 60-8.

140. Springer, B., & Mims, T. (2004). Hurricane Ivan timber damage assessment. *Alabama's TREASURED Forests*, 7–9.

141. Taillie, P. J., Moorman, C. E., Poulter, B., Ardón, M., & Emanuel, R. E. (2019). Decadal-scale vegetation change driven by salinity at leading edge of rising sea level. Ecosystems, 22(8), 1918-1930.

142. Taylor, A. R., Dracup, E., MacLean, D. A., Boulanger, Y., & Endicott, S. (2019). Forest structure more important than topography in determining windthrow during Hurricane Juan in Canada's Acadian Forest. *Forest Ecology and Management*, *434*, 255-263.

143. Van Gunst, K. J., Weisberg, P. J., Yang, J., & Fan, Y. (2016). Do denser forests have greater risk of tree mortality: A remote sensing analysis of density-dependent

forest mortality. *Forest Ecology and Management*, *359*, 19-32. https://doi.org/10.1016/j.foreco.2015.09.032

144. Van Mantgem, P. J., Stephenson, N. L., Byrne, J. C., Daniels, L. D., Franklin, J. F., Fulé, P. Z., ... & Veblen, T. T. (2009). Widespread increase of tree mortality rates in the western United States. Science, 323(5913), 521-524.

145. Vermeer, M., & Rahmstorf, S. (2009). Global sea level linked to global temperature. *Proceedings of the national academy of sciences*, *106*(51), 21527-21532.

146. Volney, W. J. A. (1998). Ten-year tree mortality following a jack pine budworm outbreak in Saskatchewan. Canadian journal of forest research, 28(12), 1784-1793.

147. Walker, L. R. (1991a). Summary of the effects of Caribbean hurricanes on vegetation. *Biotropica*, *23*(4), 442-447.

148. Walker, L. R. (1991b). Tree damage and recovery from Hurricane Hugo in Luquillo experimental forest, Puerto Rico. *Biotropica*, 379-385.

149. Wang, W., McDowell, N. G., Ward, N. D., Indivero, J., Gunn, C., & Bailey, V. L. (2019). Constrained tree growth and gas exchange of seawater-exposed forests in the Pacific Northwest, USA. *Journal of Ecology*, *107*(6), 2541-2552.

150. Wang, Y. (2004). Using Landsat 7 TM data acquired days after a flood event to delineate the maximum flood extent on a coastal floodplain. International Journal of Remote Sensing, 25(5), 959-974.

151. Waser, L. T., Küchler, M., Jütte, K., & Stampfer, T. (2014). Evaluating the potential of WorldView-2 data to classify tree species and different levels of ash mortality. *Remote Sensing*, *6*(5), 4515-4545. https://doi.org/10.3390/rs6054515

152. Williams, A. P., Allen, C. D., Macalady, A. K., Griffin, D., Woodhouse, C. A., Meko, D. M., ... & McDowell, N. G. (2013). Temperature as a potent driver of regional forest drought stress and tree mortality. Nat Clim Chang 3 (3): 292–297.

153. Williams, K., Ewel, K. C., Stumpf, R. P., Putz, F. E., & Workman, T. W. (1999). Sea-level rise and coastal forest retreat on the west coast of Florida, USA. *Ecology*, *80*(6), 2045-2063.

154. Williams, T. M., Song, B., Trettin, C. C., & Gresham, C. A. (2013). A review of spatial aspects of forest damage and recovery on the South Carolina coast following hurricane Hugo. *Journal of Geography & Natural Disasters*, *3*(2), 2167-0587.

155. Woodall, C.W., Grambsch, P.L., Thomas, W., Moser, W.K., 2005b. Survival analysis for a large scale forest health issue: Missouri oak decline. Environmental Monitoring and Assessment 108, 295-307.

156. Wyckoff, P. H., & Clark, J. S. (2000). Predicting tree mortality from diameter growth: a comparison of maximum likelihood and Bayesian approaches. Canadian Journal of Forest Research, 30(1), 156-167.

157. Xi, W., Peet, R. K., & Urban, D. L. (2008). Changes in forest structure, species diversity and spatial pattern following hurricane disturbance in a Piedmont North Carolina forest, USA. *Journal of Plant Ecology*, *1*(1), 43-57.

158. Yaussy, D. A., Iverson, L. R., & Matthews, S. N. (2013). Competition and climate affects US hardwood-forest tree mortality. *Forest Science*, *59*(4), 416-430.

159. Yu, M., & Gao, Q. (2020). Topography, drainage capability, and legacy of drought differentiate tropical ecosystem response to and recovery from major hurricanes. *Environmental Research Letters*, *15*(10), 104046.

160. Zampieri, N. E., Pau, S., & Okamoto, D. K. (2020). The impact of Hurricane Michael on longleaf pine habitats in Florida. *Scientific Reports*, *10*(1), 8483.

161. Zeng, H., Chambers, J. Q., Negrón-Juárez, R. I., Hurtt, G. C., Baker, D. B., & Powell, M. D. (2009). Impacts of tropical cyclones on US forest tree mortality and carbon flux from 1851 to 2000. *Proceedings of the National Academy of Sciences*, *106*(19), 7888-7892.

162. Zens, M. S., & Peart, D. R. (2003). Dealing with death data: individual hazards, mortality and bias. *Trends in Ecology & Evolution*, *18*(7), 366-373.

163. Zhu, Z., Woodcock, C. E., & Olofsson, P. (2012). Continuous monitoring of forest disturbance using all available Landsat imagery. *Remote sensing of environment*, *122*, 75-91.

164. Zimmerman, J. K., Everham III, E. M., Waide, R. B., Lodge, D. J., Taylor, C. M., & Brokaw, N. V. (1994). Responses of tree species to hurricane winds in subtropical wet forest in Puerto Rico: implications for tropical tree life histories. *Journal of ecology*, 911-922.

CHAPTER 3

SPATIAL PATTERNS OF TREE MORTALITY IN A COASTAL FOREST OF HOBCAW BARONY AFTER HURRICANE HUGO.

Abstract

Remote sensing technologies like satellite imagery or aerial photographs can be used to elucidate the spatial patterns of tree mortality resulting from hurricanes. This project assessed topographic factors to explain the patterns of tree mortality. Post-hurricane aerial photographs taken in October 1990 were processed in Arc GIS to derive the tree mortality areas map after Hurricane Hugo. Topographic variables such as elevation, proximity to the marsh, drainage capacity and curvature of the land data were acquired. Analysis and visualization showed higher mortality in concave areas close to the marsh at approximately 1-2m elevation and 120-180m far from streams. Variables were used to derive the model using the logistic regression analysis. All variables (water depth, curvature, distance from marsh and streams) were significant in the model, and the model has moderate accuracy. The predicted map for tree mortality after Hurricane Ian was derived based on the model, and the actual tree mortality map was generated using the Leaf Area Index change. Two maps were compared visually, and the model underestimated the mortality. Understanding how various spatial factors interact and contribute to tree mortality will enhance our capacity to evaluate the susceptibility of coastal forests to mortality due to periodic hurricane events and how they shape the growth and resilience of coastal forests.

Introduction

Hurricane Hugo of Category 4 came ashore across Sullivan's Island, South Carolina, at midnight Eastern Standard Time (EST) on September 21, 1989 (Hook et al., 1991). Supported by observation of watermarks in the field, Schuck-Kolben (1990) inferred that the Hurricane Hugo surge was up to 3.3 meters (m) above mean sea level at the North Inlet of the Hobcaw Barony. Further flood debris was discovered in the forest area at 3-4 m heights, indicating a tidal surge up to that height (Gardner et al., 1991). This enabled seawater to penetrate the nearby coastal woodland up to approximately the 3.0-m elevation mark, and the water surge passed through almost 1.5 kilometers (km) into the forest from the forest marsh edge (Gardner et al., 1992).

A range of elements, including terrain characteristics such as elevation, topography, and the arrangement of drainage systems, can create variations in stress levels due to tidal surges across a landscape and subsequent mortality of trees (Gitlin et al., 2006). Several studies examined how sea-level rise influenced the distribution of upland forests along coastlines (Clark, 1986; Ross et al., 1994) and delved into how the decline of forest stands is related to changes in elevation. While high-elevation vegetation faced more significant damage during hurricanes (Yu & Gao, 2020), this pattern might vary within coastal forests.

The curvature of the land, whether it is concave or convex, plays a role in directing the flow and collection of water (Ali & Roy, 2010; Gessler et al., 2000) and is assumed to contribute to the death of trees because it can lead to the accumulation of saltwater in the forest soil. Baguskas et al. (2014) included land curvature as one of the factors in their analysis of

how drought-induced tree mortality is spatially distributed across the forest; however, detailed research on tree mortality due to the curvature of the land is yet to be done in coastal forests.

Water flows downhill and accumulates in areas with lower elevations, indicating higher moisture availability in those areas. Typically, saltwater tends to accumulate in the flow accumulation area longer during and after storm surges following hurricanes, which can lead to tree mortality due to increased soil salinity. Following the storm, collections of surge water remained in swales with inadequate drainage for several weeks after Hurricane Hugo in 1989 (Gardner et al., 1991).

However, Yu & Gao (2020) emphasized the significance of drainage capacity for the recovery of coastal mangroves, suggesting that better drainage capacity reduces the likelihood and duration of inundation, causing less soil salinity and thus lowering tree mortality. Comprehensive investigations regarding tree mortality's relationship to drainage capacity in the coastal forest are very limited. Given the strong connection between the structure of forests and their hydrology, which is particularly pronounced in the gently sloping southeastern coastal plains, it is crucial to understand how flow accumulation and runoff are generated. This understanding is important because disruptions to forest structure can occur suddenly, such as during hurricanes, or gradually over longer periods, as with climate change (Dai et al., 2011; Dai et al., 2013).

Trees near the marsh area might face higher vulnerability to various stressors, potentially resulting in increased mortality rates (Kearney et al., 2019; Langston et al., 2017). Soon after the storm during Hurricane Hugo, the impact was severe, with trees and shrubs near the marsh's edge experiencing extensive leaf and needle damage due to salt and wind stress,

while further inland, the spatial pattern of salt stress varied, vegetation showed fewer signs of stress (Garnder et al., 1991). Generally, salt levels decreased further inland from the forest marsh boundary over time, and trees along this boundary and in swales between remaining beach ridges have experienced needle or leaf loss or browning (Garnder et al., 1991). However, Field et al. (2016) mentioned that there is not sufficient evidence to strongly support a significant recent rise in mortality rates near the marsh edge when considering the distance from the marsh in New England. These contrasting results brought attention to our understanding of tree mortality and marsh transgression in the Hobcaw Barony of South Carolina.

The field of forestry has a rich history of utilizing aerial photography to support inventory programs (Thompson et al., 2007). Remote sensing techniques can be harnessed to detect and track changes in forests as a valuable tool for assessing the spatiotemporal variations in mortality events (Neumann et al., 2017). Satellite remote sensing methodologies offer the capacity to quantify the impacts of forest disturbances on various scales, ranging from local to global, and at varying temporal resolutions (Chambers et al., 2007; Zhu et al., 2012; Negrón-Juárez et al., 2010). Many remote sensing damage assessments depend on variations in vegetation indices such as the normalized difference vegetative index (NDVI) (Hu et al., 2018; Lee et al., 2008; Parker et al., 2018), enhanced vegetation index (EVI) (Rossi et al., 2013), Leaf Area Index (LAI) (Bright et al., 2013; Wang et al., 2012; Rao et al., 2019), and normalized difference infrared index (NDII) (Wang et al., 2010). These indices are advantageous because they are extensively tested, easily accessible, and do not require external data such as field plots for analysis. Leaf Area Index (LAI) represents the proportion of green

leaf area to ground area. Cohrs et al. (2020) utilized Sentinel-2A imagery to determine the LAI for pine plantations in the southeastern United States.

Knowledge regarding the occurrence and patterns of tree mortality events caused by sea level rise and hurricanes in coastal forests is very limited. In this study, we used multispectral images captured one year after Hurricane Hugo to quantify the spatial extent of tree mortality in forests in Hobcaw Barony and analyze landscape-scale variables that affect the spatial patterns in forest disturbance. Moreover, we also used the fragment LAI index from Sentinel-2A to derive the tree mortality map after Hurricane Ian using the change in LAI in pre and post-hurricane Ian in 2022.

We aim to derive a model to illustrate the relationship between patterns of tree mortality and topographic variables such as elevation, curvature, drainage capacity, and proximity to the marsh. The major objectives of this study are to a) map the spatial pattern of tree mortality observed after Hurricane Hugo, b) map the tree mortality areas after Hurricane Hugo in relation to variables such as concavity of land, drainage capacity, distance to the marsh, and elevation, c) derive a model and predict the tree mortality areas for Hurricane Ian, and d) to derive and compare Hurricane Ian 2022 mortality maps using satellite imagery and model predictions. The findings have implications for predicting vegetation response patterns to future disturbances and highlight the need for targeted management interventions to mitigate the effects.

Methodology

Study area

Hobcaw Barony has an area of around 6800 hectares and is situated at the southernmost point of the Waccamaw peninsula, north of Georgetown, South Carolina (33.33° N latitude,

79.20° W longitude) (Figure 3.1). The Hobcaw Barony is known for its tidal freshwater forested wetlands, which play a crucial ecological role in the southeastern United States (Conner et al., 2007). There are approximately 129 flora species found across 114 genera in 48 families (Stalter et al., 2018). The existence of nearby salt marshes impacts the distribution of salt marsh vascular plants in the clamshell middens of the tidal marsh (Stalter et al., 2018). Loblolly pine (*Pinus taeda),* longleaf pine (*Pinus palustris*)*,* bald cypress (*Taxodium distichum*)*,* swamp tupelo (*Nyssa biflora*)*,* Southern live oak (*Quercus virginiana*)*,* pond pine (*Pinus serotina*)*,* laurel oak (*Quercus laurifolia*)*,* water oak (*Quercus nigra*)*,* and others are the major tree species found in the forest. Cypress and pine hardwood are present near the North Inlet salt marsh from where the saltwater intruded into the forest during Hurricane Hugo. During Hurricane Hugo in 1989, severe damage was reported for pond pine, laurel oak, water oak, loblolly pine, and longleaf pine (Heaton et al., 2023). Hobcaw Barony is approximately 5.5 km inland from the coastline and lies 72 km east of the point of landfall of the center of Hurricane Hugo.

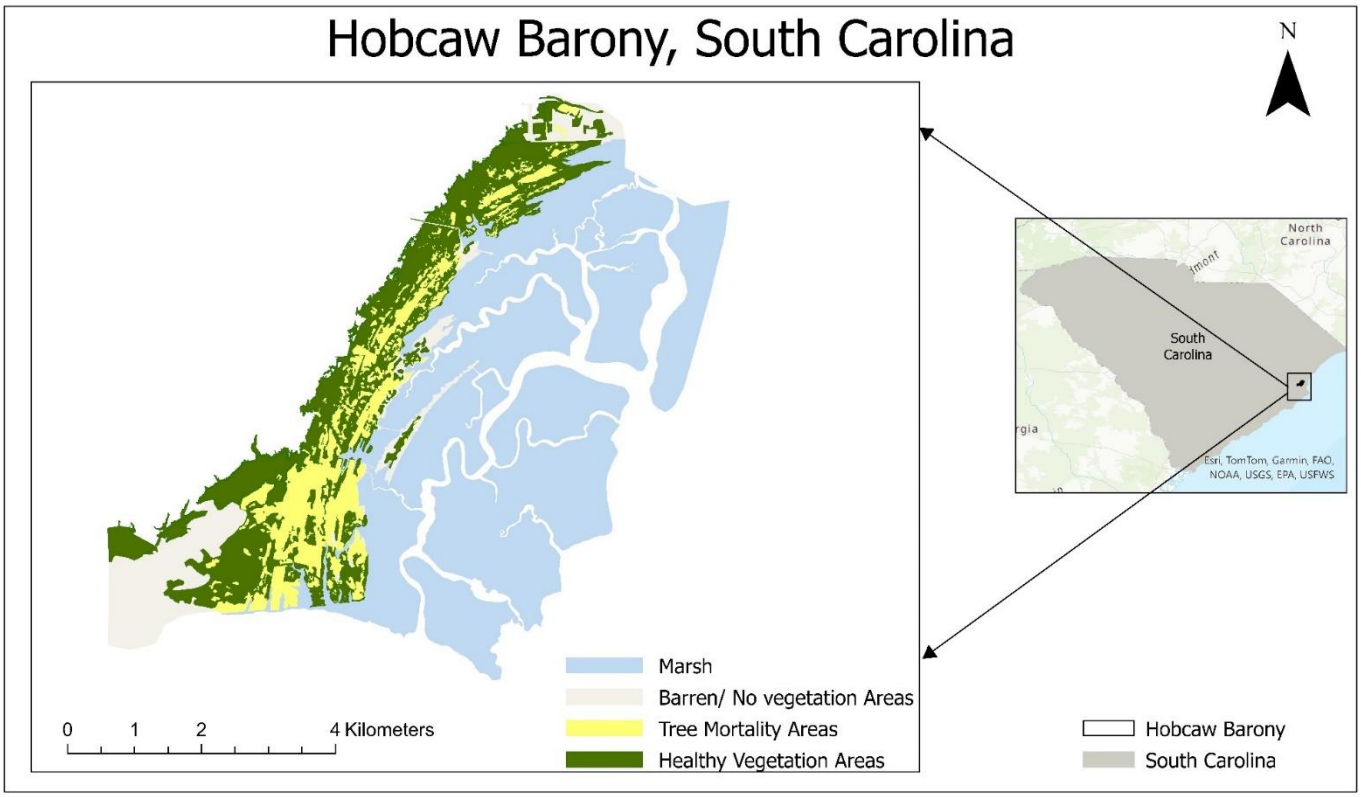

Figure 3.1: Study area map showing part of Hobcaw Barony Forest, South Carolina.

Datasets

We utilized multiple data sources to measure the spatial differences and the scale of tree mortality in the coastal regions of Hobcaw Barony. Variables used to explain the spatial patterns of tree mortality were derived from remotely sensed data. A digital elevation model (DEM) was obtained from the United States Geological Survey (USGS) and clipped to the area of interest. The concavity of the land was derived from the DEM data. The marsh area was demarcated manually using National Agriculture Imagery Program (NAIP) imagery.

ArcGIS Pro 10.2.1 was used to prepare the tree mortality maps and derive the variables for the data analysis. Aerial photographs taken one year after Hurricane Hugo in 1990 were georeferenced with the 2005 NAIP Imagery using the ground control points (GCP). GCPs were chosen from fixed and consistent features that remain unchanged over time, such as road intersections, marsh boundaries, rivers, stream channels, and buildings. After georeferencing, polygons were manually created for each image's mortality and healthy vegetation areas. Polygon contained multiple trees within them, and in each image, dying trees had a yellow-brown or dark blue appearance, while the healthy trees appeared red and pink.

We analyzed tree mortality during Hurricane Ian by comparing pre- and post-hurricane images from Sentinel-2A, taken in February 2022 and February 2024. These images were used to calculate the Leaf Area Index (LAI) for each year, which allowed us to analyze the relative change in LAI between the two years. The LAI was acquired using the Simple Ratio (SR) metric, following the formula:

$$LAI = 0.310 * SR - 0.098 \tag{1}$$

where SR is the simple ratio of the near-infrared (NIR) band (Band 8) and the red band (Band 4) calculated using Sentinel-2 Level-2A surface reflectance images (Cohrs et al., 2020).

In ecological studies, changes in LAI are often correlated with tree health and vigor. Therefore, we calculated the change in LAI using the formula:

$$Change = \frac{LAI_{2024} - LAI_{2022}}{LAI_{2022}} \quad (2)$$

Only negative values, indicating a decrease in LAI, were retained for further analysis. Any change exceeding the 22% threshold was set to 1, indicating tree mortality. A significant reduction in LAI of more than 22% can indicate severe damage to trees, making it a relevant threshold for assessing mortality. In ecological analysis, thresholds are often used to differentiate between normal variability and significant ecological changes. The 22% threshold is set to identify significant drops in LAI that are more than just normal changes, showing that trees are not only stressed but are dead.

February was determined to be the optimal month for comparison between 2022 and 2024. This choice was made because most of the areas are dominated by evergreen loblolly pine, and it was assumed that understory growth was minimal during this month, enhancing the accuracy of our LAI change analysis focused on tree mortality. Additionally, clear-cut operations in some areas during this period were manually removed from the analysis to ensure the accuracy of our results.

DEM and derived variables

Four variables (elevation, concavity, drainage capacity of the land, and proximity to the marsh) were assumed to control the spatial patterns of tree mortality in the forest area. The DEM has a 1 m ×1 m spatial resolution, which was resampled to 10 m ×10 m to perform the curvature analysis. Each pixel's size for the curvature analysis was 100 m^2, and the curvature output raster units are one over 100m units. The drainage capacity of the land was derived

using hydrology tools in the ArcGIS Pro. Drainage capacity is defined by the distance to the cumulative drainage network of the flow accumulation inside the forest, which is connected to the marsh at the forest's edge. Proximity to the marsh is the absolute perpendicular distance of the point/patch of mortality to the boundary line of the marsh.

The Hobcaw forest was inundated up to approximately 3 m during Hurricane Hugo (Gardner et al., 1992). Due to uncertainty in the precision of the 1990 estimates, Hugo's inundation depth was rounded to 3 m, and this height was used to outline the inundation area in ArcGIS Pro. Areas of healthy vegetation and tree mortality within that height were also digitized as multiple polygons. The nearest distance from any point to the marsh boundary or flow accumulation channel was calculated using the “Near” tool in ArcGIS Pro.

We used the Fishnet tool in ArcGIS to create uniformly spaced points (10 meters apart), which allowed us to generate sample points for our study. The sample points comprised 103,283 points, of which 36,927 were identified as being in the mortality class, and 66,356 were in the healthy vegetation class. For each of these points from the mortality and healthy vegetation classes, we retrieved values from the variable raster datasets and utilized these values as input for the logistic regression analysis. The dataset was then split into the training and test data (3:1) to build and train the model and validate its accuracy using the test data. Pearson correlation test was performed on the independent variables before the analysis.

We used the DEM for the visualization but used the water depth as a covariate for the logistic regression analysis. Using water depth as a variable in the model is justified because it directly measures the extent of water inundation in the forest, which influences soil infiltration

rates and subsequent changes in water salinity, as well as providing an indicator of drainage duration and overall hydrological dynamics than static DEM data.

In this case, water depth is a function of the DEM and height of the water during a surge into the forest. Water depth was determined as the absolute height above ground level for each pixel.

- For each pixel during Hurricane Hugo, the water depth = 3- DEM (m)
- For each pixel during Hurricane Ian, the water depth= 2.35- DEM (m)

Logistic regression analysis

Quantitative data analysis used R 1.2.5033 (R Core Team, 2019). Regression analysis was employed to develop the models. Bivariate logistic regression (glm() function, family=binomial) was used to assess the impact of topographic features on tree mortality in specific forest patches. In these models, tree mortality or healthy vegetation areas served as the binary response variable, indicating whether a pixel was classified as dead or dying (1) or as having healthy green vegetation (0) after the hurricane event.

We used logistic regression to explore the relationship between tree mortality at each pixel (mortality or healthy class). The equation gives our model:

$$P(Y = 1|X_1, \dots X_n) = \frac{1}{1 + e^{-(\beta_0 + \beta_1 X_1 + \dots \beta_n X_n)}} \quad (3)$$

Where P is the conditional probability that a tree falls under the mortality area (Y = 1), given predictors X1, ..., Xn as water depth, concavity, distance from drainage network and distance from the marsh.

Akaikes Information Criterion (AIC) (Anderson & Burnham, 2004) was used to determine the model best supported by mortality observations. We derived the AIC for models containing all possible combinations of the interactions among the predictors. The model most strongly supported by data was determined by the lowest AIC value (AICmin).

Accuracy Estimation

The Area Under the Curve (AUC) measures the area under the Receivers Operating Characteristics (ROC) curve, which is a graph showing the true positive rate versus the false positive rate. The ROC curve helps us see how well a model distinguishes between positive and negative cases at different thresholds. AUC is useful for model validation as it offers a single scalar value summarizing the model's performance across various decision thresholds. In binary classification, sensitivity (true positive rate) and specificity (true negative rate) are crucial metrics. Sensitivity indicates the proportion of actual positives the model correctly identifies, while specificity shows the proportion of actual negatives correctly identified. These metrics are vital for assessing a model's capability to classify positive and negative instances accurately. The cutoff point was established by choosing the threshold that optimizes the balance between sensitivity and specificity.

Additionally, we utilized the F1 score to measure accuracy. The F1 score is a metric for assessing the performance of a classification model, especially when dealing with imbalanced

classes. It is the harmonic mean of precision and recall, effectively balancing both. The formula for the F1 score is:

$$F1\ Score = \ 2 \times \frac{Precision * Recall}{Precision + Recall} \tag{4}$$

Precision is the ratio of true positive predictions to the total predicted positives, reflecting the accuracy of positive predictions. Recall, or sensitivity, is the ratio of true positive predictions to all actual positives, assessing the model's capability to identify positive instances. The F1 score, ranging from 0 to 1, with 1 indicating perfect precision and recall, is especially valuable for considering both false positives and false negatives in the evaluation.

The model was then used to predict the mortality of Hurricane Ian by changing the water depth variable, and it was compared with the actual tree mortality map of Hurricane Ian. The whole steps of the methodology are illustrated in Figure 3.2.

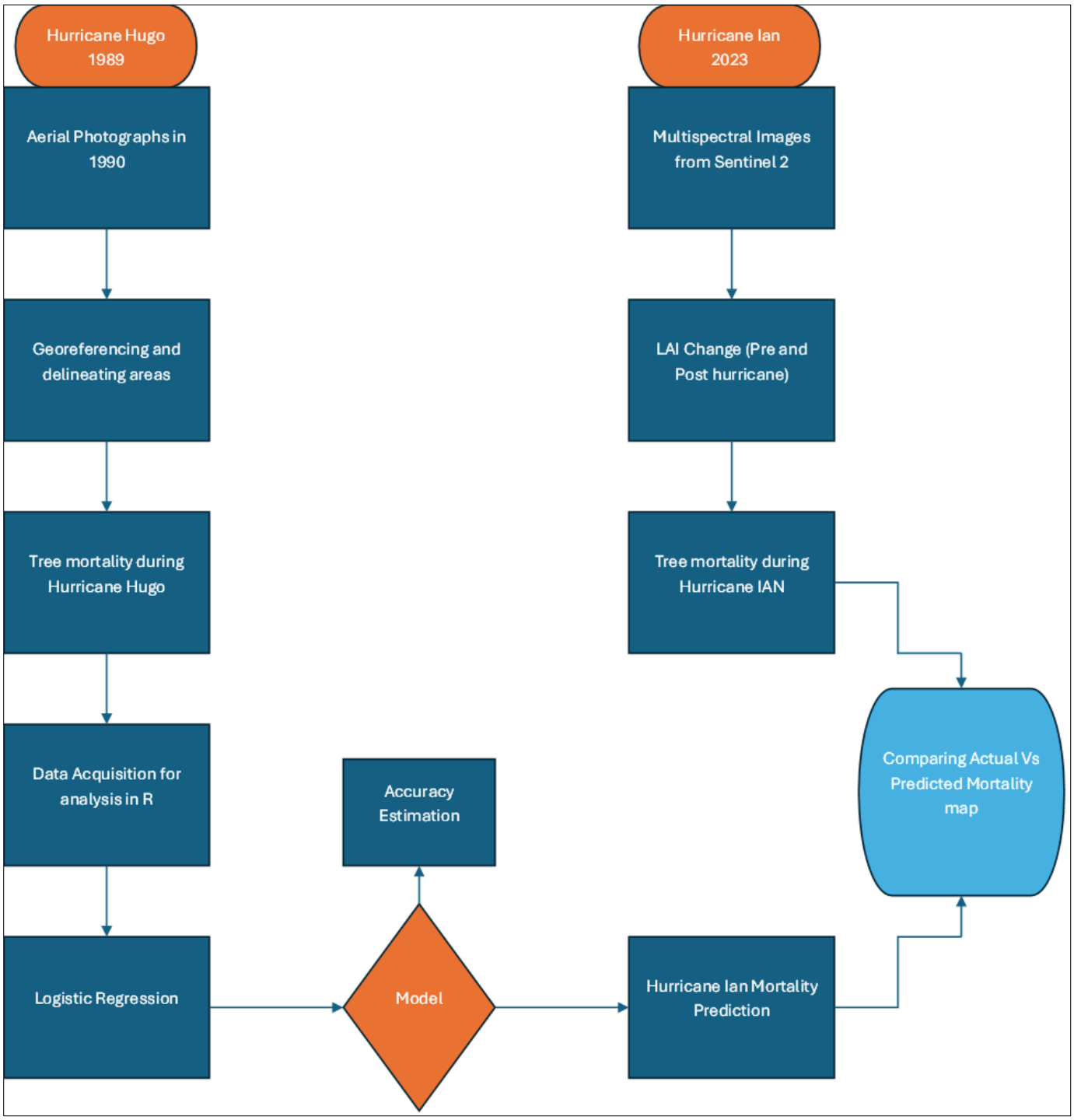

Figure 3.2: Methodology layout showing the steps from acquiring images for analysis to comparing the mortality maps.

Results

It was found that trees were dying/died in an approximately 7.01 km^2 area in the Hobcaw Barony after Hurricane Hugo (Figure 3.3).

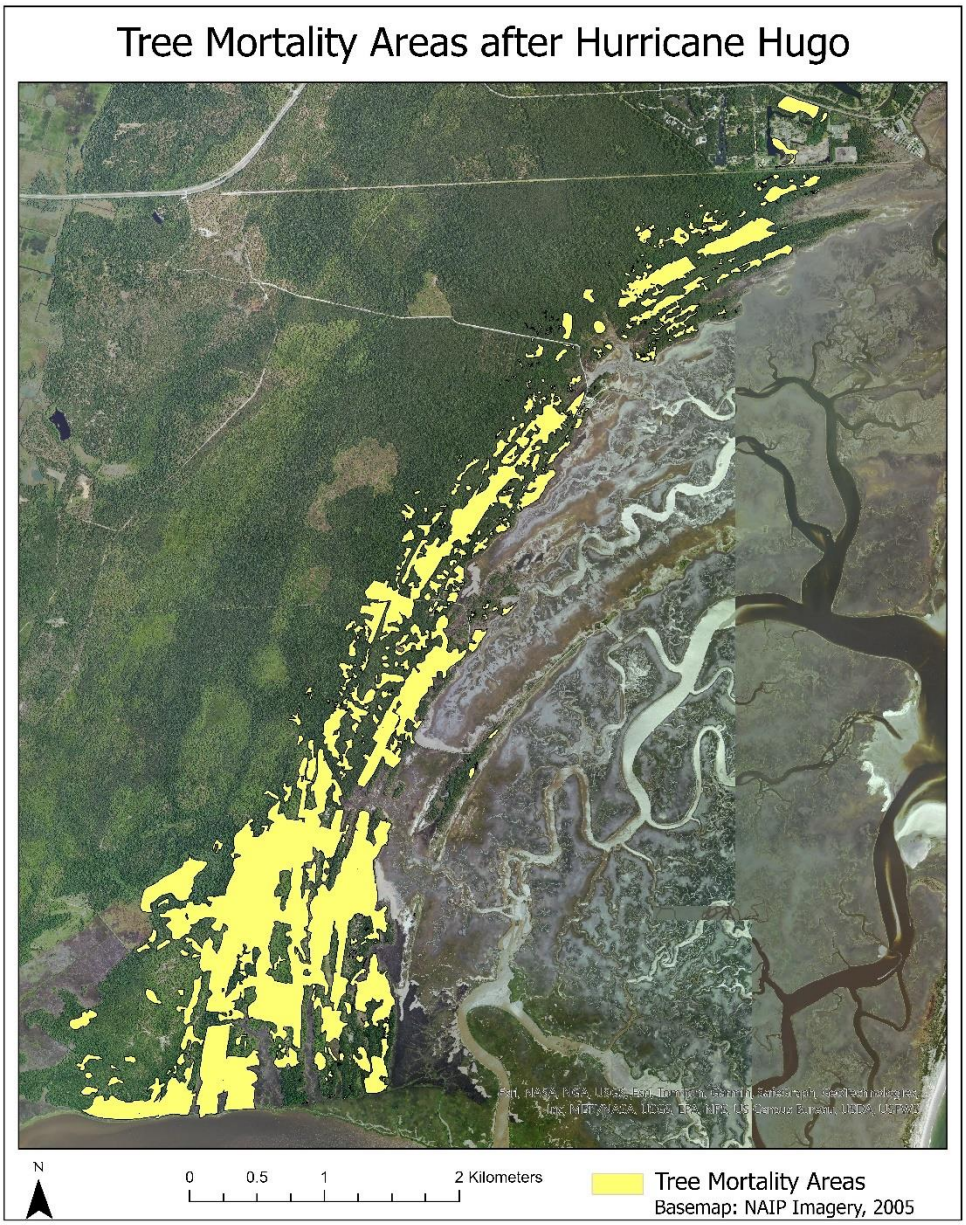

Figure 3.2: Tree Mortality Areas after Hurricane Hugo in 1989 in the Hobcaw Barony Forest, South Carolina.

Maps in Figures 3.4, 3.5, 3.6 and 3.7 further illustrates tree mortality areas in Hurricane Hugo with regard to the curvature, distance from the marsh, distance from stream networks and DEM, respectively. For better visualization, curvature of the land was categorized into three categories: Concave (< -0.01), flat (-0.01 to +0.01), and convex (>0.01) and the elevation range was categorized into three categories: less than 1 m (<1 m), 1-2 m, and greater than 2 m above mean sea level.

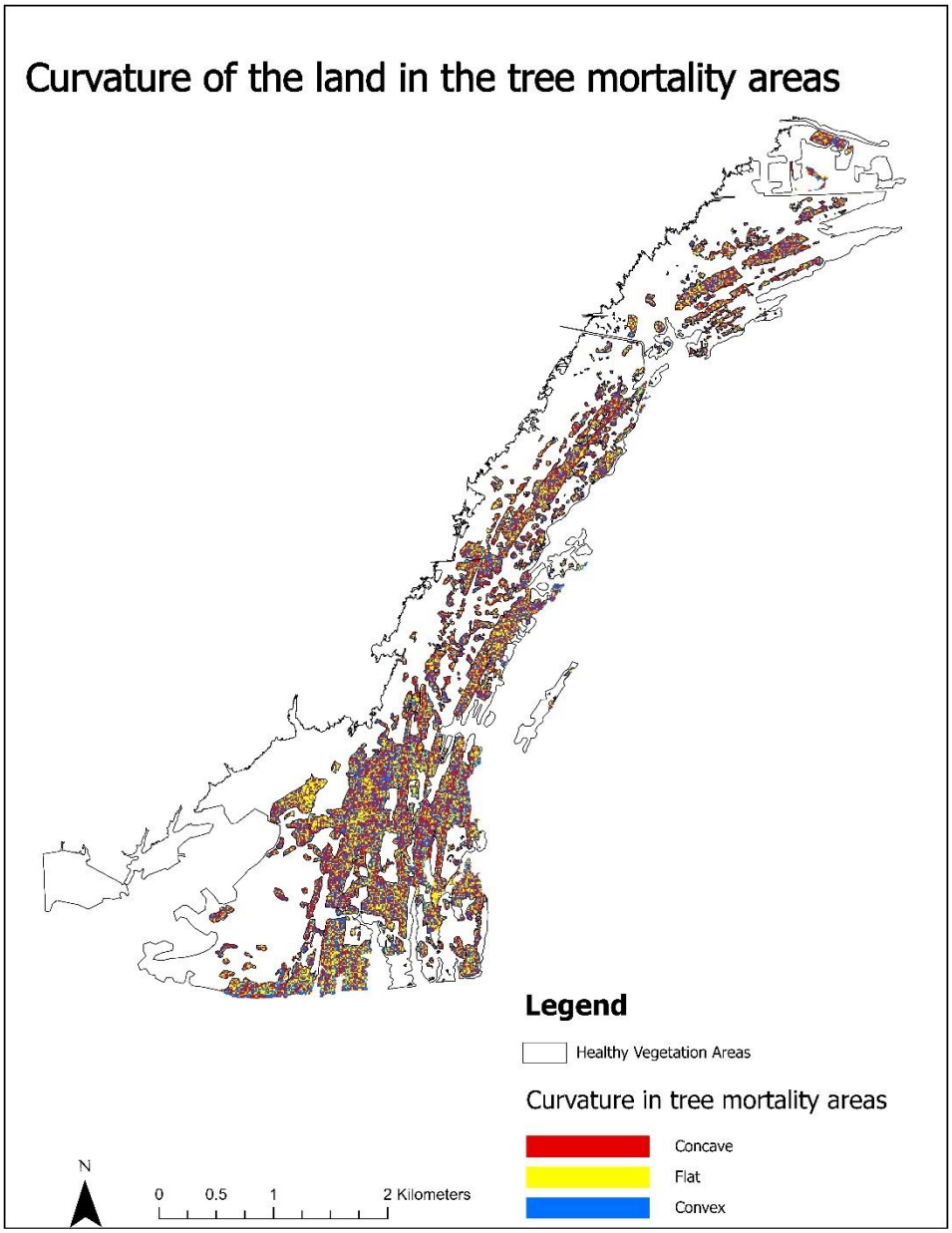

Figure 3.4:Tree mortality by curvature classes after Hurricane Hugo (1989) in Hobcaw Barony, South Carolina, USA

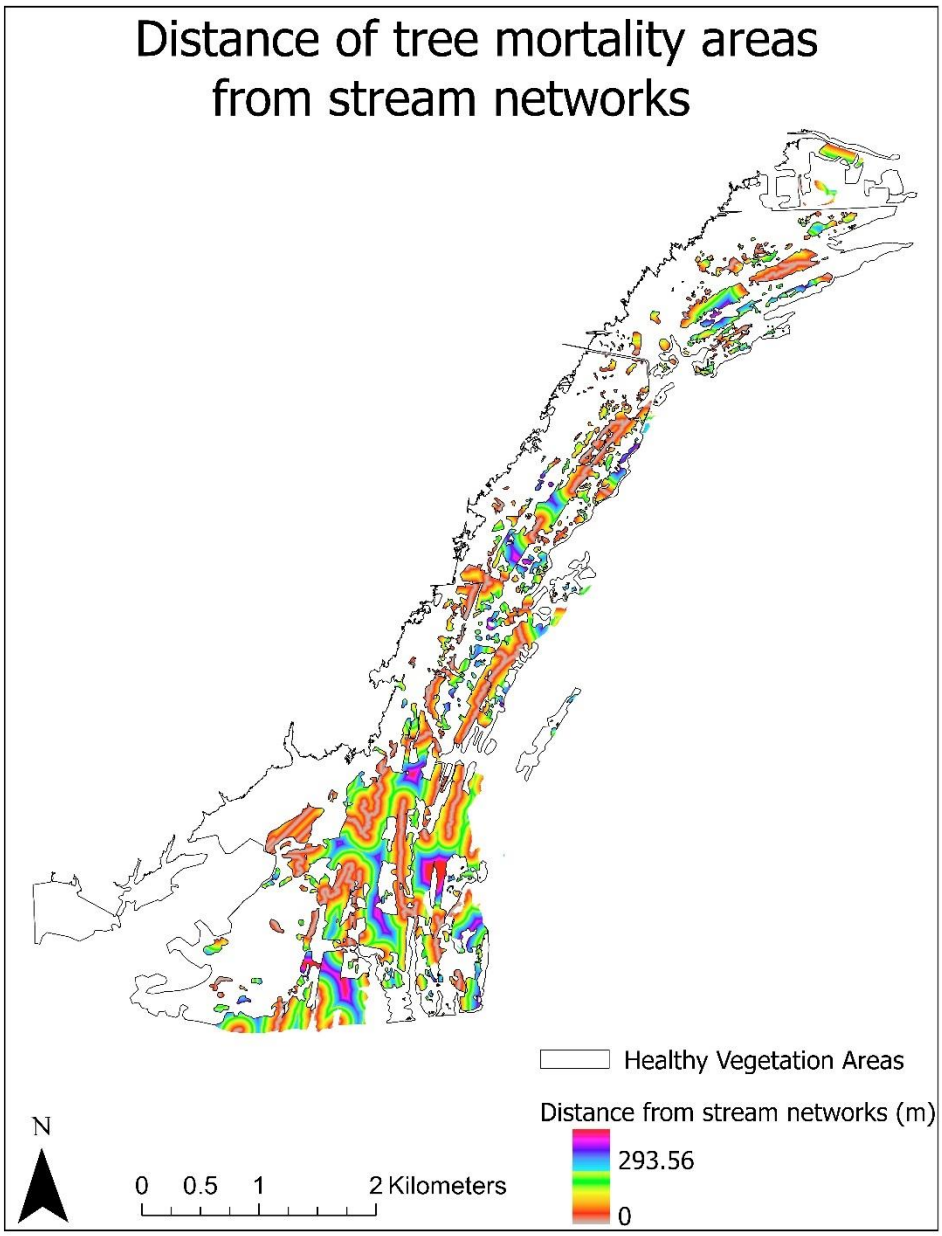

Figure 3.3: Tree mortality by distance from stream networks after Hurricane Hugo (1989) in Hobcaw Barony, South Carolina, USA.

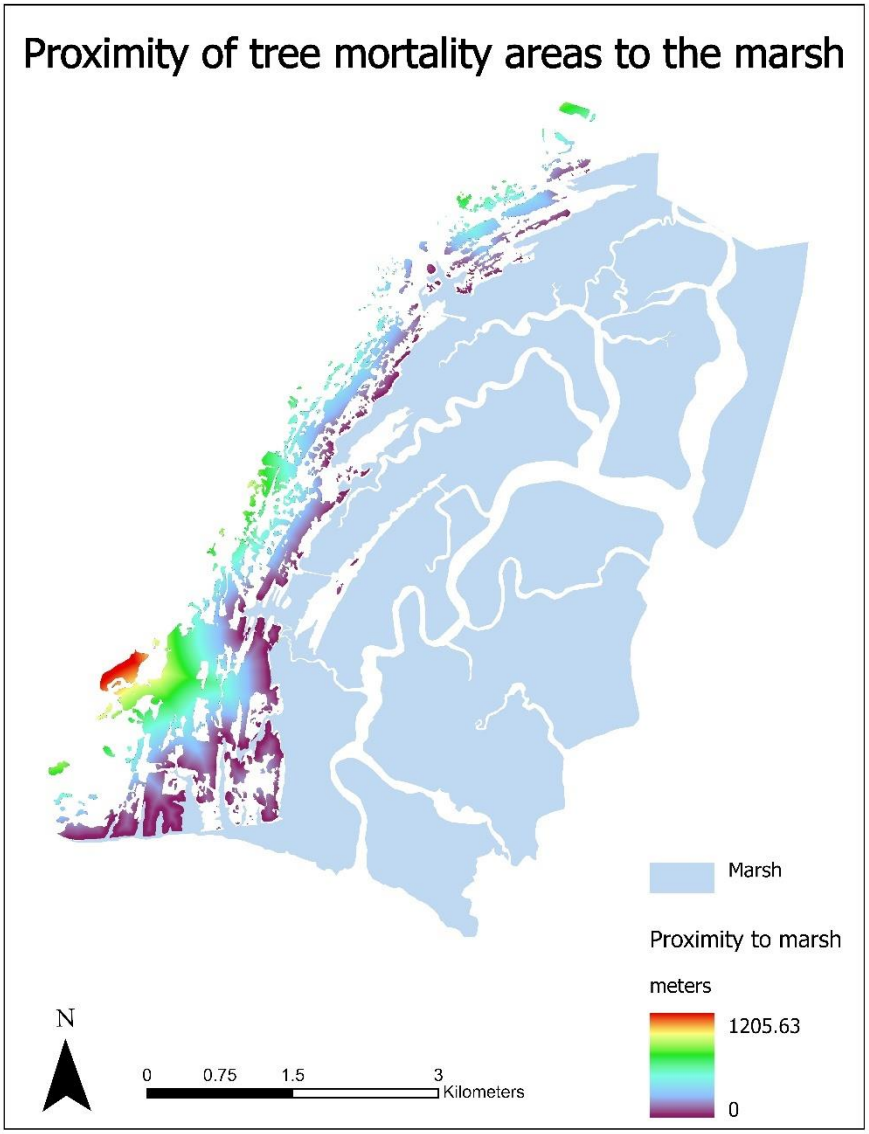

Figure 3.4: Tree mortality with distance from marsh after Hurricane Hugo (1989) in Hobcaw Barony, South Carolina, USA.

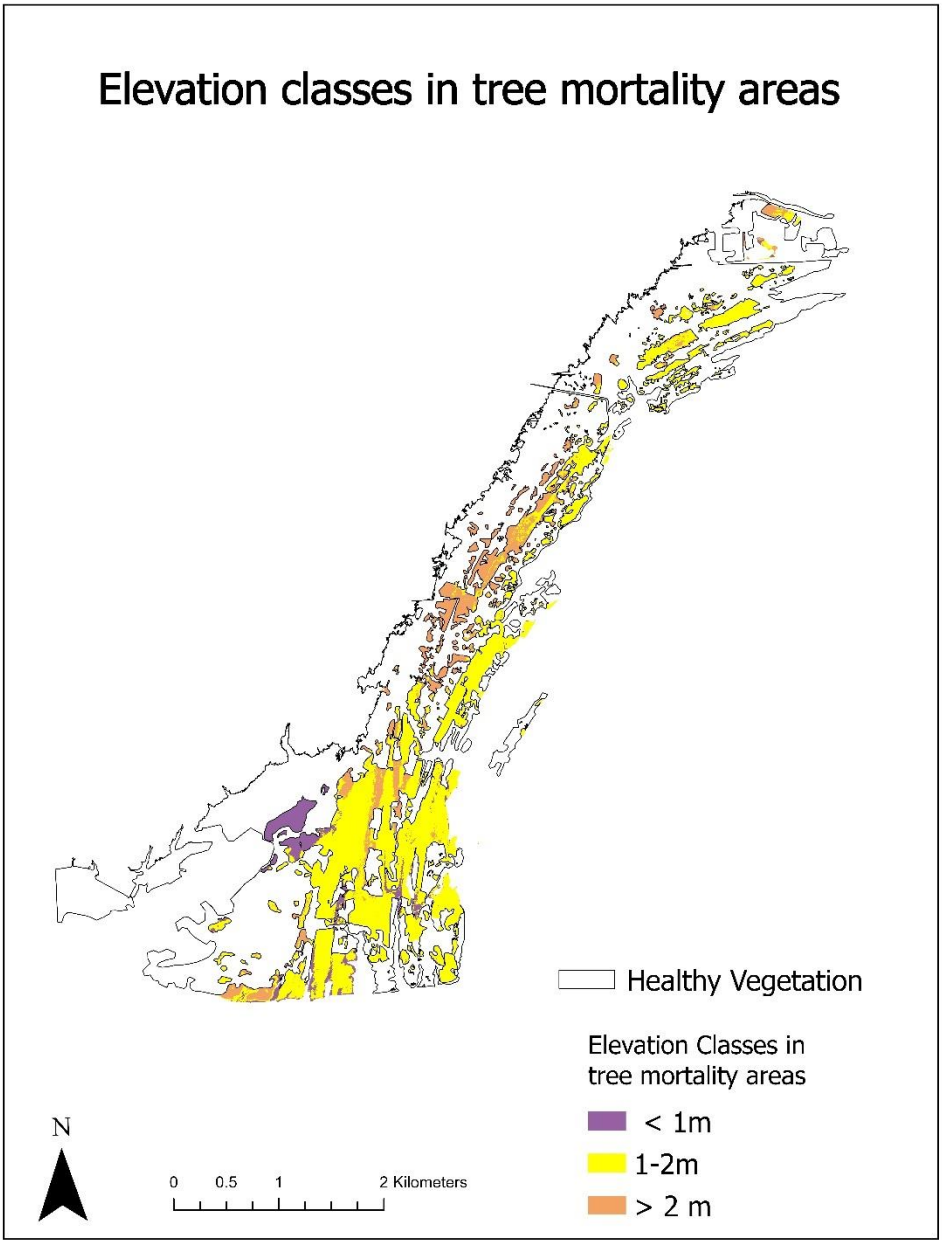

Figure 3.5: Tree mortality by elevation classes after Hurricane Hugo (1989) in Hobcaw Barony, South Carolina, USA.

Looking at the density plot to understand the distribution of pixels for each variable, curvature did not differ much in their distribution in all three cases (Figure 3.8 a). Higher tree mortality areas were between 1-2m DEM in Hurricane Hugo and Hurricane Ian mortality areas;

however, it was evenly distributed in Hurricane Hugo healthy areas. (Figure 3.8 b). Moreover, the closer the distance from the marsh, the higher the distribution was seen in Hurricane Hugo and Ian mortality areas. It was relatively even distributed in the case of Hurricane Hugo Healthy areas. (Figure 3.8 c). The density plot line graph for the distance from streams showed almost similar patterns in all three areas(Figure 3.8 d).

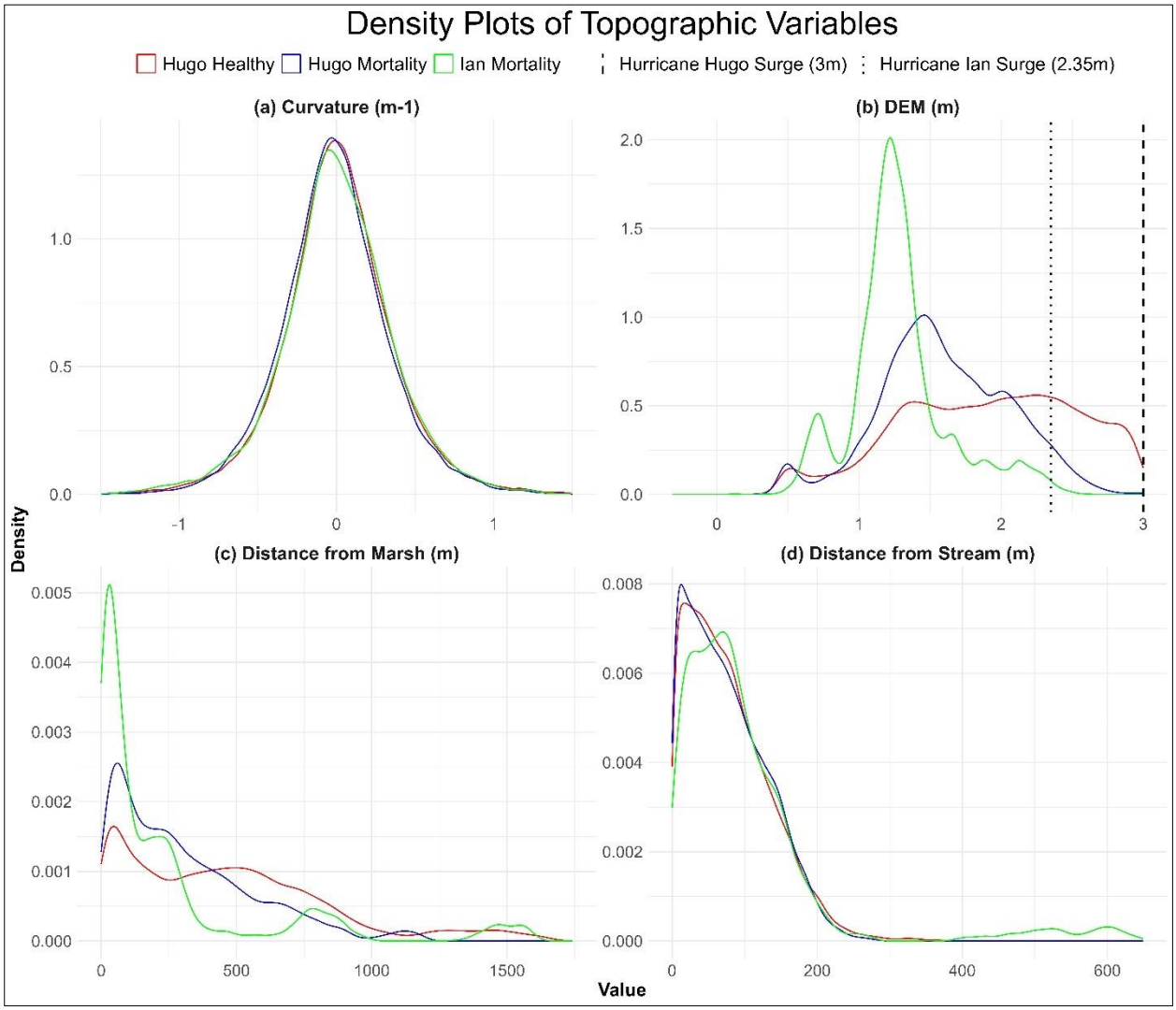

Figure 3.6: Density plots of pixel distribution of independent variables for healthy areas after Hurricane Hugo and tree mortality areas in Hurricane Hugo and Ian.

The difference in the distribution of the pixels is positive for the concave curvature and negative for the convex curvature; higher in DEM 1-2m; positive for distance from marsh up to 400m; and positive for distance from streams up to approximately 20 m and between 120-180m.(Figure 3.9)

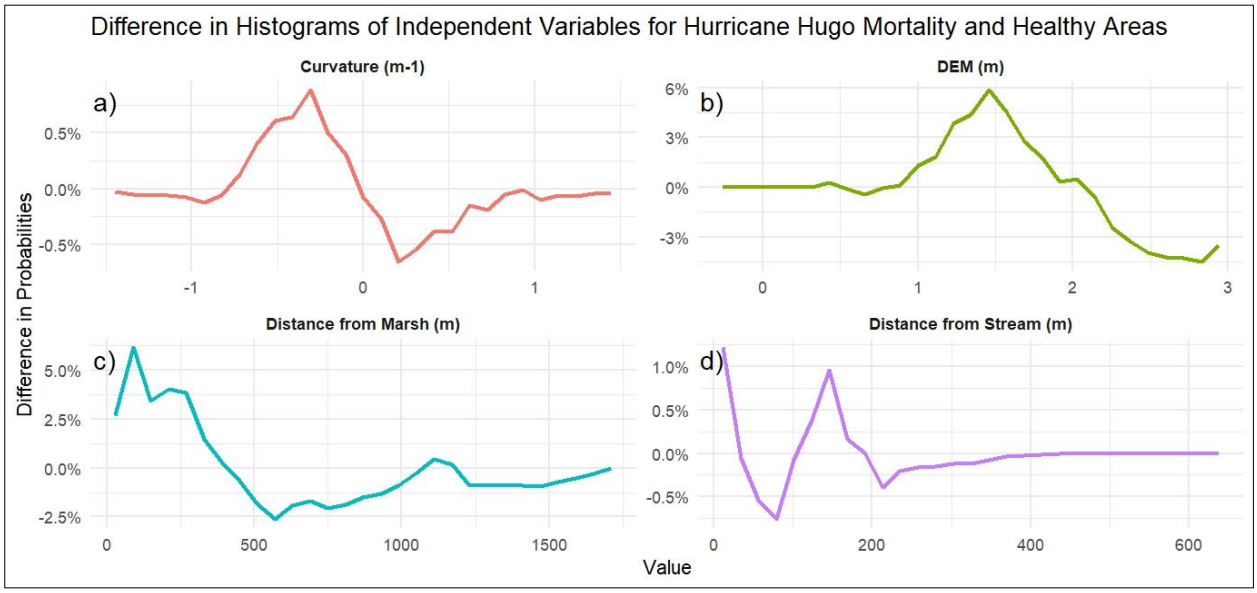

Figure 3.7: Differences in the distribution of the pixels of independent variables for tree mortality and healthy areas after Hurricane Hugo in 1989 in the Hobcaw Barony forest, South Carolina, USA.

Pearson correlation coefficient and plot indicated a low correlation between the independent variables used in the logistic regression (Figure 3.10 and Table A - 1).

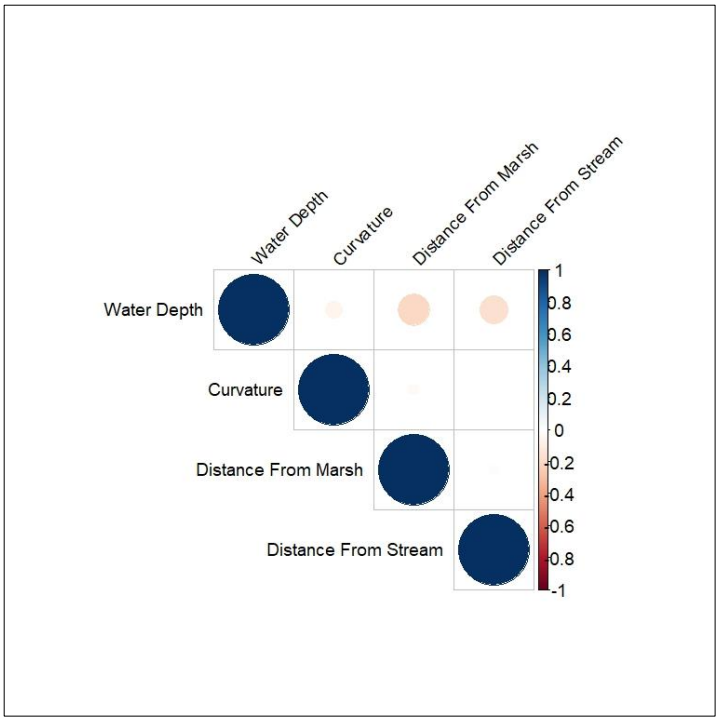

Figure 3.8: Pearson correlation matrix plots among the variables used in the analysis.

All the variables in the model were significant. The positive coefficient value for the concave curve and water depth implies that the log odds of any pixel falling into mortality areas (1) is higher with increasing concavity and water depth and vice versa for other variables. (Table 3.1)

Table 3.1: Summary of the final logistic regression analysis model tree mortality in the Hobcaw Barony Forest, South Carolina, USA

Coefficients	Estimate	Std. Error	Z value	Pr(>|z|)
Intercept	-1.097	0.044	-24.532	< 0.0001
Curvature (Concave)	0.052	0.022	2.275	0.0229*

Curvature (Convex)	-0.094	0.023	-4.065	< 0.0001
Distance From Stream	-0.001	0.001	-3.898	< 0.0001
Water Depth	0.793	0.027	29.377	< 0.0001
Distance From Marsh	-0.001	0.001	-44.232	< 0.0001
Distance From Stream * Water Depth	0.001	0.001	5.818	< 0.0001

Receiver Operating Characteristic (ROC) Curve was used to validate the model using the true positive and false positive values. The ROC curve depicts the performance of a classification model across all classification thresholds. The AUC was found to be 0.68. (Figure 3.11). However, the model with a higher AUC (>0.7) is recommended as a model with higher accuracy. The F1 score for the accuracy estimation was 0.74, which means the model is assumed to have a good performance for predictability.

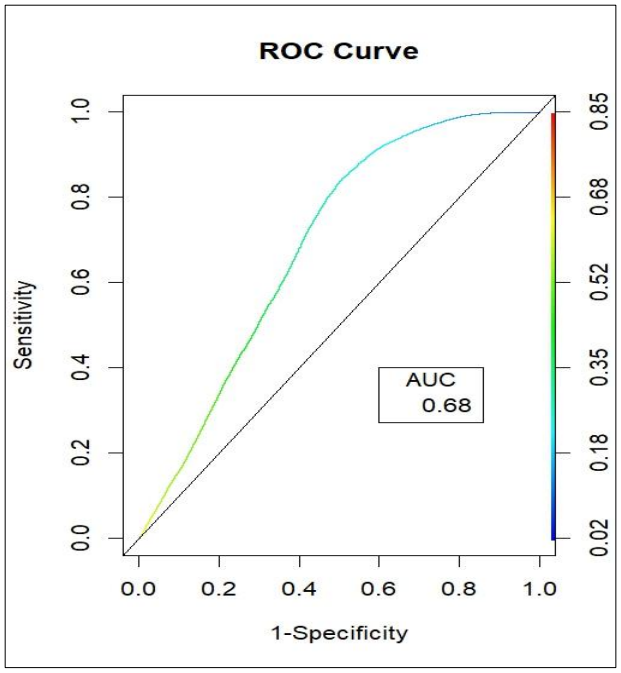

Figure 3.9: ROC Curve for the accuracy estimation

The predicted tree mortality map for Hurricane Ian, based on the logistic regression model, and the actual tree mortality area after Hurricane Ian, based on the LAI change, is illustrated in Figures 3.12 and 3.13, respectively. The model underestimated the tree mortality (Actual Mortality: 0.41 sq. km, Predicted Mortality: 0.17 sq. km); however, the spatial locations of tree mortality seem similar. Forty-one percent of the tree mortality after Hurricane Ian occurred within the same areas affected by Hurricane Hugo's mortality in 1990 (Figure 3.13).

Figure 3.10: Tree mortality areas were predicted after Hurricane Ian based on the logistic regression model prediction.


Tree Mortality after Hurricane Ian 2022
N
0
0.5
1
2 Kilometers
Overlapping Mortality Areas with Hurricane Hugo
Tree Mortality Areas

Figure 3.11: Actual tree mortality areas after Hurricane Ian based on the LAI change. Blue shades depict tree mortality areas after Hurricane Ian, which also fall inside the areas of tree mortality after Hurricane Hugo.

Discussion

A positive difference in the variable's histograms in the concave curvature shows a higher mortality in the concave curvature in the mortality areas than in the healthy areas during Hurricane Hugo (Figure 3.3). This also aligns with the model's findings, wherein the coefficient of convex curvature in the logistic regression model demonstrates a negative association with mortality (Table 3.1). This may be because concave terrain is a long-term water storage site with higher tree mortality due to salinity.

The positive value (>0) in the graph of the difference in the distribution of the pixels in tree mortality and healthy areas after Hurricane Hugo found within the 0- 40 m and 120-180m range near the streams was noteworthy, suggesting a localized impact of distance from streams (Figures 3.9 d). The distance from the stream variable is also a significant factor in our model; however, the log odds values are less (Table 3.1). Yu and Gao (2020) highlighted the importance of drainage capacity in their study on tree mortality in mangrove forests near river channels. We may also consider further investigation into incorporating the combined influence of slope and aspect gradients along the stream networks rather than solely relying on linear distance from the stream network as a determinant.

The observed higher tree mortality near marshland (Figure 3.6) and higher distribution of pixels closer to the marsh in mortality areas (Figure 3.8 c) aligns with our initial assumption that

these areas are more prone to seawater inundation, particularly during frequent hurricanes. This is also supported by an earlier study by Kearney et al. (2019). This increases the likelihood of seawater ingress, either directly through storm surges or indirectly through the dispersion of sea spray, contributing to the higher tree mortality in those areas. Furthermore, the possibility of a cumulative impact from previous hurricane events cannot be disregarded, which again exacerbates the adverse effects on vegetation. The confluence of saltier water, potentially intensified by repeated hurricane exposure, and the direct impact of salt spray within the adjacent forest zones emerge as a plausible explanation for the observed higher tree mortality rates in the areas close to the marsh. Moreover, Garnder et al. (1991) also highlighted that the trees near the marsh were more damaged during the Hurricane.

Higher tree mortality areas within the elevation range of 1-2 m (Figure 3.7 and 3.8 b); this phenomenon can be attributed to the existing marshland in areas below 1 m, which already has naturally sparse tree populations within this height range. Consequently, the greater availability of trees within the 1–2m category contributed to higher tree mortality in this elevation. Water depth, used as a derivative of DEM for the model analysis, implies that the log odds of any pixel falling into mortality areas (1) is higher with increasing water depth and vice versa (Table 3.1).

Validation after constructing the model using the training data and evaluating its accuracy on the independent test dataset quantified the model's discriminatory power. The AUC value of 0.68 reflects the model's ability to distinguish between tree mortality and healthy vegetation areas (Figure 3.11). However, this value suggests a moderate discriminatory performance, urging caution in interpreting the model's predictive capabilities. A higher AUC, preferably exceeding 0.70, is assumed to be an accurate prediction model; however, the model can still be used to

explore the significance of our independent variables and provide significant insights into the spatial variables affecting mortality. Further, using the F1 score for validation, it was 0.74, which implies the model has a moderate predicting capacity. The validation process contributes valuable insights into the model's strengths and limitations, paving the way for future refinements and improvements to enhance its overall predictive accuracy.

After deriving the actual tree mortality based on LAI change and the predicted map for Hurricane Ian using the model after the accuracy check, there are some visible discrepancies between the predicted and the actual tree mortality map (Figure 3.12 and 3.13). The predicted area of tree mortality after Hurricane Ian was 0.17 sq. km, but the actual tree mortality was 0.41 sq. km. This difference may be due to the time of the data acquisition. The Hurricane Hugo data was collected one year after Hurricane Hugo, but the multispectral images acquired for LAI after Hurricane Ian were one and a half years after the event. LAI can rapidly recover following a disturbance from vegetation regrowth, including surviving trees and new growth (Templeton et al., 2015). Many forests can restore their leaf area after such events, provided that soil fertility is maintained or improved (Norton et al., 2015). The overlap of tree mortality from Hurricane Ian within the same areas impacted by Hurricane Hugo in 1990 (Figure 3.13) indicates that 41% of the areas of tree mortality in the recent Hurricane Ian were located in regions already affected by the earlier event. However, a significant 60% of tree deaths occurred in new areas, which could be attributed to the southern pine beetle infestation in the recent year rather than the hurricane itself. This discrepancy highlights a crucial limitation of the current model, which is designed to predict tree mortality specifically resulting from hurricane impacts based on the topographic. The

model does not account for additional factors, such as beetle infestations, which can independently contribute to significant tree mortality.

Limitations of the study

The research and model may have limitations due to the absence of various environmental, biological, and hydrological variables. These omissions could introduce errors, particularly concerning hydrologic factors like artesian freshwater from aquifers, environmental factors such as temperature and precipitation, and biological factors such as bark beetle infestation.

Southern pine beetles (*Dendroctonus frontalis*) are causing tree mortality in the coastal forests. However, it is imperative to note that this hypothesis remains unexplored in the current research due to the absence of comprehensive data about the water table aquifer and the extent of pine infestation in the study area. This constraint represents a notable limitation of the present investigation, highlighting the need for future research endeavors to acquire detailed information on these critical variables. Furthermore, the observed lower value of the AUC value of the derived model may potentially be linked to the exclusion of information about these variables above.

Another limitation of this research is that tree mortality after Hurricane Ian was calculated using changes in leaf area index change pre- and post-hurricane using Sentinel-2A imagery. However, the tree mortality areas were not validated using ground-truthing methods. Ground-truthing is necessary to ensure the accuracy and reliability of remote sensing data.

Conclusion

The higher tree mortality was observed in the areas close to the marsh at an elevation 1-2 m with concave curvature and around 120-180 m away from the stream networks. From the model, the probability that a certain patch/pixel of the forest belongs to a mortality class is influenced by the topographic variables: negatively by convex curvature, proximity to the marsh, water depth (a derivative of elevation), and positively by concave curvature, distance from stream networks. Moreover, there was an interaction effect between the variables. Considering the interaction effects between the distance from streams and water depth, the model had the lowest AIC value. The model had moderate accuracy and underestimated tree mortality areas after Hurricane Ian. Furthermore, the findings of this research may have broader implications for coastal regions globally, highlighting the role of topographic factors in the changing dynamics of coastal forests, which frequently experience hurricanes. A more robust analysis to derive integrated models using machine learning techniques and comparing the models is recommended.

REFERENCES

1. Ali, G. A., & Roy, A. G. (2010). Shopping for hydrologically representative connectivity metrics in a humid temperate forested catchment. Water Resources Research, 46(12).
2. Anderson, D., & Burnham, K. (2004). Model selection and multi-model inference. *Second. NY: Springer-Verlag*, *63*(2020), 10.
3. Baguskas, S. A., Peterson, S. H., Bookhagen, B., & Still, C. J. (2014). Evaluating spatial patterns of drought-induced tree mortality in a coastal California pine forest. *Forest Ecology and Management*, *315*, 43-53.
4. Bright, B. C., Hicke, J. A., & Meddens, A. J. (2013). Effects of bark beetle-caused tree mortality on biogeochemical and biogeophysical MODIS products. *Journal of Geophysical Research: Biogeosciences*, *118*(3), 974-982.
5. Chambers, J. Q., Fisher, J. I., Zeng, H., Chapman, E. L., Baker, D. B., & Hurtt, G. C. (2007). Hurricane Katrina's carbon footprint on US Gulf Coast forests. *Science*, *318*(5853), 1107-1107.
6. Clark, J. S. (1986). Coastal forest tree populations in a changing environment, southeastern Long Island, New York. *Ecological Monographs*, *56*(3), 259-277.
7. Cohrs, C. W., Cook, R. L., Gray, J. M., & Albaugh, T. J. (2020). Sentinel-2 leaf area index estimation for pine plantations in the southeastern United States. *Remote Sensing*, *12*(9), 1406.
8. Conner, W. H., Doyle, T. W., Krauss, K. W., Williams, K., MacDonald, M., McPherson, K., & Mirti, T. H. (2007). Ecology of the coastal edge of hydric hammocks on the Gulf Coast of

Florida. *Ecology of tidal freshwater forested wetlands of the Southeastern United States*, 255-289. doi: 10.1007/978-1-4020-5095-4_10

9. Dai, Z., Amatya, D. M., Sun, G., Trettin, C. C., Li, C., & Li, H. (2011). Climate variability and its impact on forest hydrology on South Carolina coastal plain, USA. *Atmosphere*, *2*(3), 330-357.
10. Dai, Z., Trettin, C. C., & Amatya, D. (2013). *Effects of climate variability on forest hydrology and carbon sequestration on the Santee Experimental Forest in coastal South Carolina*. Asheville, NC, USA: United States Department of Agriculture, Forest Service, Southern Research Station.
11. Field, C. R., Gjerdrum, C., & Elphick, C. S. (2016). Forest resistance to sea-level rise prevents landward migration of tidal marsh. *Biological Conservation*, *201*, 363-369.
12. Gardner, L. R., Michener, W. K., Blood, E. R., Williams, T. M., Lipscomb, D. J., & Jefferson, W. H. (1991). Ecological impact of Hurricane Hugo—salinization of a coastal forest. *Journal of Coastal Research*, 301-317.
13. Gardner, L. R., Michener, W. K., Williams, T. M., Blood, E. R., Kjerve, B., Smock, L. A., ... & Gresham, C. (1992). Disturbance effects of Hurricane Hugo on a pristine coastal landscape: North Inlet, South Carolina, USA. *Netherlands Journal of Sea Research*, *30*, 249-263.
14. Gessler, P. E., Chadwick, O. A., Chamran, F., Althouse, L., & Holmes, K. (2000). Modeling soil–landscape and ecosystem properties using terrain attributes. *Soil Science Society of America Journal*, *64*(6), 2046-2056.

15. Gitlin, A. R., Sthultz, C. M., Bowker, M. A., Stumpf, S., Paxton, K. L., Kennedy, K., ... & Whitham, T. G. (2006). Mortality gradients within and among dominant plant populations as barometers of ecosystem change during extreme drought. *Conservation Biology*, *20*(5), 1477-1486.
16. Heaton, R., Song, B., Williams, T., Conner, W., Baucom, Z., & Williams, B. (2023). Twenty-Seven Year Response of South Carolina Coastal Plain Forests Affected by Hurricane Hugo. *Plants*, 12(4), 691.
17. Hook, D. D., Buford, M. A., & Williams, T. M. (1991). Impact of Hurricane Hugo on the South Carolina coastal plain forest. *Journal of Coastal Research*, 291-300.
18. Hu, T., & Smith, R. B. (2018). The impact of Hurricane Maria on the vegetation of Dominica and Puerto Rico using multispectral remote sensing. *Remote Sensing*, *10*(6), 827. doi:10.3390/rs10060827
19. Kearney, W. S., Fernandes, A., & Fagherazzi, S. (2019). Sea-level rise and storm surges structure coastal forests into persistence and regeneration niches. *PloS one*, *14*(5), e0215977. https://doi.org/10.1371/journal.pone.0215977
20. Langston, J. K. (2017). *Democratization and authoritarian party survival: Mexico's PRI*. Oxford University Press.
21. Lee, M. F., Lin, T. C., Vadeboncoeur, M. A., & Hwong, J. L. (2008). Remote sensing assessment of forest damage in relation to the 1996 strong typhoon Herb at Lienhuachi Experimental Forest, Taiwan. *Forest ecology and management*, *255*(8-9), 3297-3306.

22. Negrón-Juárez, R., Baker, D. B., Zeng, H., Henkel, T. K., & Chambers, J. Q. (2010). Assessing hurricane-induced tree mortality in US Gulf Coast forest ecosystems. *Journal of Geophysical Research: Biogeosciences*, *115*(G4).

23. Neumann, M., Mues, V., Moreno, A., Hasenauer, H., & Seidl, R. (2017). Climate variability drives recent tree mortality in Europe. *Global change biology*, *23*(11), 4788-4797. doi:10.1111/gcb.13724

24. Norton, U., Ewers, B. E., Borkhuu, B., Brown, N. R., & Pendall, E. (2015). Soil nitrogen five years after bark beetle infestation in lodgepole pine forests. *Soil Science Society of America Journal*, *79*(1), 282-293.

25. Parker, G., Martínez-Yrízar, A., Álvarez-Yépiz, J. C., Maass, M., & Araiza, S. (2018). Effects of hurricane disturbance on a tropical dry forest canopy in western Mexico. *Forest Ecology and Management*, *426*, 39-52.

26. R Core Team. (2019). R: A language and environment for statistical computing. Vienna, Austria: R Foundation for Statistical Computing. Retrieved from https://www.R-project.org/

27. Rao, K., Anderegg, W. R., Sala, A., Martínez-Vilalta, J., & Konings, A. G. (2019). Satellite-based vegetation optical depth as an indicator of drought-driven tree mortality. *Remote Sensing of Environment*, *227*, 125-136.

28. Ross, M. S., O'Brien, J. J., & da Silveira Lobo Sternberg, L. (1994). Sea-level rise and the reduction in pine forests in the Florida Keys. *Ecological Applications*, *4*(1), 144-156.

29. Rossi, E., Rogan, J., & Schneider, L. (2013). Mapping forest damage in northern Nicaragua after Hurricane Felix (2007) using MODIS enhanced vegetation index data. GIScience & remote sensing, 50(4), 385-399.

30. Schuck-Kolben, R. E. (1990). *Storm-tide elevations produced by Hurricane Hugo along the South Carolina coast, September 21-22, 1989* (No. 90-386). US Geological Survey.

31. Stalter, R., Baden, J., DePratter, C., & Kenny, P. (2018). The vascular flora of Coastal Indian clam shell middens in South Carolina, USA. *Journal of the Botanical Research Institute of Texas*, *12*(2), 697-706. https://doi.org/10.17348/jbrit.v12.i2.972

32. Templeton, B. S., Seiler, J. R., Peterson, J. A., & Tyree, M. C. (2015). Environmental and stand management influences on soil CO2 efflux across the range of loblolly pine. *Forest Ecology and Management*, *355*, 15-23.

33. Thompson, I. D., Maher, S. C., Rouillard, D. P., Fryxell, J. M., & Baker, J. A. (2007). Accuracy of forest inventory mapping: Some implications for boreal forest management. *Forest Ecology and Management*, *252*(1-3), 208-221.

34. Wang, W., Peng, C., Kneeshaw, D. D., Larocque, G. R., & Luo, Z. (2012). Drought-induced tree mortality: ecological consequences, causes, and modeling. Environmental Reviews, 20(2), 109-121.

35. Wang, W., Qu, J. J., Hao, X., Liu, Y., & Stanturf, J. A. (2010). Post-hurricane forest damage assessment using satellite remote sensing. *Agricultural and forest meteorology*, *150*(1), 122-132.

36. Yu, M., & Gao, Q. (2020). Topography, drainage capability, and legacy of drought differentiate tropical ecosystem response to and recovery from major hurricanes. *Environmental Research Letters*, *15*(10), 104046.

37. Zhu, Z., Woodcock, C. E., & Olofsson, P. (2012). Continuous monitoring of forest disturbance using all available Landsat imagery. *Remote sensing of environment*, *122*, 75-91.

CHAPTER 4

TREE MORTALITY DUE TO HURRICANES AND ASSOCIATED VARIABLES IN THE COASTAL FOREST IN SOUTH CAROLINA.

Abstract

Assessing tree mortality after disturbances is a key area of interest for researchers in forestry science. Data were collected from long-term monitoring plots established in 1994 in the pine-dominated Hobcaw Barony Forest of South Carolina. We hypothesize that tree mortality on the coast is influenced by various factors, including biotic interactions, climatic variations, and hydrographic features, and that these covariates have a measurable impact on the survival rates of trees since the establishment of the plot. We use simple numerical analysis to estimate tree mortality and a nonparametric Kaplan-Meier method to describe the effects of covariates on survival probability. There was higher tree mortality in 2003-2007 and 2022-2023 and higher for the evergreen species with less DBH values. The Kaplan-Meier Curve indicated that any tree has a survival probability of around 20% after 29 years or upon reaching a diameter at breast height (DBH) of 10 cm. The results can be incorporated into ecological simulations to evaluate the vulnerability of coastal tree species under different scenarios and thus can be used to inform management strategies.

Introduction

Tree mortality is a critical ecological process within forest ecosystems. Therefore, early warning indicators that predict imminent mortality events are crucial for effective ecosystem management (Carpenter & Gunderson, 2001; Dakos et al., 2008). Predicting tree death is challenging because it typically results from a combination of interconnected factors affecting the tree over varying periods and intensities rather than from a single cause (Waring, 1987). Tree mortality may result from the mutuality between external environmental conditions, such as climate, hydrology, and internal life-history strategies, reflected in traits such as DBH, leaf habits, etc. Rather than solely attributing tree fatalities to hurricane-induced saltwater intrusion, integrating local climatic variables into the model enhances its capacity to illustrate how diverse factors collectively impact tree survival.

Studying the changes in vegetation over time, with a comprehensive evaluation of factors like tree mortality, growth, and regeneration/recruitment, can deepen our understanding of the ecological processes regulating plant communities (Phillips et al., 2011). Due to differences in how various plant species can be resilient to inundation and saltwater exposure, these stressors can lead to significant alterations in plant communities' structure and composition (Williams et al., 1999; Osland, 2016), and it may become evident well in advance of a transition of forest to a marsh (Field et al., 2016). Post-hurricane investigations have revealed variations in tree resistance to damage and mortality rates (Walker, 1991; Zimmerman et al., 1994). The extent of damage incurred to a tree may be linked to its size (Walker, 1991; Herbert et al., 1999). The diameter at breast height (DBH) of the plant species is an important variable in assessing tree growth and health. Larson et al. (2015) studied the spatial aspects of tree mortality in young and old-growth forests. They noticed the significant distinctions in

mortality among the two forest types with different diameter classes. Deciduous trees shed their leaves periodically, resulting in a bare canopy for at least one month during the dry season. On the other hand, evergreen trees retain their leafy canopy throughout the entire year. The type of leaf habit in trees significantly impacts their ecological and physiological traits and their allocation of metabolic resources, influencing their growth rate and capacity to manage stress (Singh & Kushwaha, 2016). Deciduous forests are generally more resistant to hurricane damage compared to evergreen forests. (Yu & Gao, 2020). Basal areas in the stands are also an important predictor of the tree's survival. Timilsina and Staudhammer (2012) used the basal areas per hectare for the tree mortality analysis, and it was also a significant predictor of mortality. Furthermore, Zhou et al. (2021) highlighted that basal area per hectare is a crucial continuous variable for comprehending forest dynamics and mortality, underscoring its importance in predicting and assessing tree survival within forest ecosystems.

Forecasts related to climate change suggest an increased likelihood of droughts due to rising temperatures and greater fluctuations in precipitation patterns (Allen et al., 2015). In trees, increased temperature causes increased respiration costs, increased heat stress, and a greater risk of cavitation (McDowell et al., 2008; Allen et al., 2010), consequently leading to higher mortality with increasing temperature. The rise in tree mortality rates is linked with climatic variations, including increased warm season temperature (Park Williams et al., 2013), intensity and the period of dry season (Adams et al.; 2017) and rainy seasons (Mori & Becker, 1991), as well as storms (Nelson et al., 2010), etc. In six of the eight hardwood species in the United States, the annual temperature was significant in the model, and the mortality risk was considerably higher with higher temperatures (Yaussy et al., 2013). Tree mortality could rise when high temperatures coincide with low summer precipitation (Bigler et al., 2006).

However, in the western USA, none of the precipitation-related variables played a role in predicting dead trees from any mortality factor. (McNellis et al., 2021).

By increasing salinity levels in the forest, tree mortality is also affected by various hydrologic factors like high tides, tide frequencies, etc. Due to rising sea levels, many coastal ecosystems face the threat of increased tidal flooding, which elevates soil salinity and significantly impacts their structure and function. (Williams et al., 1999; Twilley et al., 2001; Morris et al., 2002, Thorne et al., 2018). The inland extent of flooding and the infiltration of saltwater have expanded, leading to a larger area impacted by hurricane and storm surge occurrences. (Poulter & Halpin, 2008; Nicholls & Cazenave 2010; Church et al., 2013).

Prior studies have explored relationships between tree mortality and certain variables using logistic regression analysis, a commonly used statistical method (e.g., Fernández, 2008). This method relies on a binary response variable modeled over uniform time intervals, which often does not align with the nature of inventory data (Boeck et al., 2014; Hülsmann et al., 2016). Individuals with unknown event times must be censored, meaning those who do not experience the event during the observation period. Such censored data necessitate the use of survival models, including the nonparametric Kaplan–Meier estimator (Kaplan & Meier, 1958), the semi-parametric Cox model (Cox, 1995), and parametric models like the Accelerated Failure Time (AFT) Model. Parametric models offer the advantage of being based on a distribution and estimating the effect of predictors in absolute terms (e.g., years). Although initially developed for medical studies, these models are increasingly adopted in forest science (Staupendahl & Zucchini, 2011; Neuner et al., 2014; Neumann et al., 2017). In this study, we

utilized survival analysis, a method that enables the estimation of time-specific survival probabilities and the evaluation of covariate effects on survival.

Survival analysis has been effectively used in forest research before (e.g., Nothdurft, 2013; Neuner et al., 2015; Neumann et al., 2017). In this study, we utilized survival analysis, a method that enables the estimation of time-specific survival probabilities and the evaluation of covariate effects on survival. For this, we used the following: (i) a comprehensive individual tree database from the long-term monitoring project, consisting of long-term detailed census records of trees in 4 sample plots in pine-dominated cover type in Hobcaw Barony (Song et al., 2012;); (ii) a compilation climatic, hydrologic, and biotic database to establish a predictor variable to represent the tree by tree mortality and survival probability (iii) survival analysis model in which the attribute of tree mortality status (alive or dead) will be modeled as the response variable with time. Understanding how periodic hurricane events and other associated variables interact and contribute to tree mortality and survival will enhance our capacity to evaluate the susceptibility of coastal and how it shapes the growth and resilience of coastal forests; therefore, to address this issue, this study looked into the following hypotheses. Particularly, we hypothesize that

- The mortality rates of trees in coastal forests have significantly increased over the years.
- Climatic variables, such as temperature fluctuations and changes in precipitation patterns, significantly contribute to the mortality rates of trees in coastal forests.
- Hydrologic factors, such as increased frequency and heights of storm surges, are critical determinants of tree mortality in coastal forests.
- Biotic features, including size, leaf habits and competition among trees, determine the mortality of trees in coastal forests.

- A survival analysis model incorporating climatic, hydrologic, and biotic variables will provide a robust framework for the assessment of tree mortality in coastal forests.

Methodology

<u>Study area: (Please refer to Chapter 3: Figure 3.1)</u>

Field data collection:

Data was gathered in the four sample plots (46, 47, 48, and 49) of 20 m × 100 m, established in 1994. We collected tree DBH in 1994, 1997, 2000, 2003, 2007, 2010, 2013, 2016, 2017, 2021 and 2022. In 2023, we only collected the data on the mortality of the tree, not the DBH. Consistent tree measurement methods, as outlined by Song et al., 2012, were followed throughout the study. All trees with a DBH ≥2.5 cm were given permanent identification tags, numbered, and measured at the diameter at the breast height of 1.3 meters. Plots were subdivided into subplots and marked by aluminum poles for ease of relocation of trees by their numbers. A systematic numbering process was implemented within each subplot to ensure an accurate count of all trees, starting from the southwest corner of the first subplot. A designated tally person from the previous measurement confirmed and cross-referenced the measurements of the two field technicians so that no tree was missed during the process. New aluminum tags were used to mark ingrowth, which reached 2.5 cm DBH in the field season cycle, while mortality was often confirmed by locating tags on dead trees. A dead tree is a broken or uprooted, or erect tree that is damaged and lacks leaves. However, the trees will be considered alive if they are found with resprouting leaves. At the end of the study, all data were reviewed to find missed trees and counted as “missing on arrival’ for the field season. Marked trees were categorized by species and assigned a damage class. Data collected during each field season consisted of DBH, the current damage class of trees, and regeneration (<2.5 cm DBH). Stems with a DBH ≥ 10 cm

were classified as trees, while stems with a DBH of 2.5 to 9.9 cm were classified as saplings. For some analysis, trees were classified based on DBH as Small (<5cm), Medium (5-10 cm) and Large (>10cm).

Data Acquisition:

Tree mortality is a slow process, so it is important to consider climatic and hydrologic data from the last three years and long-term trends (lagged). Field data are typically collected in the summer, which is already halfway through the year. Using data from earlier years rather than the current year's data gives a more accurate understanding of the factors affecting tree death and survival.

Climatic data

The climatic data from 1993 to 2023 was acquired from PRISM (https://prism.oregonstate.edu/). We used two important predictors to assess how climatic factors impact tree mortality in the coastal forest: a) mean annual temperature and precipitation of the past three years and b) lagged mean annual temperature and precipitation. Lagged data is the mean of the climatic data throughout the tree's observation period. For example, if the tree were observed from 2000 to 2013, the lagged climatic data is the mean of the annual climatic data for that period. Since tree mortality is a slow process and trees respond with delays (lag times), we analyzed data from the past three years and incorporated lagged climatic information into the analysis. The slow progression of tree dying suggests that prior years' stressors substantially influence current mortality rates. This approach acknowledges the cumulative impact of survival time climatic conditions on forests.

Hydrologic Data

Hydrologic variables included the highest tide and tide frequency in the plot in the past three years. Tide height data from 1994 to 2023 was acquired from the NOAA website (https://www.noaa.gov/). The verified hourly tide data in datum NAVD was obtained from the website. The Oyster Land Creek weather station had the data from 2001 to 2020. The rest of the data was acquired from the Springmaid Pier in Myrtle Beach weather station. The center of the sample plot was taken as a reference to gather the data for tide frequency. If the height of the tide was greater than the elevation of the center of the plot, it was assumed that the tide inundated the trees in the plot.

Biotic data

We acquired the biotic data for the species, like species, size (DBH), mortality (dead or alive), etc., from the field data collection and leaf habit data from the secondary sources (published papers, books, internet, etc.). Over 29 years (beginning from 1994), 6,815 mature trees (DBH>2.5cm) of 18 species were monitored in different years for their basal growth (diameter at breast height 1.3m) and survivorship (dead or alive). There are many more plant species in the area; the chosen species were selected based on their abundance. Trees are usually selected by a minimum diameter of 2.5 cm and continuously monitored, and new individuals are introduced in each new period through natural replacement (recruitment) (Lawrence et al., 2012; Sliver et al., 2013). Thus, the start date of monitoring varied between individuals as they were measured only after their DBH>2.5cm.

Leaf habit data was obtained for species from the www.missouribotanicalgarden.org. The models included the stand structure variables to account for the possible effect of the study plot and the competition between trees in the same plot. Stand structure variables include total basal area (BA) per plot.

$$\text{BA per plot} = \left(\left(\Sigma \frac{\pi \left(\frac{d}{2}\right)^2}{10{,}000}\right)\right) \ldots\ldots\ldots\ldots\ldots\ldots\ldots\ldots\ldots\ldots\ldots\ldots\ldots\ldots\ldots\ldots\ldots\ldots\ldots\ldots\ldots\ldots\ldots Eqn\ 1$$

Where d is the diameter at breast height for each tree species in the sample plot.

Data Analysis

R 1.2.5033 (R Core Team, 2019) was used for data analyses and visualization. Statistical significance for each test was determined on a 95% confidence interval. Survival analysis was done using the survival and coxed packages (R Core Team, 2019).

Mortality Analysis

We calculated the annual tree mortality rates for the time series of collected data as

$N_{(t+1)} = N_t e^{-rt}$ ……………………………………………………………………Eqn 2

thus, $r = -\ln\left(\frac{N(t+1)}{N(t)}\right) / \text{t}$ ………………………………………………………………Eqn 3

, where *N(t)* is the number of survivors at time t, $N_t$is the initial number of trees, r is the mortality rate, and $N_{(t+1)}$ is the number of survivors at time t + 1 (Sheil et al., 1995). This annual mortality rate is used in subsequent graphical representations and analysis.

We performed the exploratory data analysis using line graphs, bar charts, violin plots, etc.. We used the Kaplan-Meier estimator for the survival analysis, which models survival as a function of time and other covariates (Table 4.1).

The variable "Time" (T) represents the number of years from when a tree was first measured until the year it died. Trees that lived past the 29-year observation period are treated as censored observations that are considered alive.

Table 4.1: Biotic, climatic and hydrologic variables selected for the analysis and their units.

Variable	Description	Abbreviation	Data source	Units
Time Variable	Period of observation (years) for each tree	Tree	Field Data	Years
Biotic	Dead(1) or Alive (0)	Status	Field Data	
	Tree Species	Species	Field Data	
	Diameter at Breast Height	DBH	Field Data	cm
	Basal Area Per Plot for each year of the measurement	Basal Area Per Plot	Derived from DBH	
	Leaf habit (Evergreen or Deciduous)	Leaf Habit	TRY database	
Climatic	Mean Annual temperature of the last three years	Past Three Years' Temperature	PRISM	Celsius
	Mean annual temperature throughout the period of observation for each tree	Lagged Temperature	PRISM	Celsius
	Mean annual precipitation of the last three years.	Past Three Years Precipitation	PRISM	mm
	Mean annual precipitation throughout the period of observation for each tree	Lagged Temperature	PRISM	mm

Hydrologic	Highest Tide height in the past three years	Past Three Years Highest Tide	NOAA	m
	Tide Frequency in the past three years	Past Three Years Tide Frequency	NOAA	$3yr^{-1}$

We used the nonparametric Kaplan-Meier estimator, implemented in the survival package (Therneau, 2018), to evaluate significant differences in observed survival probabilities among various tree species. Our analysis focused on the observation period up to 29 years, T, at the beginning (1994) and end of the observation interval (2023) to determine survival outcomes. Each tree's observation period was based on its dead (1) or alive (0) condition. The observation period was considered the time variable in the analysis instead of other parameters, such as DBH or height, because this can be indirectly interpreted as tree age (Paul et al., 2019; Brandl et al., 2020). The nonparametric Kaplan–Meier estimator of the survival function $S'(T)$ of T is defined as (Kaplan & Meier, 1958):

$$S'(T) = \prod_{i:T_{(i)} \leq T} \left(1 - \frac{d_i}{n_i}\right) \ldots\ldots\ldots\ldots\ldots\ldots\ldots\ldots\ldots\ldots\ldots\ldots\ldots Eqn\ 4$$

where $S'(0) = 1$, d_i is the trees that die at time $T_{(i)}$, and n_i represents the total number of subjects at risk at $T_{(i)}$.

The Kaplan–Meier estimator was employed to provide a descriptive overview of a tree's survival probability based on a single predictor, with all models being individual-based and using the time variable (T) as the period (years) between the tree's introduction into the inventory and its death. Since continuous variables cannot be represented in a Kaplan-Meier curve, they were

split into ranges above and below their median. Some variables like leaf habit and DBH (small, medium and large) were kept in the categorical format.

Results

Mortality Analysis

The annual tree mortality rate was lowest in the year 2000 (0.6%) and increased in 2007 (10.7%). There was a fluctuation in tree mortality from 2007 to 2023; however, it reached the highest of 12.3 % in 2022-2023 (Figure 4.1 and Table A - 2).

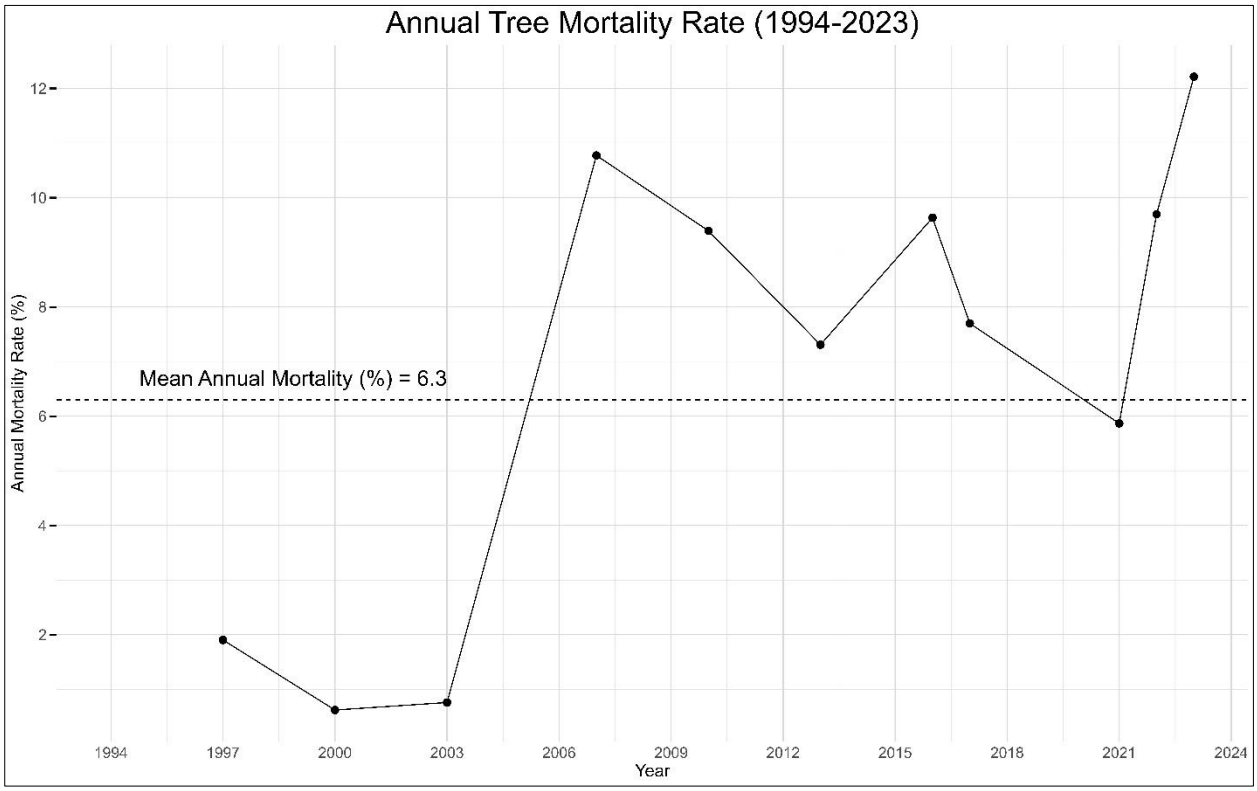

Figure 4.1: Annual tree mortality for a whole tree data set collected from 1994 to 2023 in the sample plots in Hobcaw Barony. Mean dashed line shows the mean annual mortality rate over the period of 29 years.

Overall, the mean annual tree mortality throughout 29 years was higher (7.01 %) in Plot 47 (Figure 4.2 b). Interestingly, every other plot had increasing tree mortality in 2022- 2023, but not plot 46 (Figure 4.2 and Table A - 3)

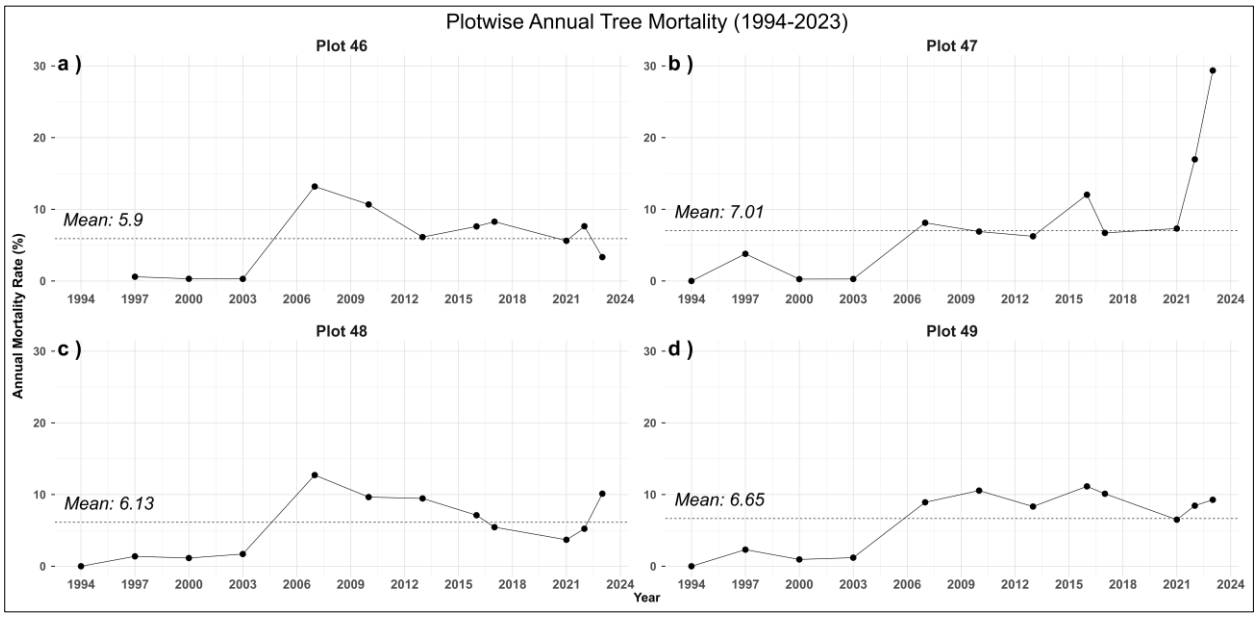

Figure 4.2: Annual mortality rates in the four sample plots in the Hobcaw Barony. Mean dashed line in each plot shows the mean annual mortality over the period of 29 years.

Of the identified 18 taxa, *Pinus taeda* emerged as the dominant species, constituting 4950 occurrences within the surveyed four sample plots. Following *Pinus taeda, Morella cerifera* exhibited a notable presence with 741 occurrences. Similarly, *Ilex vomitoria, Liquidambar styraciflua, Persea borbonia and Quercus virginiana* were other major species in the area. (Figure 4.3).

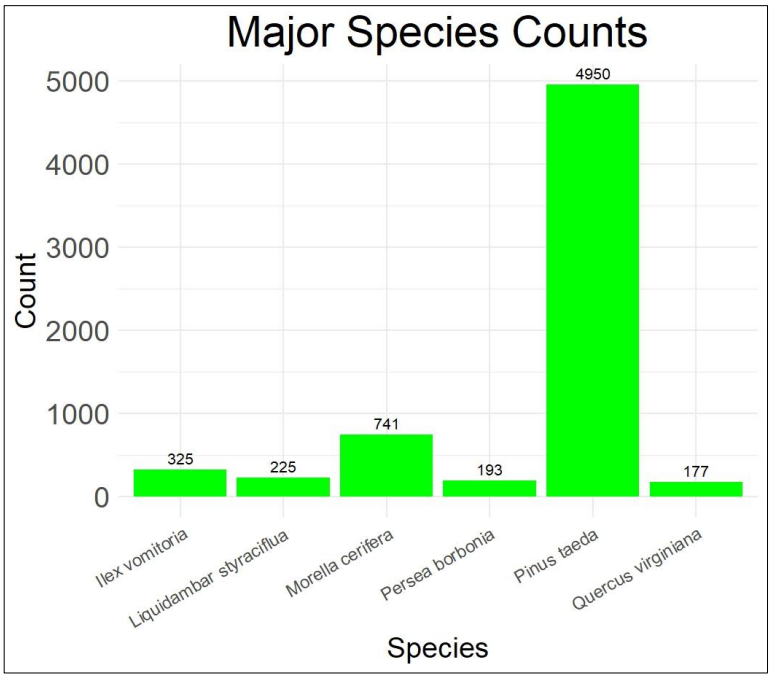

Figure 4.3: Major species counts observed in the sample plots from 1994 to 2023.

Among the species, the dominant species, *Pinus taeda* and the second dominant, *Morella cerifera*, showed a similar pattern of annual tree mortality. *Pinus taeda* had the highest mortality in the year 2007. Most of the species mortality increased in the year 2021 to 2022 while decreasing in the year 2023. Interestingly, *Persea borbonia* had the highest tree mortality of around 61% from 2013 to 2016 (Figure 4.4 and Table A - 3).

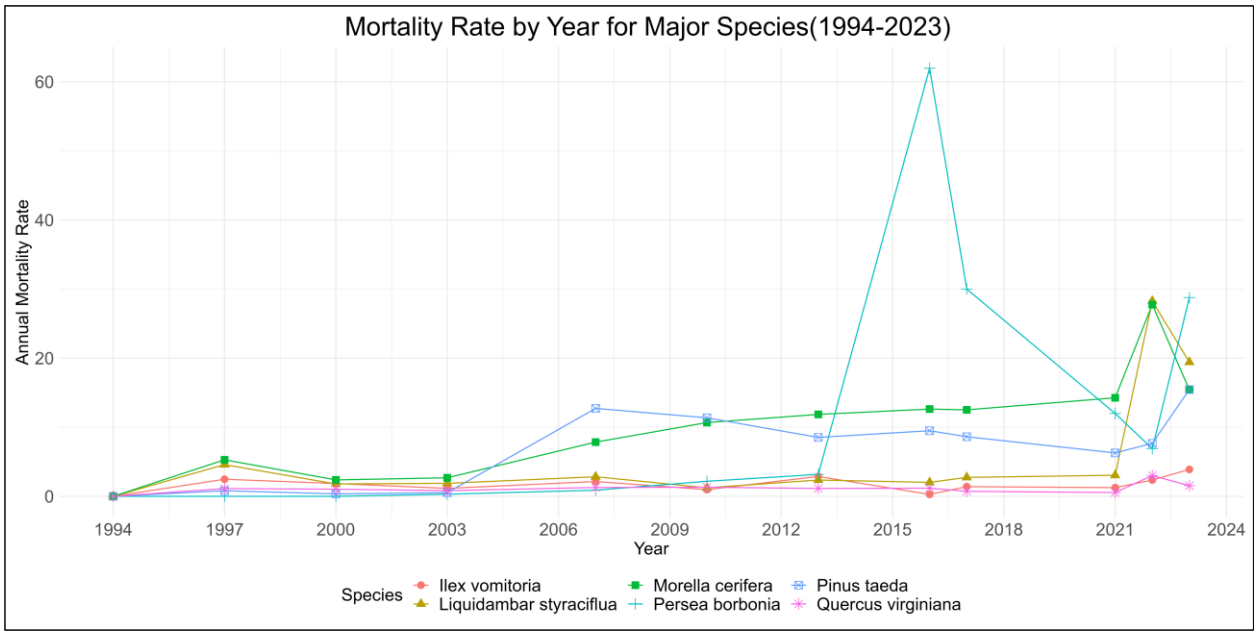

Figure 4.4: The mortality rate of major species over 29 years in a coastal forest in Hobcaw Barony, South Carolina, USA.

Evergreen plants, mostly Loblolly pine, highly dominated the area. We surveyed 6448 evergreen and 361 deciduous plants in the sample plots (Figure 4.5).

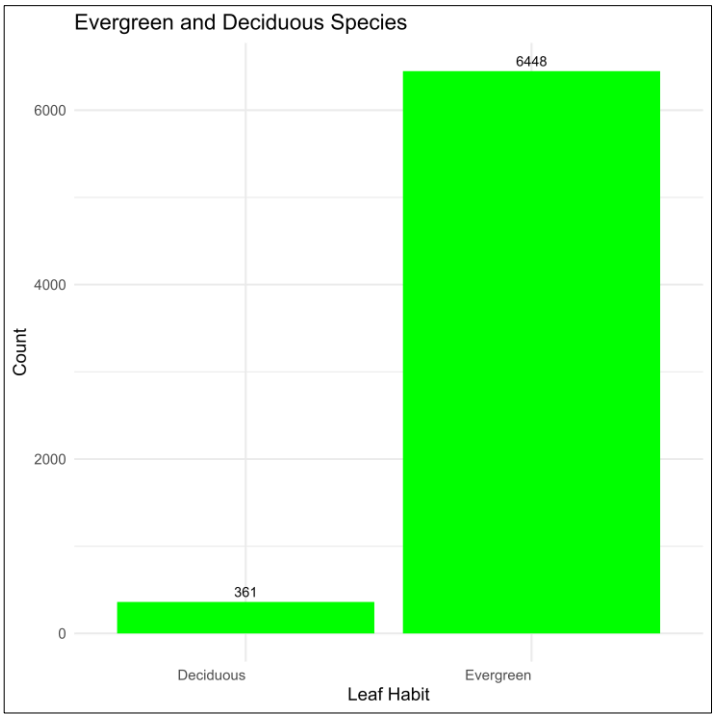

Figure 4.5: Evergreen and Deciduous Species

Evergreen plants had a higher mortality rate between the years 2003 to 2021. However, the deciduous plant had higher annual mortality from 2021 onwards (Figure 4.6).

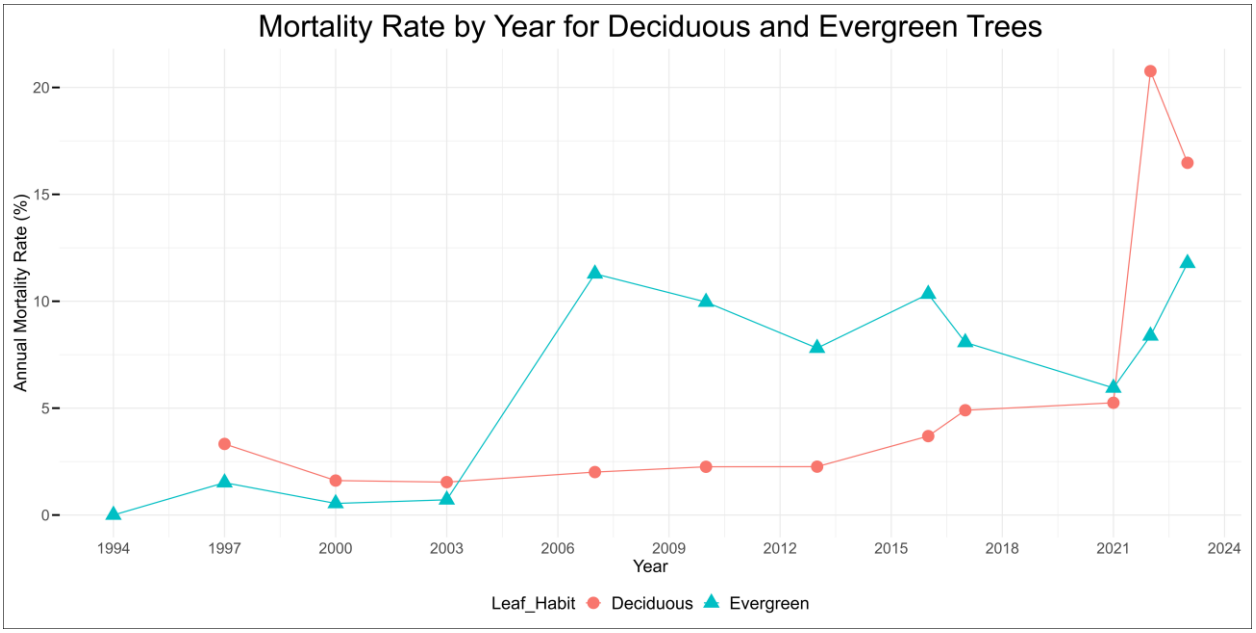

Figure 4.6: Mortality rate by year for Evergreen and Deciduous Species.

Most of the trees that died were of DBH less than 10 cm. At the species level, *Liquidambar styraciflua* showed a bit different pattern than others (Figure 4.7).

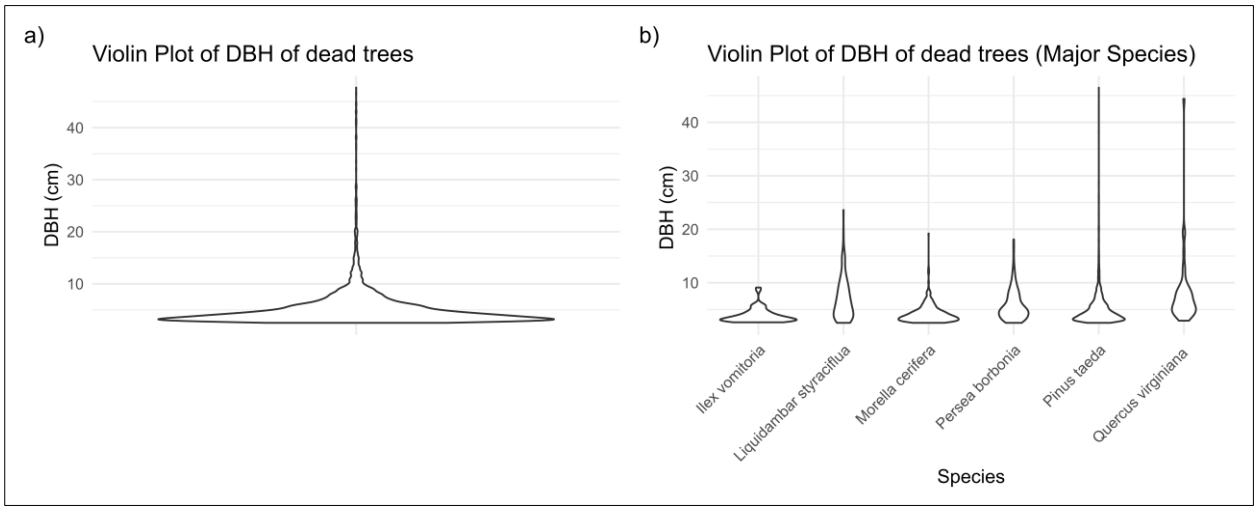

Figure 4.7: Violin plot for DBH distribution for all trees in the dataset and for trees of major species that have died.

Mean annual temperature and precipitation varied throughout the period (Figure 4.8). The scatter plot shows higher annual tree mortality with an increase in the past three years' temperature and vice versa (Figure 4.9 a). Similarly, annual tree mortality patterns fluctuated throughout the mean precipitation range of the past three years (Figure 4.9 b).

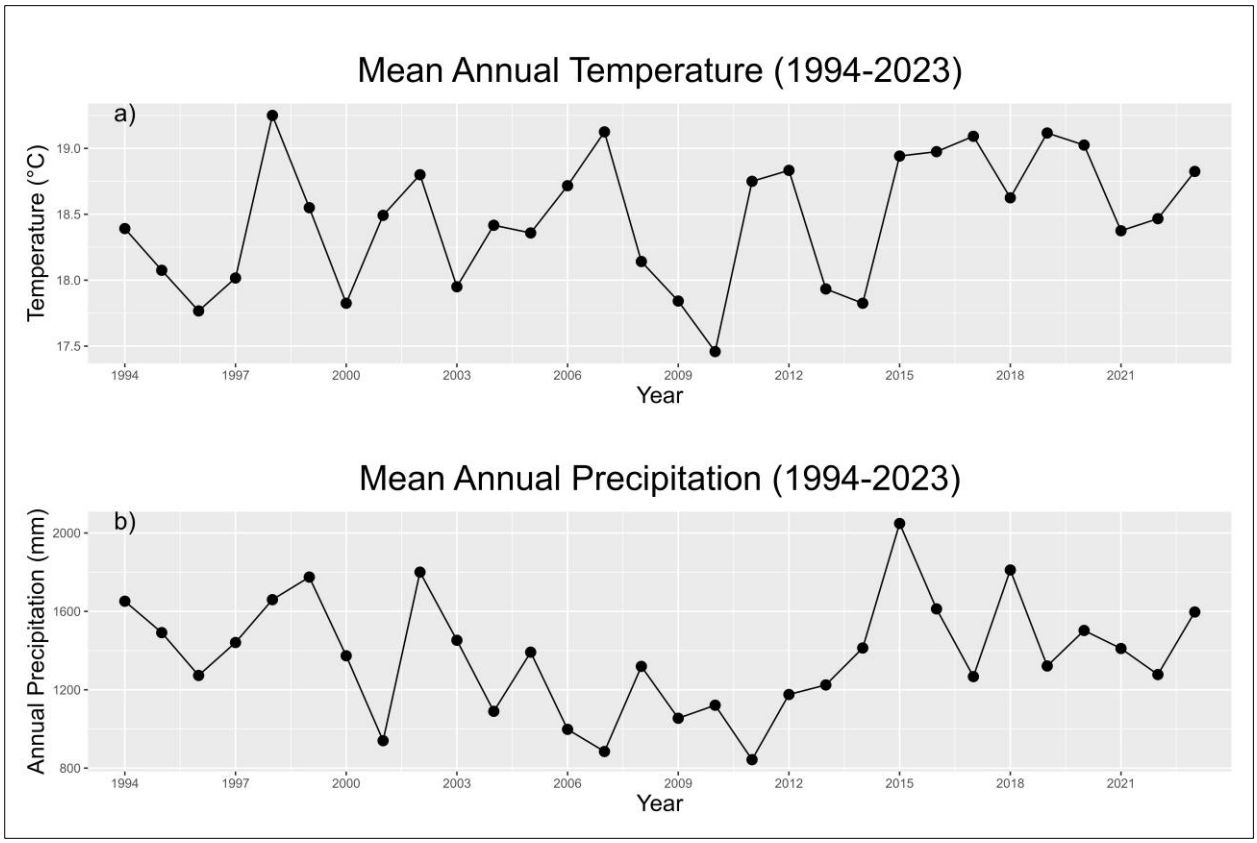

Figure 4.8: Patterns of mean annual temperature and precipitation from 1994 to 2023 in the Hobcaw Barony Forest, South Carolina, USA.

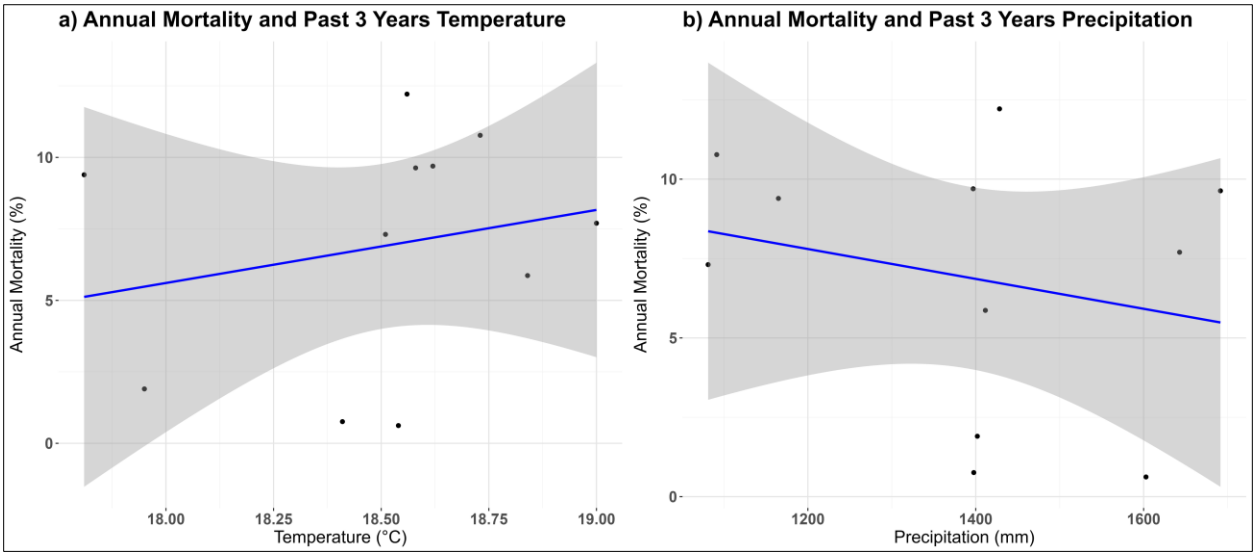

Figure 4.9: Mortality rate by year for temperature and precipitation variables.

The highest tide occurred in 2022 during Hurricane Ian, and the trend line shows the tide height increasing over the years (Figure 4.10). By examining the graph of the highest tides from the past three years alongside annual tree mortality rates, we can identify a pattern: annual tree mortality tends to rise and fall in correlation with the increasing and decreasing tide heights from 2017 to 2023. Moreover, there were higher tides after 2015 (Figure 4.11).

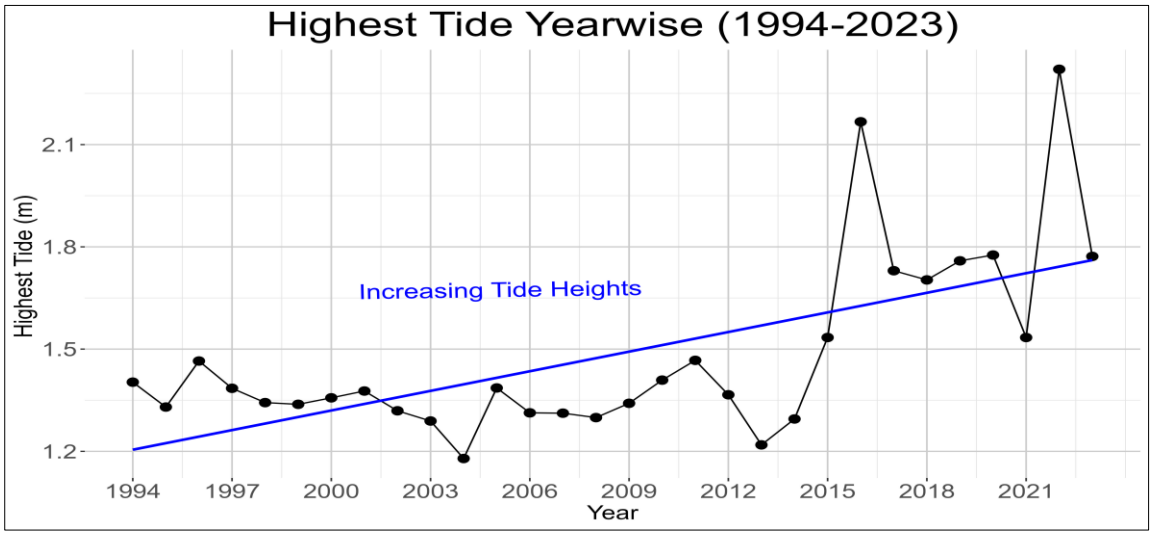

Figure 4.10: Highest tides since 1994 and increasing trend of the tide heights.

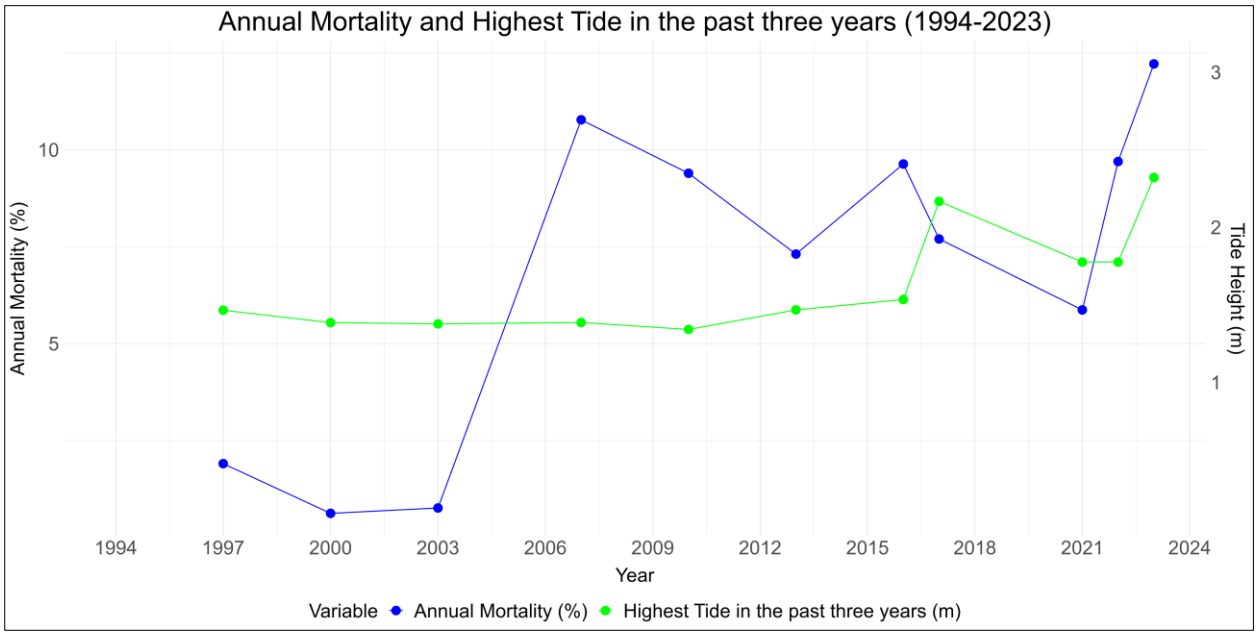

Figure 4.11: Annual mortality rate and the highest tide in the past three years for the period of 29 years from 1994-2003.

Kaplan-Meier survival analysis indicated that the survival probability of trees rapidly decreased up to 10 cm DBH and tapered off thereafter (Figure 4.12 a). Furthermore, survival probability gradually decreased with time, and there was only a 20% probability that a tree would survive for 30 years (Figure 4.12 b).

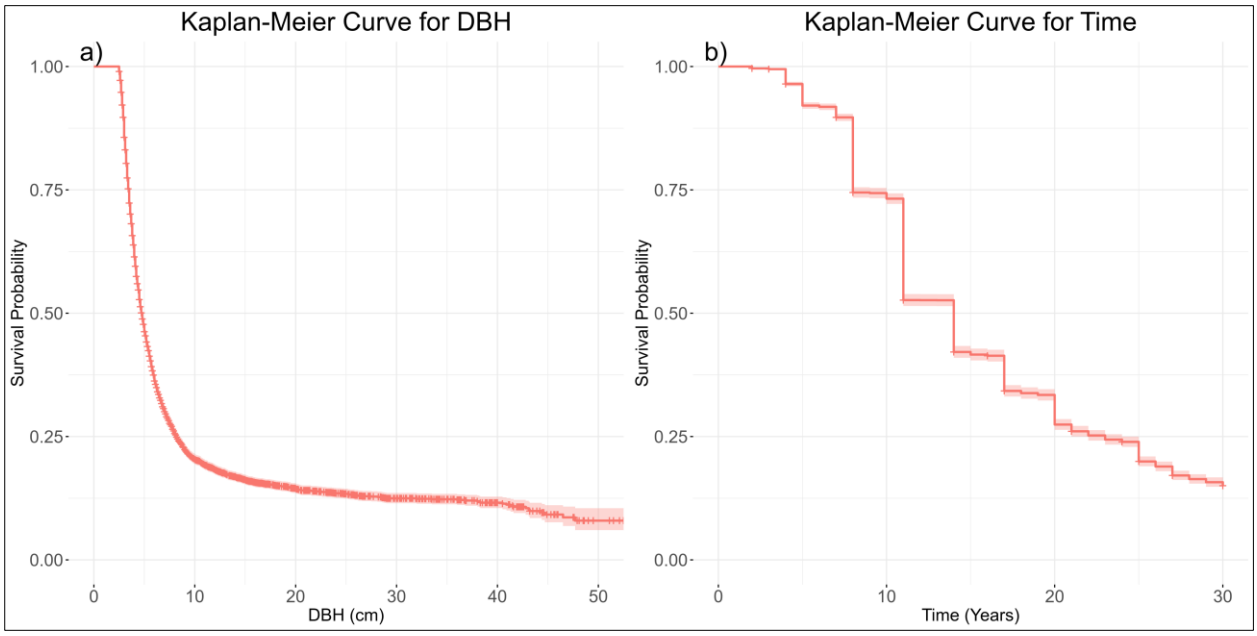

Figure 4.12: Kaplan Meier curve for the tree mortality with DBH and period of observation in years (Time) as a time variable.

The survival probability ranking of various major species is as follows: Live Oak (*Quercus virginiana*), Yaupon (*Ilex vomitoria*), Sweetgum (*Liquidambar styraciflua*), Loblolly Pine (*Pinus taeda*), Wax Myrtle (*Morella cerifera*), and Red Bay (*Persea borbonia*). Specifically, Loblolly Pine (*Pinus taeda*) exhibited a survival probability of approximately 15% over a span of 29 years. Interestingly, Red Bay (*Persea borbonia*) demonstrated highly fluctuating survival rates after the first 18 years (Figure 4.13).

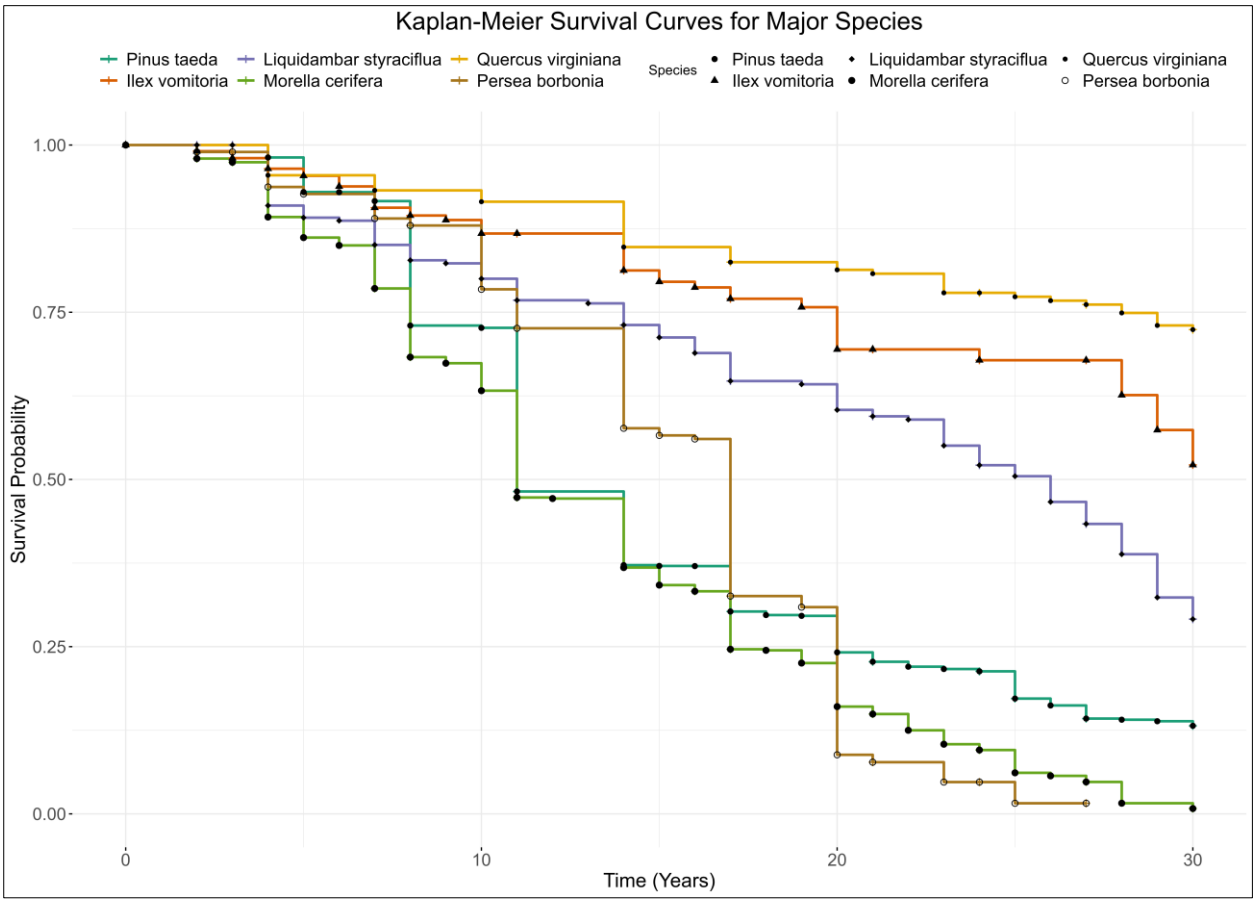

Figure 4.13: Kaplan Meier Survival Analysis for major species over the period of 29 years from 1994 to 2023.

Larger trees with a DBH greater than 10 cm exhibited a higher survival probability (Figure 4.14 a). Deciduous trees also demonstrated a higher survival probability (Figure 4.14 b). Moreover, trees in plots with higher total basal areas had a lower survival probability (Figure 4.14 c).

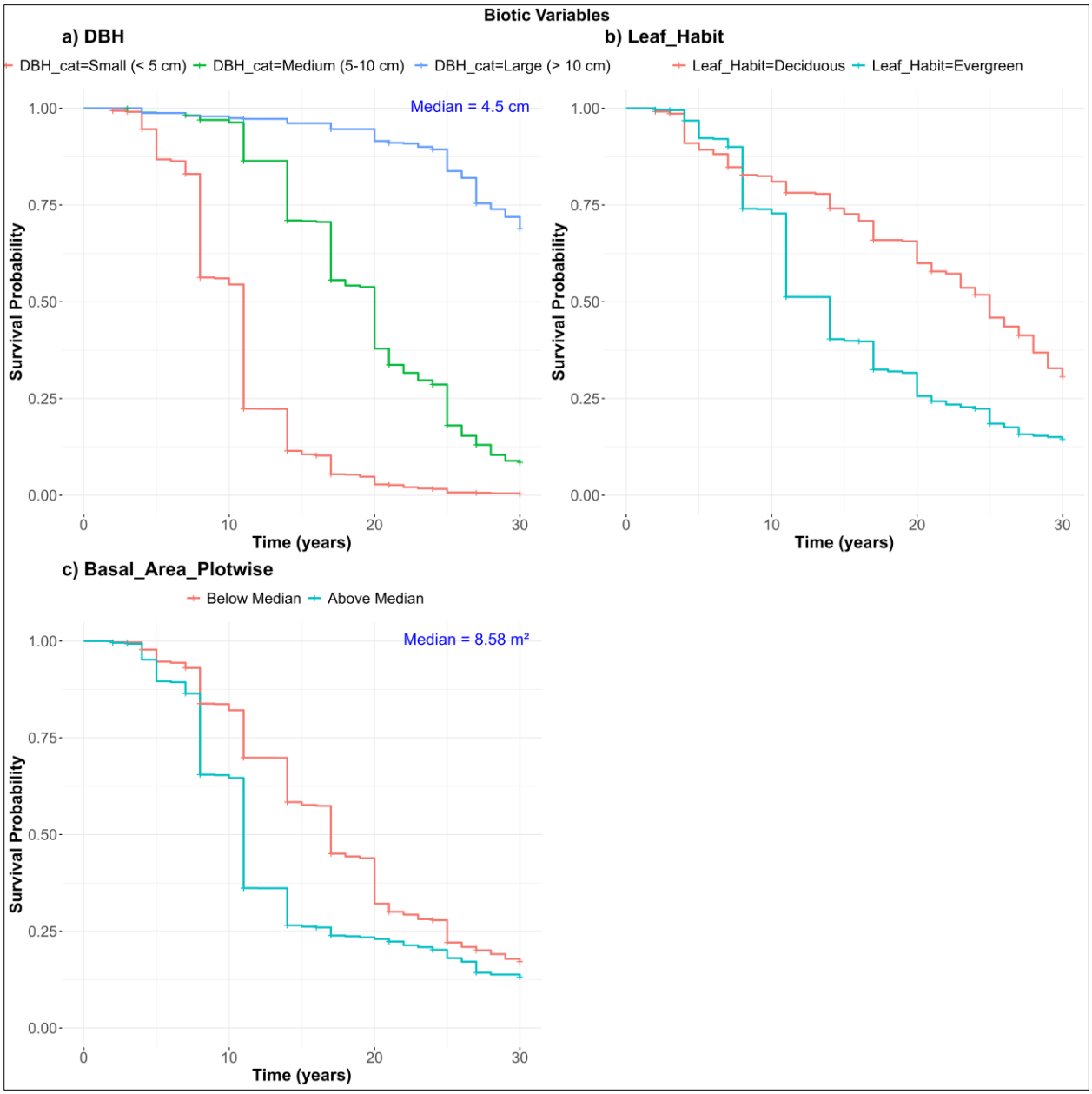

Figure 4.14: Kaplan-Meier Survival Analysis curve for the biotic variables for the period of 29 years. Biotic variables included the DBH, leaf habit and total basal area in a plot. DBH is further categorized as small, medium and large.

There was a higher survival probability when the mean annual temperature and precipitation in the past three years were below the median of 18.63 °C and 1164 mm, respectively. (Figure 4.15 a, c). Lagged climate (climate throughout the tree's survival period)

also influenced tree survival, and there was a higher survival probability in low lagged temperatures and precipitation (Figure 4.15 b, d).

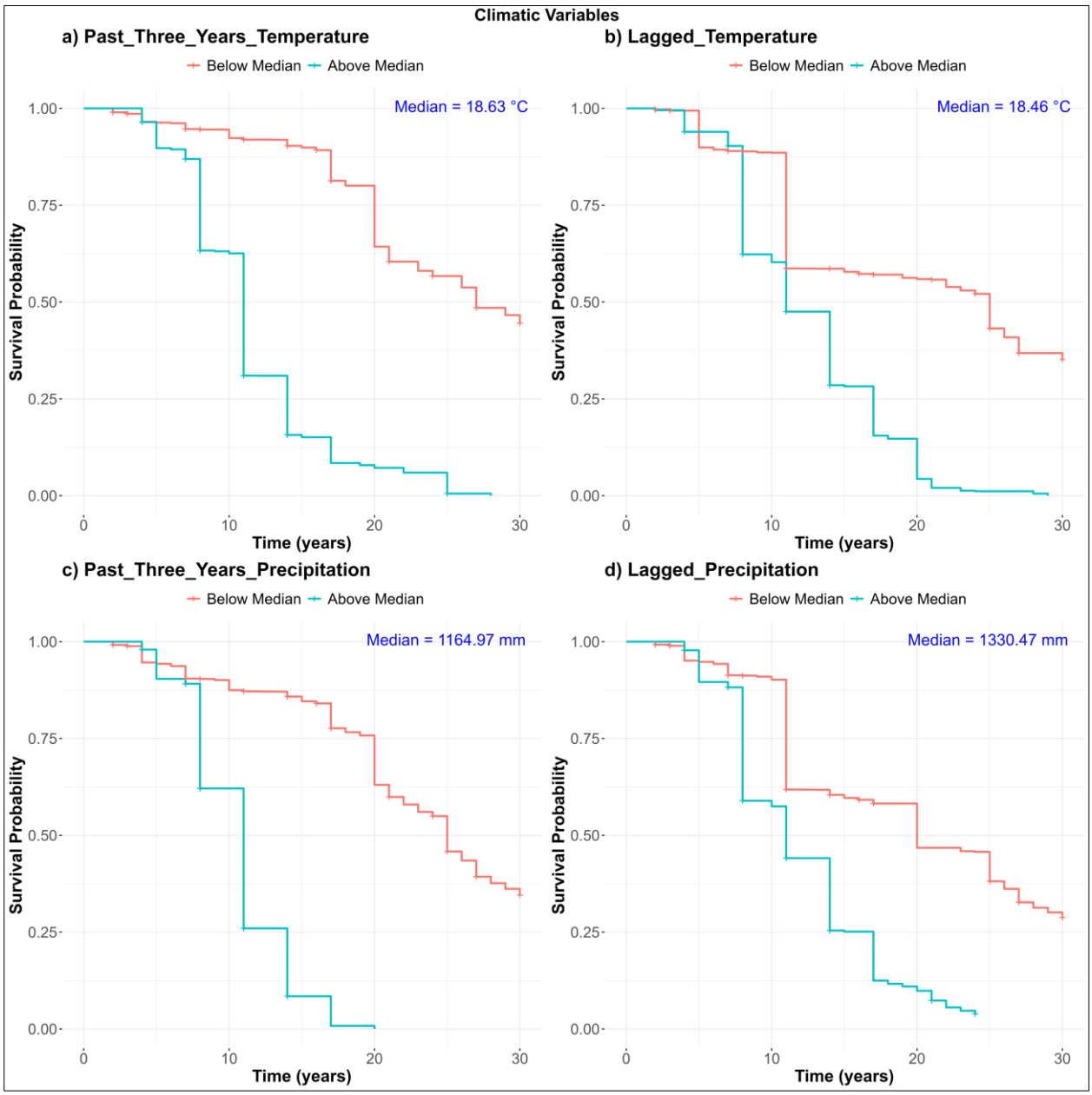

Figure 4.15: Kaplan-Meier Survival Analysis curve for the climatic variables for the period of 29 years. Climatic variables included temperature and precipitation data for the past three years,

as well as for a lagged period corresponding to the observation duration during the survival of each tree.

Hydrologic Variables

The tree did not survive for a longer period when there were higher tide frequencies (Figure 4.16 a) and when the height of the tides was more than the median values (Figure 4.16 b). The median value for the cumulative tide frequencies for sample plots was 7, implying that trees that faced more than 7 tides in the last three years are highly likely to die within 29 years. Moreover, if the tide height in the last three years was more than 1.47 m, there was a lower probability of survival.

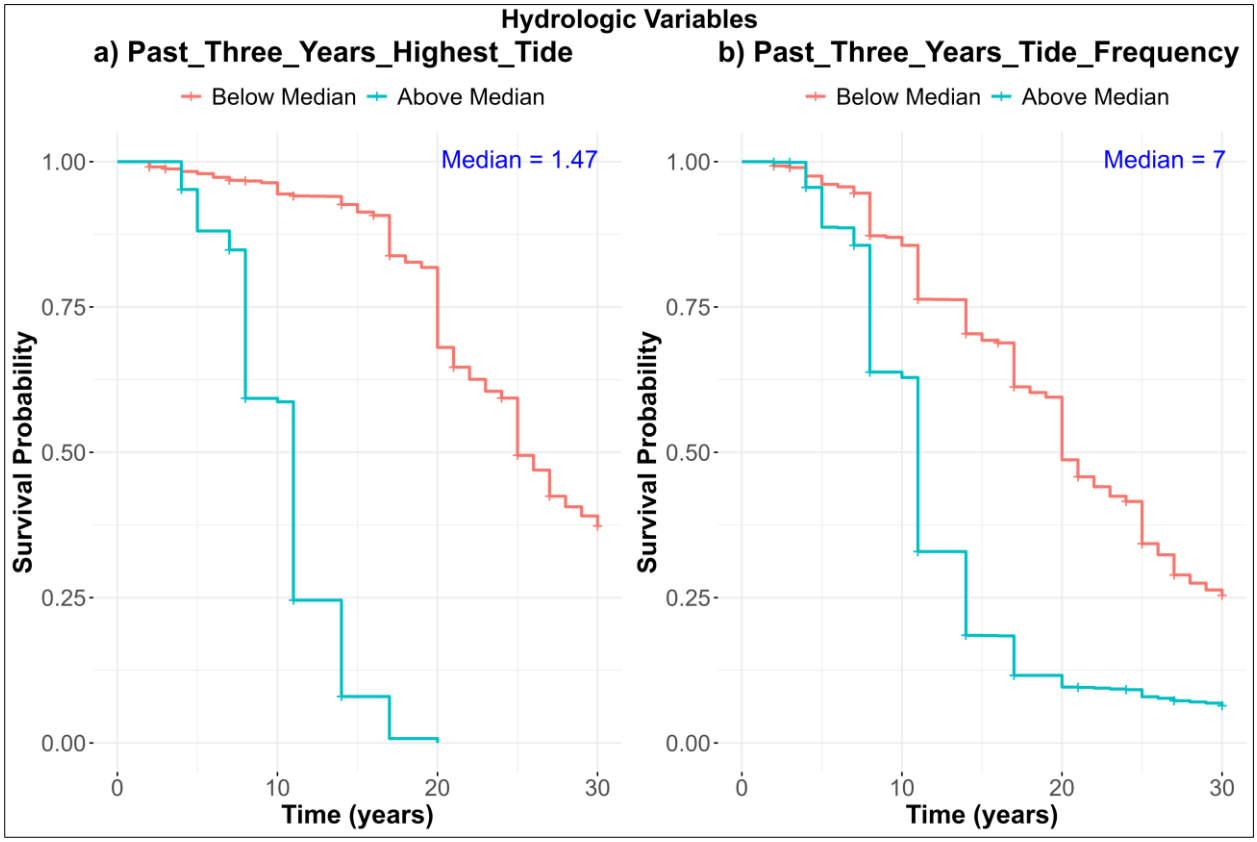

Figure 4.16: Kaplan-Meier Survival Analysis curve for the hydrologic variables for the period of 29 years. Hydrologic variables included the tide frequency and the highest tide in the past three years in each tree.

Discussion

This study assessed the mortality rates and the driving factors in the Hobcaw Barony Forest over the period of 29 years from 1994 to 2023. Annual mortality rates varied considerably across the years, with the lowest (0.6%) in 1997-2000 and the highest (12.2%) in 2022-2023. (Figure 4.1). Our results further show that the mortality rates differed among the plots for different periods of time (Figure 4.2). For major species, tree mortality increased in the year period 2022-2023 (Figure 4.3). These results, with high tree mortality in this period, may be attributed to various variables and the exceptional storm, Hurricane Ian and the recent outbreak of Southern Pine beetle in the forest, which weakened trees after the hurricane. Bellingham et al. 1996 observed species-level canopy changes in montane forests in Jamaica after Hurricane Gilbert.

Our results show that most trees died at the younger stage within a DBH of 10 cm (Figure 4.12 a). Jimenez et al. (1985) also found higher mortality in younger stands with small DBH than in mature stands in mangrove forests. Similarly, Langston et al. (2017) also underscored the harmful impact of saltwater intrusion caused by sea-level rise on the survival of young trees in coastal forests, stressing the necessity of preserving freshwater sources for the health and longevity of trees. The duration (years) after the establishment of the plot was taken as a time variable for the analysis. This duration, however, does not signify the exact tree age for most of the trees (because of right and left truncation) but can be used as a rough estimate of the tree age. This data type is common in forestry, and tree age is a significant factor influencing tree mortality (van Mantgem et al., 2009; Peng et al., 2011), with tree mortality rates in younger trees

more than double those of trees 100 years older. In this research, we also found a decreasing survival probability with time, with approximately 20% survival probability in the period of 30 years. (Figure 4.12 b). As a result, our findings are significant for bio-economic studies, which aim to integrate survival probabilities into evaluating economic risks and returns for different species in coastal forests.

Our results show that most trees died at the younger stage within a DBH of 10 cm (Figure 4.7). In the Kaplan-Meier survival curve of biotic variables (Figure 4.14 a), the larger trees tend to have a higher survival probability, which aligns with other studies (Hämäläinen et al., 2016). This may be because larger trees have established root systems and greater access to resources to efficiently absorb nonsaline water and nutrients, even during environmental stress. Additionally, their greater height and canopy spread enable them to outcompete smaller trees for sunlight, ensuring sustained growth and resilience.

Our research concludes that live oak has a higher survival probability and a lower survival probability for red bay. These results are comparable to those of Lucas & Carter (2013), who reported greater survival rates for live oak compared to pine species (slash pine) on Horn Island after Hurricane Katrina; however, we focused on the loblolly pine. Interestingly, Red Bay (*Persea borbonia*) exhibited significantly fluctuating survival rates, with a noticeable decline in survival after the 18-year period. Extensive mortality of *Persea borbonia* has been observed in the coastal plain counties of southeastern South Carolina (Fraedrich et al., 2008), with numerous studies identifying a trend of increased mortality in larger red bay stems (Shields et al., 2011; Spiegel & Leege, 2013). Kendra et al. (2013) discovered that red bay stems with larger DBH had more beetle entrance holes and advanced

disease stages than smaller stems, indicating that beetles preferentially target larger stems, possibly leading to increased tree mortality in these larger stems.

Our data is highly dominated by evergreen plants, mostly Loblolly pine, which had a higher mortality rate overall than deciduous plants (Figure 4.6). The time-based Kaplan-Meier survival model also revealed significant differences in survival probabilities between evergreen and deciduous species (Figure 4.14 b). Deciduous species exhibited higher survival probabilities at various stages. This finding is consistent with the conclusions of Aleixo et al. (2019), who also observed variations in survival linked to the leaf habits of the species. This finding can also be attributed to the research done by Givnish (2002), who investigated the adaptive significance among species and found that deciduous species acquire substantial amounts of nutrients, such as phosphorus and nitrogen, which provide a competitive advantage when coexisting with evergreen species.

Additionally, to refer to practical forest management, it is also necessary to show tree survival as a function of the basal area since it is also a component of silviculture. Woodall et al. (2005) discovered that the influence of covariates basal area in the plot was significant in the smaller diameter at breast height (DBH) classes. We found a lower survival probability in the plots with higher basal area (Figure 4.14 c). Bradford & Bell et al. (2017) found lower mortality in the plot with the lower basal area and suggested reducing forest basal area to decrease the tree competition; however, it was the case of drought-induced tree mortality. An increase in basal area per hectare can lead to overcrowding, leading to intense competition that may raise the tree mortality rate in the forest (Wiegand et al., 2006; Moustakas et al., 2008; Zhang et al., 2015). Interestingly, after a 15-year period, the Kaplan-Meier curves for above and below the median

basal area per plot appear to converge (Figure 4.14 c), suggesting that the effect of basal area per plot on survival probability becomes relatively minor or decreases over time after a certain period.

Annual tree mortality increased with higher temperatures in the past three years, though mortality patterns varied across different precipitation levels. (Figure 4.9 a, b). Moreover, the Kaplan-Meier curve analysis also depicts the varying results for climatic variables (Figure 4.15). Understanding the impact of climate variability on mortality is more challenging than just a straightforward relationship with temperature (Adams et al., 2009), and our result asserted this statement. Survival probability was higher at lower lagged temperatures. This is supported by studies on plant physiological processes, which indicate that higher temperatures lead to increased respiration costs and faster carbon starvation in trees, causing greater stress (Atkin et al., 2007). Neumann et al. (2017) also concluded that maximum temperatures significantly affect mortality, with extremely hot conditions increasing the likelihood of tree death.

The trees sampled for this study were all subjected to varying degrees of hydrologic factors like tide height and frequency. The height of the tides has been increasing in recent years since 2015 (Figure 4.10). We also noticed trends linking increased annual tree mortality with the higher tide in the last three years in the period from 2017 to 2023. (Figure 4.11). Kaplan Meier survival curve analysis also showed a higher survival probability when there was lower tide frequency and low tide height in the last three years (Figures 4.16 a, b). The higher the tide frequency and the higher the tide in the storm surge, the higher the probability of salt stress in the plots, which might be the reason for such results. In the research done by Williams et al. (1999),

the plants in the plots had a high survival rate when there was less tidal flooding on the west coast of Florida.

Limitations of the study

Firstly, the absence of GPS coordinates for each tree species necessitated using the sample plot center to represent all trees when calculating distances from marshes and streams. This approach may have introduced spatial inaccuracies and limited the precision of our distance measurements.

Secondly, we didn't have data on freshwater aquifers and soil salinity, as well as critical hydrologic and edaphic factors influencing tree mortality, which is another significant limitation. Moreover, the tide heights and tide frequency data were not available at the nearest Oyster Creek station all the time. We had to gather the data from another station, Springmaid Pier, which is almost 20 miles far from the study site. This might also have brought some discrepancies in the analysis and results.

Furthermore, the study did not encompass biological factors such as pest and pathogen infestations, which are known to play pivotal roles in tree mortality dynamics. The exclusion of these variables may have restricted our ability to fully elucidate the complex interactions between environmental stressors and tree mortality rates observed in the coastal forest ecosystem.

Conclusion

We found fluctuations in the years of tree mortality throughout the observation period of 29 years. There were differences in mortality among species, which was obvious due to

differences in how each species responds to each variable. Despite some limitations due to the unevenly distributed data (pine-dominated), we could fit nonparametric and parametric survival models to the data. Survival models were applied using the R survival package, which enables the incorporation of time-varying covariates into the models.

This approach allowed for the comparison of the impacts of various potential mortality drivers, including time-varying covariates that changed annually (such as temperature, precipitation, basal area plotwise, DBH, highest tide, and tide frequency) with those that remained constant throughout the study (such as leaf habit and species). Most variables showed obvious differences in the survival probabilities while looking at the Kaplan-Meier curves. Regarding the underlying data, it is crucial to highlight the importance of continuous observation programs and obtaining more precise information on tree age and location (GPS coordinates). We can monitor some sample seedlings for each species for the long term and estimate the age of the other trees of the same species to incorporate the exact age information in the data. The models can be integrated into ecological simulations to assess risk to coastal tree species under various future climate scenarios, and survival probability functions can inform species selection strategies in coastal areas.

REFERENCES

1. Adams, H. D., Guardiola-Claramonte, M., Barron-Gafford, G. A., Villegas, J. C., Breshears, D. D., Zou, C. B., ... & Huxman, T. E. (2009). Temperature sensitivity of drought-induced tree mortality portends increased regional die-off under global-change-type drought. Proceedings of the national academy of sciences, 106(17), 7063-7066.
2. Adams, H. D., Zeppel, M. J., Anderegg, W. R., Hartmann, H., Landhäusser, S. M., Tissue, D. T., ... & McDowell, N. G. (2017). A multi-species synthesis of physiological mechanisms in drought-induced tree mortality. *Nature ecology & evolution*, *1*(9), 1285-1291.
3. Aleixo, I., Norris, D., Hemerik, L., Barbosa, A., Prata, E., Costa, F., & Poorter, L. (2019). Amazonian rainforest tree mortality driven by climate and functional traits. Nature Climate Change, 9(5), 384-388. https://doi.org/10.1038/s41558-019-0458-0
4. Ali, G. A., & Roy, A. G. (2010). Shopping for hydrologically representative connectivity metrics in a humid temperate forested catchment. Water Resources Research, 46(12).
5. Allen, C. D., Macalady, A. K., Chenchouni, H., Bachelet, D., McDowell, N., Vennetier, M., ... & Cobb, N. (2010). A global overview of drought and heat-induced tree mortality reveals emerging climate change risks for forests. *Forest ecology and management*, *259*(4), 660-684.
6. Allen, T. D., Golden, T. D., & Shockley, K. M. (2015). How effective is telecommuting? Assessing the status of our scientific findings. *Psychological science in the public interest*, *16*(2), 40-68.
7. Atkin, O. K., Scheurwater, I., & Pons, T. L. (2007). Respiration as a percentage of daily photosynthesis in whole plants is homeostatic at moderate, but not high, growth temperatures. New Phytologist, 174(2), 367-380.

8. Bellingham, P. J., Tanner, E. V. J., Rich, P. M., & Goodland, T. C. R. (1996). Changes in light below the canopy of a Jamaican montane rainforest after a hurricane. Journal of Tropical Ecology, 12(5), 699-722.
9. Bigler, C., Bräker, O. U., Bugmann, H., Dobbertin, M., & Rigling, A. (2006). Drought as an inciting mortality factor in Scots pine stands of the Valais, Switzerland. *Ecosystems*, *9*, 330-343.
10. Boeck, A., Dieler, J., Biber, P., Pretzsch, H., & Ankerst, D. P. (2014). Predicting tree mortality for European beech in southern Germany using spatially explicit competition indices. Forest Science, 60(4), 613-622.
11. Bradford, J. B., & Bell, D. M. (2017). A window of opportunity for climate-change adaptation: Easing tree mortality by reducing forest basal area. Frontiers in Ecology and the Environment, 15(1), 11-17. https://doi.org/10.1002/fee.1445
12. Brandl, S., Paul, C., Knoke, T., & Falk, W. (2020). The influence of climate and management on survival probability for Germany's most important tree species. *Forest Ecology and Management*, *458*, 117652.
13. Carpenter, S. R., & Gunderson, L. H. (2001). Coping with Collapse: Ecological and Social Dynamics in Ecosystem Management: Like flight simulators that train would-be aviators, simple models can be used to evoke people's adaptive, forward-thinking behavior, aimed in this instance at sustainability of human–natural systems. BioScience, 51(6), 451-457.
14. Church, J. A., Clark, P. U., Cazenave, A., Gregory, J. M., Jevrejeva, S., Levermann, A., ... & Unnikrishnan, A. S. (2013). *Sea level change*. PM Cambridge University Press.

15. Cox, R., Lowe, D. R., & Cullers, R. L. (1995). The influence of sediment recycling and basement composition on evolution of mudrock chemistry in the southwestern United States. *Geochimica et Cosmochimica Acta*, *59*(14), 2919-2940.
16. Dakos, V., Scheffer, M., Van Nes, E. H., Brovkin, V., Petoukhov, V., & Held, H. (2008). Slowing down as an early warning signal for abrupt climate change. Proceedings of the National Academy of Sciences, 105(38), 14308-14312.
17. Fernández-Berrocal, P., & Aranda, D. R. (2008). La inteligencia emocional en la educación. *Electronic Journal of Research in Education Psychology*, *6*(15), 421-436.
18. Field, C. R., Gjerdrum, C., & Elphick, C. S. (2016). Forest resistance to sea-level rise prevents landward migration of tidal marsh. Biological Conservation, 201, 363-369. https://doi.org/10.1016/j.biocon.2016.07.035
19. Fraedrich, S. W. (2008). California laurel is susceptible to laurel wilt caused by Raffaelea lauricola. Plant Disease, 92(12), 1469.
20. Givnish, T. J. (2002). Adaptive significance of evergreen vs. deciduous leaves: solving the triple paradox. Silva fennica, 36(3), 703-743.
21. Hämäläinen, A., Hujo, M., Heikkala, O., Junninen, K., & Kouki, J. (2016). Retention tree characteristics have major influence on the post-harvest tree mortality and availability of coarse woody debris in clear-cut areas. Forest Ecology and Management, 369, 66-73. https://doi.org/10.1016/j.foreco.2016.03.037
22. Herbert, R. A. (1999). Nitrogen cycling in coastal marine ecosystems. *FEMS microbiology reviews*, *23*(5), 563-590.
23. Hook, D. D., Buford, M. A., & Williams, T. M. (1991). Impact of Hurricane Hugo on the South Carolina coastal plain forest. *Journal of Coastal Research*, 291-300.

24. Hülsmann, L., Bugmann, H. K., Commarmot, B., Meyer, P., Zimmermann, S., & Brang, P. (2016). Does one model fit all? Patterns of beech mortality in natural forests of three European regions. Ecological applications, 26(8), 2465-2479.

25. Jimenez, J. A., Lugo, A. E., & Cintron, G. (1985). Tree mortality in mangrove forests. Biotropica, 177-185.

26. Kaplan, E. L., & Meier, P. (1958). Nonparametric estimation from incomplete observations. *Journal of the American statistical association*, *53*(282), 457-481.

27. Kendra, P. E., Montgomery, W. S., Niogret, J., & Epsky, N. D. (2013). An uncertain future for American Lauraceae: A lethal threat from red bay ambrosia beetle and laurel wilt disease (a review). American Journal of Plant Sciences, 4(5), 727–738.

28. Langston, A. K., Kaplan, D. A., & Putz, F. E. (2017). A casualty of climate change? Loss of freshwater forest islands on Florida's Gulf Coast. *Global Change Biology*, *23*(12), 5383-5397. https://doi.org/10.1111/gcb.13805

29. Larson, A. J., Lutz, J. A., Donato, D. C., Freund, J. A., Swanson, M. E., HilleRisLambers, J., ... & Franklin, J. F. (2015). Spatial aspects of tree mortality strongly differ between young and old-growth forests. https://doi.org/10.1890/15-0628.1

30. Lawrence, A. B., Escobedo, F. J., Staudhammer, C. L., & Zipperer, W. (2012). Analyzing growth and mortality in a subtropical urban forest ecosystem. Landscape and Urban Planning, 104(1), 85-94.

31. Lucas, K. L., & Carter, G. A. (2013). Change in distribution and composition of vegetated habitats on Horn Island, Mississippi, northern Gulf of Mexico, in the initial five years following Hurricane Katrina. Geomorphology, 199, 129-137.

32. McDowell, N., Pockman, W. T., Allen, C. D., Breshears, D. D., Cobb, N., Kolb, T., ... & Yepez, E. A. (2008). Mechanisms of plant survival and mortality during drought: why do some plants survive while others succumb to drought?. *New phytologist*, *178*(4), 719-739.

33. McNellis, B. E., Smith, A. M., Hudak, A. T., & Strand, E. K. (2021). Tree mortality in western US forests forecasted using forest inventory and Random Forest classification. *Ecosphere*, *12*(3), e03419.

34. Mori, S. A., & Becker, P. (1991). Flooding affects survival of Lecythidaceae in terra firme forest near Manaus, Brazil. *Biotropica*, *23*(1), 87-90.

35. Morris, J. T., Sundareshwar, P. V., Nietch, C. T., Kjerfve, B., & Cahoon, D. R. (2002). Responses of coastal wetlands to rising sea level. Ecology, 83(10), 2869-2877.

36. Moustakas, A., Wiegand, K., Getzin, S., Ward, D., Meyer, K. M., Guenther, M., & Mueller, K. H. (2008). Spacing patterns of an Acacia tree in the Kalahari over a 61-year period: How clumped becomes regular and vice versa. acta oecologica, 33(3), 355-364.

37. Nelson, R., Kokic, P., Crimp, S., Martin, P., Meinke, H., Howden, S. M., ... & Nidumolu, U. (2010). The vulnerability of Australian rural communities to climate variability and change: Part II—Integrating impacts with adaptive capacity. *Environmental Science & Policy*, *13*(1), 18-27.

38. Neumann, M., Mues, V., Moreno, A., Hasenauer, H., & Seidl, R. (2017). Climate variability drives recent tree mortality in Europe. Global Change Biology, 23(11), 4788. https://doi.org/10.1111/gcb.13724

39. Neuner, G. (2014). Frost resistance in alpine woody plants. *Frontiers in plant science*, *5*, 654.

40. Neuner, S., Albrecht, A., Cullmann, D., Engels, F., Griess, V. C., Hahn, W. A., ... & Knoke, T. (2015). Survival of Norway spruce remains higher in mixed stands under a dryer and warmer climate. Global change biology, 21(2), 935-946.

41. Nicholls, R. J., & Cazenave, A. (2010). Sea-level rise and its impact on coastal zones. *science*, *328*(5985), 1517-1520.

42. Nothdurft, A. (2013). Spatio-temporal prediction of tree mortality based on long-term sample plots, climate change scenarios and parametric frailty modeling. Forest ecology and management, 291, 43-54.

43. Osland, M. J., Enwright, N. M., Day, R. H., Gabler, C. A., Stagg, C. L., & Grace, J. B. (2016). Beyond just sea-level rise: Considering macroclimatic drivers within coastal wetland vulnerability assessments to climate change. *Global Change Biology*, *22*(1), 1-11.

44. Osland, M. J., Enwright, N., Day, R. H., & Doyle, T. W. (2013). Winter climate change and coastal wetland foundation species: salt marshes vs. mangrove forests in the southeastern United States. *Global change biology*, *19*(5), 1482-1494. https://doi.org/10.1111/gcb.12126

45. Park Williams, A., Allen, C. D., Macalady, A. K., Griffin, D., Woodhouse, C. A., Meko, D. M., ... & McDowell, N. G. (2013). Temperature as a potent driver of regional forest drought stress and tree mortality. *Nature climate change*, *3*(3), 292-297.

46. Paul, R., & Elder, L. (2019). *The miniature guide to critical thinking concepts and tools*. Rowman & Littlefield.

47. Peng, C., Ma, Z., Lei, X., Zhu, Q., Chen, H., Wang, W., ... & Zhou, X. (2011). A drought-induced pervasive increase in tree mortality across Canada's boreal forests. *Nature climate change*, *1*(9), 467-471.

48. Phillips, O. L., Lewis, S. L., Baker, T. R., & Malhi, Y. (2011). The response of South American tropical forests to recent atmospheric changes. *Tropical Rainforest Responses to Climatic Change*, 343-358.

49. Poulter, B., & Halpin, P. N. (2008). Raster modelling of coastal flooding from sea-level rise. *International Journal of Geographical Information Science*, *22*(2), 167-182.

50. R Core Team. (2019). R: A language and environment for statistical computing. Vienna, Austria: R Foundation for Statistical Computing. Retrieved from https://www.R-project.org/

51. Sheil, D., Burslem, D. F., & Alder, D. (1995). The interpretation and misinterpretation of mortality rate measures. *Journal of Ecology*, 331-333.

52. Shields, J., Jose, S., Freeman, J., Bunyan, M., Celis, G., Hagan, D., Morgan, M., Pieterson, E. C., & Zak, J. (2011). Short-term impacts of laurel wilt on red bay (Persea borbonia [L.] Spreng.) in a mixed evergreen-deciduous forest in northern Florida. Journal of Forestry, 109(4), 828–838.

53. Silver, E. J., D'Amato, A. W., Fraver, S., Palik, B. J., & Bradford, J. B. (2013). Structure and development of old-growth, unmanaged second-growth, and extended rotation Pinus resinosa forests in Minnesota, USA. Forest Ecology and Management, 291, 110-118.

54. Singh, K. P., & Kushwaha, C. P. (2016). Deciduousness in tropical trees and its potential as indicator of climate change: A review. *Ecological indicators*, *69*, 699-706.

55. Song, B., Gresham, C. A., Trettin, C. C., & Williams, T. M. (2012). Recovery of coastal plain forests from Hurricane Hugo in South Carolina, USA, fourteen years after the storm. *Tree For Sci Biotechnol*, *6*(Special Issue 1), 60-8.

56. Spiegel, K. S., & Leege, L. M. (2013). Impacts of laurel wilt disease on red bay (Persea borbonia [L.] Spreng.) population structure and forest communities in the coastal plain of Georgia, USA. Biological Invasions, 15(11), 2467–2487.

57. Staupendahl, K., & Zucchini, W. (2011). Estimating survival functions for the main tree species based on time series data from the forest condition survey in Rheinland-Pfalz, Germany.

58. Therneau, T. (2018). Survival analysis (Version 2.42-6): CRAN R Development Team

59. Thorne, K., MacDonald, G., Guntenspergen, G., Ambrose, R., Buffington, K., Dugger, B., ... & Takekawa, J. (2018). US Pacific coastal wetland resilience and vulnerability to sea-level rise. Science Advances, 4(2), eaao3270.

60. Timilsina, N., & Staudhammer, C. L. (2012). Individual Tree Mortality Model for Slash Pine in Florida: A Mixed Modeling Approach. Southern Journal of Applied Forestry, 36(4), 211-219. https://doi.org/10.5849/sjaf.11-026

61. Twilley, R. R., Barron, E. J., Gholz, H. L., Harwell, M. A., & Zimmerman, R. J. (2001). Confronting climate change in the Gulf Coast region: Prospects for sustaining our ecological heritage. Union of Concerned Scientists and The Ecological Society of America. UCS Publication, Cambridge, MA.

62. Van Gunst, K. J., Weisberg, P. J., Yang, J., & Fan, Y. (2016). Do denser forests have greater risk of tree mortality: A remote sensing analysis of density-dependent forest mortality. Forest Ecology and Management, 359, 19-32. https://doi.org/10.1016/j.foreco.2015.09.032

63. Van Mantgem, P. J., Stephenson, N. L., Byrne, J. C., Daniels, L. D., Franklin, J. F., Fulé, P. Z., ... & Veblen, T. T. (2009). Widespread increase of tree mortality rates in the western United States. Science, 323(5913), 521-524.

64. Walker, L. R. (1991). Tree damage and recovery from Hurricane Hugo in Luquillo experimental forest, Puerto Rico. *Biotropica*, 379-385.

65. Waring, R. H. (1987). Characteristics of trees predisposed to die. Bioscience, 37(8), 569-574.

66. Wiegand, T., Kissling, W. D., Cipriotti, P. A., & Aguiar, M. R. (2006). Extending point pattern analysis for objects of finite size and irregular shape. Journal of Ecology, 94(4), 825-837.

67. Williams, K., Ewel, K. C., Stumpf, R. P., Putz, F. E., & Workman, T. W. (1999). Sea-level rise and coastal forest retreat on the west coast of Florida, USA. *Ecology*, *80*(6), 2045-2063.

68. Woodall, C., Grambsch, P., & Thomas, W. (2005). Applying survival analysis to a large-scale forest inventory for assessment of tree mortality in Minnesota. Ecological Modelling, 189(1-2), 199-208. https://doi.org/10.1016/j.ecolmodel.2005.04.011

69. Yaussy, D. A., Iverson, L. R., & Matthews, S. N. (2013). Competition and climate affects US hardwood-forest tree mortality. *Forest Science*, *59*(4), 416-430.

70. Yu, M., & Gao, Q. (2020). Topography, drainage capability, and legacy of drought differentiate tropical ecosystem response to and recovery from major hurricanes. *Environmental Research Letters*, *15*(10), 104046.

71. Zhang, J., Huang, S., & He, F. (2015). Half-century evidence from western Canada shows forest dynamics are primarily driven by competition followed by climate. Proceedings of the National Academy of Sciences, 112(13), 4009-4014. https://doi.org/10.1073/pnas.1420844112

72. Zimmerman, J. K., Everham III, E. M., Waide, R. B., Lodge, D. J., Taylor, C. M., & Brokaw, N. V. (1994). Responses of tree species to hurricane winds in subtropical wet forest in Puerto Rico: implications for tropical tree life histories. *Journal of ecology*, 911-922.

APPENDICES

Table A - 1: Correlation among the variables

Variables	Water Depth	Curvature	DistanceFrmMarsh	DistanceFrmStream
Water Depth	1	-0.05903	-0.20953	-0.1632
Curvature	-0.05903442	1	-0.02238	0.00837
Distance From Marsh	-0.20952645	-0.02238	1	-0.01848
Distance From Stream	-0.16320335	0.008373	-0.01848	1

Table A - 2: Annual mortality rate over the years for the period of 29 years (1994-2023)

Year	Annual Mortality Rate (%)
1994	NA
1997	1.90
2000	0.62
2003	0.75
2007	10.77
2010	9.39
2013	7.30
2016	9.63

2017	7.69
2021	5.86
2022	9.69
2023	12.21

Table A - 3: Plotwise annual mortality rate

Plot	Year	Annual_Mortality_Rate	Mean_Annual_Mortality
46	1994	0	5.90
46	1997	0.59	5.90
46	2000	0.30	5.90
46	2003	0.29	5.90
46	2007	13.18	5.90
46	2010	10.68	5.90
46	2013	6.12	5.90
46	2016	7.61	5.90
46	2017	8.27	5.90
46	2021	5.60	5.90
46	2022	7.64	5.90
46	2023	3.33	5.90
47	1994	0.00	7.01
47	1997	3.79	7.01
47	2000	0.26	7.01

47	2003	0.28	7.01
47	2007	8.12	7.01
47	2010	6.89	7.01
47	2013	6.23	7.01
47	2016	12.03	7.01
47	2017	6.71	7.01
47	2021	7.32	7.01
47	2022	16.97	7.01
47	2023	29.36	7.01
48	1994	0.00	6.13
48	1997	1.38	6.13
48	2000	1.14	6.13
48	2003	1.70	6.13
48	2007	12.72	6.13
48	2010	9.65	6.13
48	2013	9.46	6.13
48	2016	7.12	6.13
48	2017	5.45	6.13
48	2021	3.69	6.13
48	2022	5.23	6.13
48	2023	10.12	6.13
49	1994	0.00	6.65
49	1997	2.31	6.65

49	2000	0.95	6.65
49	2003	1.19	6.65
49	2007	8.92	6.65
49	2010	10.55	6.65
49	2013	8.33	6.65
49	2016	11.14	6.65
49	2017	10.11	6.65
49	2021	6.50	6.65
49	2022	8.45	6.65
49	2023	9.27	6.65

Table A - 4: Species-wise annual mortality rate (%) for major species

Species/ Year	1994	1997	2000	2003	2007	2010	2013	2016	2017	2021	2022	2023
Ilex vomitoria	0	2.47	1.852	1.143	2.14	0.96	2.87	0.27	1.39	1.25	2.35	3.89
Liquidambar styraciflua	0	4.59	1.78	1.88	2.83	1.23	2.35	2.020	2.73	3.05	28.27	19.41
Morella cerifera	0	5.28	2.37	2.68	7.84	10.67	11.85	12.62	12.51	14.26	27.76	15.41
Persea borbonia	0	0	0	0.30	0.88	2.17	3.177	61.96	30.01	11.98	6.89	28.76
Pinus taeda	0	0.81	0.35	0.52	12.72	11.36	8.52	9.49	8.62	6.28	7.6693	15.45
Quercus virginiana	0	1.12	1.03	0.82	1.28	1.31	1.137	1.17	0.722	0.549	3.0077	1.53

Table A - 5: Species code, common name, scientific name, counts and leaf habits.

Species code	Common Name	Scientific Name	Count	Leaf Habit
Lobp	loblolly pine	*Pinus taeda*	4950	Evergreen
Waxm	wax myrtle	*Morella cerifera*	741	Evergreen
Live	live oak	*Quercus virginiana*	177	Evergreen
Sgum	Sweetgum	*Liquidambar styraciflua*	225	Deciduous
Pndp	pond pine	*Pinus serotina*	36	Evergreen
Rbay	Redbay	*Persea borbonia*	193	Evergreen
Yaup	Yaupon	*Ilex vomitoria*	322	Evergreen
Tall	Chinese tallow	*Triadica sebifera*	66	Deciduous
Hsug	horse sugar	*Symplocos tinctoria*	20	Deciduous
Laur	laurel oak	*Quercus laurifolia*	13	Deciduous
Bgum	black gum	*Nyssa sylvatica*	11	Deciduous
Woak	water oak	*Quercus nigra*	3	Deciduous
Blue	Blueberry	*Vaccinium elliottii*.	20	Deciduous
Ahol	American holly	*Ilex opaca*	19	Evergreen
Poak	post oak	*Quercus stellata*.	1	Deciduous
Inkb	Inkberry	*Ilex glabra*	7	Evergreen
Wlok	willow oak	*Quercus phellos*.	1	Deciduous
Dhol	deciduous holly	*Ilex decidua*	1	Deciduous
Unkn	Unknown		3	

Table A - 6: Temperature, Precipitation and Highest tide Variables from 1994 to 2023.

Year	Highest Tide (m)	Temperature (Celsius)	Precipitation (mm)
1994	1.40	18.39	1651.88
1995	1.33	18.08	1491.57
1996	1.47	17.77	1272.97
1997	1.39	18.02	1441.18
1998	1.34	19.25	1659.83
1999	1.34	18.55	1775.08
2000	1.36	17.83	1373.47
2001	1.38	18.49	940.05
2002	1.32	18.80	1800.29
2003	1.29	17.95	1452.57
2004	1.18	18.42	1089.94
2005	1.39	18.36	1391.74
2006	1.31	18.72	997.90
2007	1.31	19.13	884.80
2008	1.30	18.14	1319.24
2009	1.34	17.84	1054.57
2010	1.41	17.46	1121.09
2011	1.47	18.75	843.28
2012	1.37	18.83	1175.76

2013	1.22	17.93	1224.64
2014	1.30	17.83	1413.19
2015	1.53	18.94	2048.51
2016	2.17	18.98	1612.73
2017	1.73	19.09	1267.22
2018	1.70	18.63	1811.32
2019	1.76	19.12	1321.32
2020	1.78	19.03	1502.62
2021	1.53	18.38	1410.49
2022	2.32	18.47	1277.66
2023	1.77	18.83	1596.86